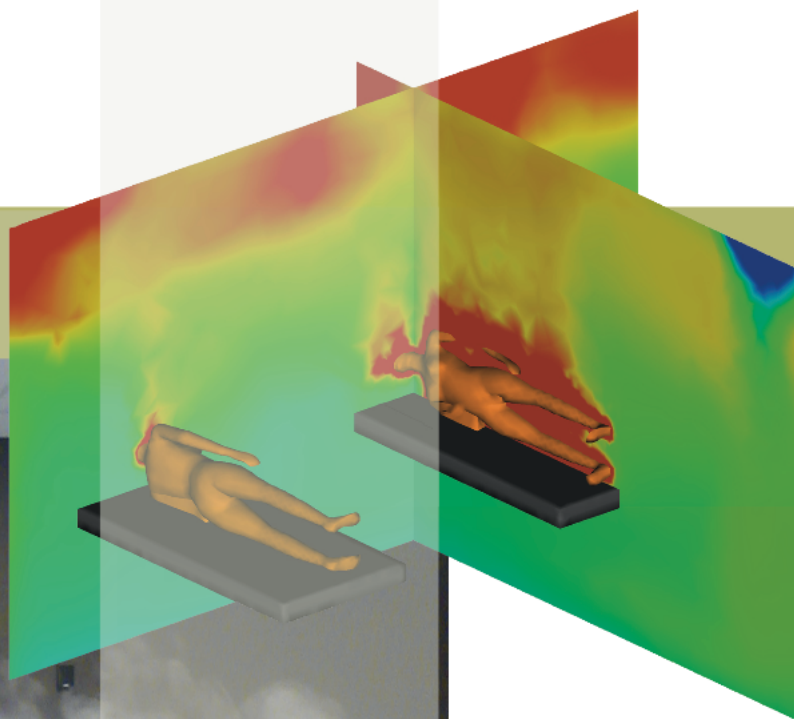


Cross infection in hospital wards

Farzad Khalegi
Anders Møllerskov



Main report

Titel:

Cross infection of hospital wards

Project period:

Master of science thesis,
Fall 2010
Spring 2011

Authors:

Anders Hornum Møllerskov

Farzad Khalegi

Supervisors:

Peter V. Nielsen

Rasmus L. Jensen

Yuguo Li

Copies:4

Pages :119

Attachments:

1 appendix and 1 dvd

Finished: 10. June 2011

Synopsis:

The present report contains three main parts; (I) Droplet nuclei, (II) CFD and (III) Particle distribution. Part I is split up in three minor part. The first part is with one thermal breathing exhaling under different conditions in a ventilated room. It is looked at the exhalation jets trajectory is in the room. In the second part is two manikins located opposite each other. they are located different places in a room ventilated with downward ventilation. it is looked upon how the distance between the manikins effect the personal exposure index. In the third part is two hospitalized manikins investigated. It is looked at how the location in the room, the influence of changed ACH and location of exhaust influence the personal exposure index. Part II is about CFD. CFD predictions are made of the hospital ward to see how CDF fits with measurements and to get a understanding of what happens in the room that is not measured. Part III is about particle deposition, the particle distribution of deposited particles on the floor are found for a single manikin exhaling particles and with two manikins opposite each other where only one of them exhales particles.

Preface

The present report presents the results of the work done in the last year of the Master of Science in Indoor Environmental Engineering at Aalborg University. Part of the project is done in Aalborg where experiments with tracergas are conducted and part of the project is done in Hong Kong where computational fluid dynamics simulations are performed and experiments using particles.

The project are divided into three major parts. The first part contains background information needed to understand the what is examined in the rest of the project and measurements using tracergas. The second part contains the CFD predictions of the flows in the hospital ward and the third part contains measurements on the particle deposition of a manikin that exhales.

Through out the report are the experiments performed named by a case number. If more information is wanted about a case e.g. case 13 it can be found on the enclosed dvd by looking in the Aalborg section and then the folder named case 13.

References in the report are given by a number, information about the reference can then be found in the bibliography in the end of the report.

The authors would like to thank all the supervisors, Prof. Yuguo Li, Prof. Peter Vilhelm Nielsen and Associate Proffesor Rasmus Lund Jensen for their guidance and help through the project. Further more would the authors like to send a thank to the technicians in both Denmark, Jan Laursen, and in Hong Kong Mr. Leung. Special thanks to senior clerk Bente Kjærgaard for always being willing to help. Mr. Liu Li for his assisting with almost anything in Hong Kong. To Mr. Vincent for helping us finding a apartment in Hong Kong. Finally also thanks to Dr. Hang for assisting with the CFD predictions.

Resumé

Dette projekt omhandler risikoen for smittespredning. Der bliver i den første del af projektet kigget på luftbåren smittespredning, som er den form hvor meget små dråbers indtørrede kerne er i stand til, at holde sig svævende i luft i meget lang tid og dermed følge lufstrømningerne. Forsøgene bliver udført i et rum på Aalborg Universitet hvor det er muligt at ændre positionen af indblæsning og udsugnings armaturer og have forskellige temperaturer på indblæsningsluften. Ventilationsprincippet som benyttes i alle målingerne er vertikal ventilation, det vil sige at den friske luft blæses ind med vertikal retning. På vej fra loftet mod gulvet sker der opblanding med rumluften. Når indblæsnings luften rammer gulvet spreder den sig langs gulvet, da den er koldere end resten af luften i rummet. Den relativt friske indblæsnings luft vil herefter stige til vejrs når det når til en varmekilde som vil transportere det opad. På den måde bliver der ført frisk luft op til personen. Der bliver i forsøgene brugt manikiner som er i stand til at afgive varme og have en åndingsfunktion ligesom mennesker. Det er muligt at indstille varmeafgivelsen på manikiner alt efter hvilket aktivitets niveau den er tiltænkt, skal den simulere en stående, løbende, liggende eller noget andet.

Først er der dog set på hvordan udåndingen fra en person udvikler sig i et rum under forskellige forhold. Det er både når personen er placeret under indblæsningsarmaturerne og under udsugningen. Det viser sig at hastigheden af udåndingen i de to tilfælde er tæt på at være den samme mens koncentrationen af sporgas, som er anvendt til at repræsentere de indtørrede dråber i luften, er forskellig for de to placeringer i rummet. Efter de indledende undersøgelser af hvordan udåndingen fra en person strømmer indføres der en manikin mere i rummet så der nu er to manikiner overfor hinanden. Manikinerne placeres forskellige steder i rummet for at se hvordan strømningerne i rummet påvirker risikoen for luftbåren smittespredning. Den vigtigste parameter i forsøgene er afstanden mellem manikinerne. Det viser sig at når manikinerne står tæt på hinanden under indblæsnings armaturet skabes der en "klokke" om dem hvor koncentrationen af sporgas er større end udenfor "klokken". Det viser sig også at jo længere manikinerne er fra hinanden jo mindre er risikoen for luftbåren smittespredning. Når manikinerne er så langt fra hinanden at deres indbyrdes "plume" ikke længere er stærk nok til at fortrænge den nedadgående strømning fra indblæsnings armaturet falder risikoen for luftbåren smittespredning gevaldigt, deres indbyrdes "klokke" er brudt.

Rummet hvor de andre målinger er foretaget har en størrelse som kunne passe til en topersoners stue på et hospital. To senge bliver tilføjet rummet og manikinerne bliver lagt ned for at simulere syge patienter, der ligger i deres syge seng. Der bliver set på hvilken indflydelse forskellige luftskifte har på risikoen for luftbåren smittespredning, det bliver undersøgt hvor i rummet de skal ligge for at risikoen for at den ene smitter den anden er mindst mulig, der bliver set på hvilken indflydelse forskellige placeringer af udsugningsarmaturet har for risikoen for at blive smittet. Det viser sig at placeringen af udsugningen spiller en stor rolle når det kommer til at minimere risikoen for at den ene patient smitter den anden. Forsøgene viser rigtig gode resultater når det kommer til personal exposure index som siger noget om forskellen mellem koncentrationen af sporgas i udsugningen og i indåndingen. Strømningerne

i rummet er styret af termisk opdrift fra varmekilder specielt manikinerne og det er derfor et meget følsomt system, men lige meget hvor store forstyrrelser der er i rummet og derved opblanding vil det altid være mindst lige så effektivt som opblandings ventilation.

Der er foretaget CFD beregninger på hospitalsstuen. CFD beregningerne laves med data fra faktiske målinger. De data som anvendes er overflade temperaturer, varmeafgivelser og temperaturer på flows, indblæsning og udånding. Dette gøres da det giver resultater tættest på de målte. Der laves CFD beregninger på 5 cases hvor ACH og udsugnings højde er det samme som målingerne. Derudover laves der en ekstra beregning som der ikke er lavet målinger på. Det viser sig at CFD beregningerne og målingerne stemmer rimeligt over ens når det kommer til temperatur fordelingen og flowet i i rummet. Fordelingen af sporgas er dog ikke helt den samme ved CFD beregningerne som for målingerne, dette kan skyldes forskellen i udåndings funktionen. I målingerne er der en pulserende udånding mens der i CFD beregningerne er konstant udånding.

Der er udført målinger med partikler i et laboratorium i Hong Kong. Disse målinger er lavet for at undersøge hvor langt en partikel er i stand til at bevæge fra en syg person. Der er hidtil blevet angivet en sikkerhedsafstand på en meter, men der er ikke vedlagt nogen dokumentation for hvorfor den afstand er valgt. Det er derfor interessant at undersøge om det er tilstrækkeligt eller om den afstand kan forkortes. Forsøgene viser at én manikin der står alene i et uventileret rum uden temperatur gradient ikke er i stand til at udånde partikler over en meter væk. Det viser også at afstanden partiklerne bevæger sig fra manikinen afhænger af aktivitetsniveauet, udåndings volumen per minut og udåndings frekvens. Målingerne viser at størstedelen af de store partikler der er i udåndingen fra manikinen aflejres indenfor 60 *cm* fra manikinen. Når to manikiner står overfor hinanden er partiklerne i stand til at afleje sig længere væk fra den manikin som udånder dem. Det viser sig at der aflejres store partikler på brystet af den modstående manikin og derfor kan det også antages at der indåndes store partikler.

Contents

I	Droplet Nuclei	13
1	Introduction	15
2	Background	17
2.1	Droplet nuclei	17
2.2	Cross infection	18
2.3	Micro environment	19
2.4	Thermal plume	21
2.5	Respiration	22
2.6	Manikin	25
3	Ventilation principles	30
3.1	Displacement ventilation	30
3.2	Mixing ventilation	31
3.3	Piston ventilation	31
3.4	Downward ventilation	32
4	Set up in Aalborg	34
4.1	The test room	34
4.2	Setup for one standing manikin	35
4.3	Setup for two standing manikins	36
4.4	Setup for the hospital ward	36
4.5	Cases	38
5	One standing manikin	41
5.1	One manikin under inlet diffuser; Case 1	41
5.2	One manikin under the exhaust; Case 2	45
5.3	Discussion	48
5.4	Conclusion	49
6	Micro environment between two standing persons	51
6.1	Vertical temperature distribution	52
6.2	Air velocity	56
6.3	Concentration	57
6.4	Personal exposure index	58
7	Results for the hospital ward	61
7.1	Where should the beds be located	61
7.2	Influence of position in the beds	62
7.3	Two exhaust heights compared to one	63
7.4	Influence of air changes on personal exposure index	65
7.5	Influence of the exhaust height	66

7.6	Conclusion	68
II Computational fluid dynamics		70
8	Computational Fluid Dynamic	71
8.1	Introduction	71
8.2	Case 1	73
8.3	Case 2	77
8.4	Case 3	81
8.5	Case 4	86
8.6	Case 5	88
8.7	Case 6	90
8.8	Conclusion	95
III Particle distribution		96
9	Set up in Hong Kong	97
9.1	The test room	97
9.2	Equipment	97
9.3	The setup for one manikin	98
9.4	The setup for two manikins	99
9.5	Cases	100
10	Particle deposition	101
10.1	Isothermal flows	101
10.2	Comparison between isothermal and non isothermal flow	103
10.3	Influence of varying activity levels	105
10.4	Micro environment between two people	107
10.5	Uncertainties	108
10.6	Conclusion	112
IV Conclusion		113
11	Conclusion	114
	Bibliography	118

Part I

Droplet Nuclei

Introduction

The purpose of hospitalization is to recover and get medical attention in order to overcome injuries and diseases. However study cases conducted by [22] [21] has revealed super spreading events inside hospitals. Patients are put together in hospital wards during their hospitalization period making them vulnerable to receive potentially highly contagious diseases from other patients or the very health care workers (HCW). This unfortunate phenomena is caused by cross infection which has several ways to target an in-patient. The ways of which a person can be targeted to a communicable disease are either by direct/indirect contact or by airborne transfer of pathogen-laden aerosols. When dealing with direct contact the general hygiene precautions are to be carefully considered and any lack or inattention can have fatal results for the bed bound patients as well as HCW. The consequences or signs of inappropriate and insufficient hygiene procedures have a larger impact on the patients with an already depressed immunological condition. Transfer of diseases and infections by direct contact is however an issue discussed thoroughly worldwide and can be prevented or controlled by handling the procedures correctly. Several diseases are known to be transferred from a host to a target by other routes than those of direct- or indirect contact where a medium or vector is involved.

During the last decade countries worldwide has witnessed epidemics and one of these epidemics evolved to a pandemic posing great threat for the global population. Diseases, viruses and human caused threats such as measles, tuberculosis, chickenpox, anthrax, smallpox, influenzas including the world known H1N1 (swine flu) and H1N5 (birds flu) and severe acute respiratory syndrome(SARS) are examples of former and novel diseases and viruses which has displeased humans in multiple extends. Although flues and viruses has existed in centuries it is still a volatile issue since it has the ability to mutate. The ability to mutate makes several viruses difficult to treat and vaccine treatments may first be available after a outbreak has arrived. The last pandemic, the swine flu, which origin is not known [13] attracted a lot of attention from the global community and also from the scientists. A credit, in part to medical discoveries and the work done by scientists has reduced the severity of the spread. Investigations made by scientists and other inquiring interested parties has during the years, since the last outbreak, revealed how the diseases are spread by investigations, substantiated with measurements and simulations of full scale test rooms and high end computer simulations. Since direct and indirect contact disease transfer is well covered and ensured other transfer routes are investigated and it has been proven that several diseases and viruses are transferred through the air when a source person is expelling contaminant diseases into the environment where other persons are present. In such situations, general

standard precautions are insufficient since the diseases are no longer acting through controllable media. Here the ventilation systems play a vital role in removing pathogen-laden droplets expelled into the air by an infected patient or other sources.

In the present study the scope is turned towards an investigation concerning the performance of a well established air distribution system. It is also of interest to gain knowledge on spread of droplet nuclei in hospital wards as to minimizing cross infection in hospital wards. In general the purpose of ventilation in hospital wards is to remove as much contaminants from the room as possible. This is mainly achieved by a diluting process where the concentration of contaminants is minimized by mixing with fresh and clean air and then the contaminated air is removed through the return openings. The location of supply openings and also the supply airflow pattern should be placed and designed in an appropriate way so fresh air is supplied to the work areas of HCW and then across the possible infected patients to the return openings. According to the guidelines presented by the Center for Disease Control and Prevention (CDC), this can be achieved by supplying air from the ceiling height and by placing return openings close to the floor [5].

Full scale experiments along with computational fluid dynamics (CFD) simulations are carried out in order to describe the contaminant distribution in the room as well as the air flow pattern. During the present study, air is supplied into the room through rectangular ceiling mounted textile diffusers. Thermal breathing manikins are used to imitate source and target patients. These are given different postures and positions in order to investigate the efficiency of the ventilation system and also the contaminant distribution in the room.

Three sets of experiments will be conducted in Aalborg. The first set of experiments are with one manikin located in the room it is investigated how the exhalation jet acts dependent on the manikins location in the room. After the measurements with only one manikin, the micro environment around two thermal breathing manikins is investigated. It is desirable to investigate the connection between different distances between two persons, one source and the other a target, and the contamination concentration near the target person. By a review of a study conducted by it has been proven that a low personal exposure index is obtained when the distance between the manikins is decreased, meaning that the exhalation jet takes a shortcut into the micro environment around persons.

In contrast to large droplets expelled from the source patient, droplet nuclei, smaller than 5 μm , stay almost weightless in the air and can travel long distances in the room until extracted by the exhaust or inhaled by a target person [19] [2]. The third set of measurement conducted in Aalborg is to investigate the risk of cross infection in a hospital ward. It is desirable to investigate the case where the risk of cross infection in the hospital ward is greatest and optimize that to reach the most effective removal of contaminants can be obtained, whether it is in accordance to CDC guidelines or not.

In Hong Kong measurements using manikins and particles performed. It is investigated how far particles travel under different conditions. It is looked upon the influence of varying the activity level with appertaining minute volume and breathing frequency and the influence of adding another manikin in front of the source.

CFD predictions of the measurements performed in Aalborg are also performed, in order to investigate whether measurements and CFD gives the same results.

Background

In the following section are descriptions of important parameters for understanding the results presented later in the report. The topics are droplets and droplet nuclei, the differences between them. The concept of cross infection, the micro environment within a macro environment. The concept of thermal plumes and how they can affect the personal exposure index. A description of the important characteristics of the respiration, such as the correlation between activity level, breathing frequency and minute volume. Finally there are also a section about the construction of the thermal breathing manikins used to simulate humans.

2.1 Droplet nuclei

In order to spread an airborne disease, droplets expelled through sneeze, laugh, cough or breathing, must sustain airborne for as long as possible. Large droplets fall down quickly whereas droplet nuclei, residues of evaporated droplets, sustain airborne for much longer time hence increased opportunity to be spread by air carriage. Droplet nuclei is a designation for small droplet residues in a size range of 0.5 to 12 μm . Droplet nuclei can threaten human health if originated from pathogen laden air, which from the beginning is descended from a sick person or other sources. Pathogen laden air means air that contains droplets containing pathogenic microorganisms which may be a source of infectious disease. Droplet nucleus smaller than 5 μm can be deposited by settlement in the alveoli of the lungs and cause lung infections. Larger droplet nucleus, larger than 5 μm can get deposited by centrifugal forces in the upper respiratory tract [14]. Due to their small size and the ability to sustain airborne for long periods of time, droplet nucleus are able to travel long distances in the build environment. This means that respiratory droplets which are small enough to remain airborne must not be underestimated and the hygienic importance of these must neither be underrated. The size of threat that pathogen laden air pose, i.e highly contaminated air that contains harmful micro-organisms or virus, is specially emerging in environments where numerous humans are clustered in the same environment. For instance a hospital ward. If a single sick person is hospitalized with a highly contagious disease, like SARS, the remaining hospitalized patient who are sharing the same ward can potentially get contaminated by way of cross infection. An effective measure to reduce the risk of cross infection is by implementing air distribution systems which can remove the contaminated air effectively.

Through the present study N_2O is used to simulate pathogen laden droplet nucleus expelled through the source manikins exhalation and received by a target manikins inhalation. The received concentration of the tracer gas N_2O is used to quantify the ventilation effectiveness

in a simulated hospital ward. The quantification of the ventilation effectiveness is realized by quantities such as personal exposure indexes and ventilation effectiveness indexes. These indexes will help reflecting the conditions in the simulated hospital ward and also highlight the risk of cross infection.

2.2 Cross infection

Cross infection is the transmission of pathogenic laden organisms from one person to another. In a hospital ward cross infection can occur between two or multiple patients or other persons in the environment. The occurrence of cross infection in a hospital ward may be caused by several reasons and the route it originates from may also have a connection to the cause. Cross infection can occur through direct contact. Direct contact implies the transfer of a infectious agent through surface contact. An infectious agent can be secretion on hands left on a doorknob or other surfaces which later is picked up by another person who then can get infected. This sort of cross infection may occur due to lack of maintenance of sanitary conditions, lack of rigorous personal hygiene at all times, inadequately sterilized surgical instruments and the hospital staff transporting bacteria.

Cross infection can also occur when some infectious agents are secreted in large droplets. When a sick person coughs or sneezes, large droplets are expelled in the direction of the "spray". Because droplets are relatively large in size they fall down in a short distance from where they are "launched". But if another person is in the vicinity environment, there is a risk of cross infection by this path. Although large droplets may fall down quickly the risk of cross infection is still present. The next route of cross infection originates from when large droplets are expelled and evaporation of these droplets are taking place.

If the distance between source and target individuals are large and precautions are made with respect to the first two routes, cross infection can still occur. This is cross infection where diseases are transmitted through an airborne route. Droplet nuclei, residues of evaporated droplets may sustain airborne for long periods and spread by air carriage into large distances from where it is originated, [21], [6], [17].

As mentioned sufficient handling and precautions may reduce the risk of the first two cross infection routes, but cross infections due to airborne pathogen laden droplet nuclei require other measures in prevention of spread. Properly installation and design of air distribution systems are of utmost importance. Within the design and installation procedure of any air distribution systems in a hospital ward is it essential to consider and take into account all parameters that can affect the air flow patterns in the build environment. Heat loads, i.e number of patients and appliances, postures and positions of the heat loads. Position and type of supply and return openings etc.. These are some of the parameters that can affect the risk of cross infection in a hospital ward.

Through the present study, cross infection with respect to droplet nuclei is investigated in a simulated hospital ward. Various set ups involving two manikins are considered. The influence of two types of return opening are investigated with respect to cross infection. The quantification of the ventilation effectiveness and thereby the risk of cross infection is enabled by using personal exposure and ventilation effectiveness indexes respectively.

2.3 Micro environment

In a ventilated space, such as a hospital ward, air distribution systems contribute to a diluting and removal process of pollutants and contaminants. In this context the whole ventilated volume of the hospital ward is designated as the macro environment. Within the macro environment some specific areas may be influenced or dominated by other flow patterns or entirely unaffected by the general air flow patterns. This area in which the flow patterns are dominated by other forces than those induced in the macro environment is called the micro environment. Hence within the micro environment homogeneous conditions may prevail that are only finding place here. When a single person is standing in a ventilated space the micro environment of that person can be thought as a cylindrical envelope surrounding the person. This is caused by the human thermal plume which is the result of a thermal convection process which transfers heat from the body to the surrounding environment. In situations where two or multiple persons are close enough to each other, their plumes can coincide to a single plume creating a joint micro environment. Within the micro environment conditions may differ from those in the remaining part of the room. Individuals within the micro environment may expose each other to contagious diseases if one of the individuals is a carrier of one. This transfer of disease is called cross infection and is the airborne type presumed that no direct contact is finding place. Another disadvantageous effect of being in a micro environment is that the risk of cross infection is high because the general flow patterns may not effectively be able to penetrate the plumes and thereby remove the contamination. Thus the contaminants expelled by a sick person can possibly make a "shortcircuit" into the target persons inhalation. As the persons move further and further away from each other the combined micro environment also vanishes. A way to investigate the risk of cross infection and the effect of increasing the gap between a source and target person is to measure the personal exposure index.

2.3.1 Personal exposure index

Amongst other purposes ventilation systems are used as remedies to remove contaminants from enclosed environments as hospital wards. It is therefore relevant to ensure that the ventilation system performs effectively. To describe the efficiency of an air distribution system different quantities are commonly used. Besides the ventilation effectiveness index, the personal exposure index is an useful quantity. The personal exposure index expresses the ventilation effectiveness which is actually experienced by a person in the ventilated environment. In order to clarify the term exposure one could think of exposure as an specific incident. The incident at which a person is in contact with a pollutant of a certain concentration during a certain period of time. Another term to be clarified is the dose. Dose occurs when the pollutant crosses the physical boundary of a person. Exposure without a dose can occur but not vice versa. Different doses may be received by persons although exposed to same level. The received dose depends on the activity level as well as the persons physiology. Another fact that has an influence on the exposure and need to be considered is the ventilation principle. Whether displacement or mixing ventilation principles are utilized, both principles affect the way the exposure can be measured. With regard to mixing ventilation it is often stated that the room air is fully mixed and the exposure can be measured anywhere in the room as the concentration is assumed to be the same in the entire room. This approach may not be appropriate when dealing with a displacement ventilated

environment because of the combined effect due to entrainment of room air into the human boundary layer and the concentration gradients in the displacement ventilated room. Fresh and contaminated air can be transported in the human boundary layer and thereby affect the inhaled concentration. A possible outcome of this behavior may be reflected as a deviation between the inhaled concentration and the concentration outside the breathing zone. The personal exposure index is defined as:

$$\varepsilon_e = \frac{c_R}{c_e} \quad (2.1)$$

Where:

ε_e	Personal exposure index [-]
c_R	Concentration of the exhaust air [ppm]
c_e	Concentration of the inhaled air [ppm]

It is desirable to attain the highest personal exposure index possible. A value of one indicates that the air is fully mixed and that the inhaled air has the same amount of pollutants as the exhausted air. A high level indicates that there is a lower risk of cross infection and a effective ventilation system.

2.3.2 Ventilation effectiveness

Similar to personal exposure index, the ventilation effectiveness can be quantified by use of quantities such as the ventilation effectiveness index and a local ventilation index. The quantity, ventilation effectiveness index gathers information about the concentrations in the occupied zone and the concentration in the return opening and gives out a single value which quantifies the air quality. Unlike this index the local ventilation index only needs concentration in a single point in the room and the concentration in the return opening. By definition the ventilation effectiveness index, ε_{oc} , is dependent of the concentration, c_{oc} , in the occupied zone and the concentration, c_R , in the return opening giving:

$$\varepsilon_{oc} = \frac{c_R}{c_{oc}} \quad (2.2)$$

Similarly the local ventilation index, ε_p , can be defined as the concentration, c_p , in a point in the room compared to the concentration, c_R , in the return opening, giving

$$\varepsilon_p = \frac{c_R}{c_p} \quad (2.3)$$

Since the patients in the hospital ward both act as heat and contaminant sources the ventilation effectiveness may be affected and it is therefor important to define the conditions in beforehand measurements are carried out. Through the present study, in all cases, the manikins are taken into account when analyzing the ventilation effectiveness, i.e the activity level etc..

2.4 Thermal plume

The thermal plume is a parameter that must be considered when designing air distribution systems in hospital wards. The intensity of the thermal plume depends on the human physiology and activity level. The human skin is approximately $32 - 34^{\circ}\text{C}$ at a normal activity level. The skin temperature is thereby several degrees warmer than the surrounding air at room temperature i.e $20 - 25^{\circ}\text{C}$. This excessive temperature causes a steady thermal convection process which transfers heat from the body to the surrounding environment and leading wast body heat away, this and other factors such as radiation, evaporation etc. maintains thermal equilibrium. As a result of this process the air which is heated by the skin rises upward and generates a free convection thermal plume above the body see illustration in figure 2.1[24].



Figure 2.1: Schlieren photograph illustrates the thermal plume around a person.

Since every section of the body release heat, the convective boundary layer of a person who stands still in quiet air begins at the feet and travels up the legs and torso, growing thicker and faster as it moves up. For a standing person who is approximately 1.7m in height the boundary layer is laminar until about 1m above floor level, and is fully turbulent above 1.5m . This natural boundary layer grows to approximately $15 - 20\text{cm}$ thickness around the head, where the maximum upward air velocity is reached in the range of $0..25\text{m/s}$ [24]. This upward flow separates from the shoulders and the top of the head, as the body surface becomes horizontal. The resulting human thermal plume continues to rise above the body itself where it reaches a typical overall flow rate of about 50 l/s . This natural human convective airflow pattern is similar for everyone despite the usual differences in body height, weight, sex, clothing, etc.. From this it is clear that the air in contact with the human body can never be stagnant, but rather is in a constant state of upward motion.

As insinuated this thermal plume is an inseparable power which is accountable in the presence of a human being or a group of humans. In the latter case the plumes will coincide into one single larger plume as long as the persons are close enough together. Another fact that can affect the intensity or size of the plume is posture. Whether a person is standing sitting or lying, different flow patterns will arise, confer figure 2.2.



Figure 2.2: When lying, the flows are generally slower and thinner than when standing. Sitting produces flows that are intermediate between lying and standing.

In the present study, humans are replaced by thermal breathing manikins. Some of the physiological and thermal abilities of humans are transferred to these manikins enabling the manikins to breathe and emit heat through their body surfaces. These abilities are controllable, enabling the user to regulate the pulmonary frequency and heat, i.e. by defining a specific activity level. Given breathing and thermal abilities, it is interesting to investigate the effect of the thermal plumes generated by the manikins.

2.5 Respiration

The primary function of respiration is to obtain oxygen for use by the bodies cells and eliminate the carbon dioxide that cells produce, respiration is also thought as a direct source of dissemination of several contagious diseases. Transportation of pathogen laden aerosols from one person to another entails that pathogen laden droplets and droplet nuclei must be carried through air when expelled from a source person. For this reason it is important to investigate the parameters such as the exhalation temperature and pulmonary ventilation rate.

The human exhalation with its pulsating and intermittent nature is a buoyant jet since its temperature is usually higher than the ambient room temperature. The exhalation jets further progress into the room depends on its momentum, the temperature conditions in the room, and of interaction with other main flows, like e.g. the boundary layer flow around a person or those induced by the ventilation system. The momentum of the exhalation jet depends on the pulmonary ventilation rate and the cross sectional area of the respiratory openings, while the exhalation temperature depends on the ambient air temperature that is inhaled. The intermittent nature of the exhalation jet is due to varying temperatures during the exhalation. The exhalation temperature tends to be higher at the end of exhalation than

2.5. Respiration

at the beginning due to the heat recovering properties of the upper airway passage. Since it acquires an almost constant, maximum value for the majority of the exhalation period, the maximum value is used, see figure 2.3 [9] [3].

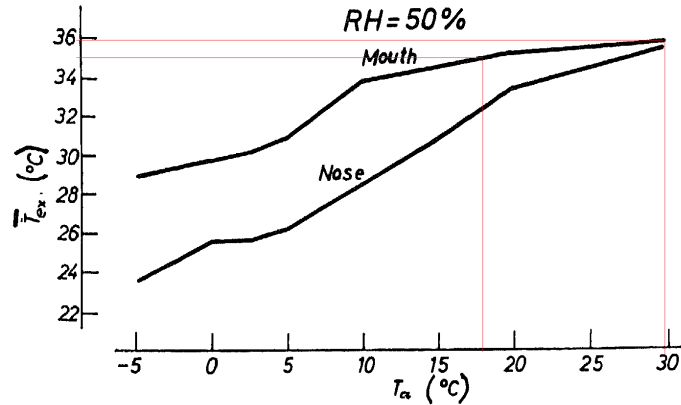


Figure 2.3: Exhalation temperature (T_{ex}) as a function of ambient temperature (T_a) [9]

The graph above shows the exhalation temperature at a relative humidity (RH) of 50% but the RH does not influence the exhalation temperature as much as the ambient air temperature. This can be seen in figure 2.4.

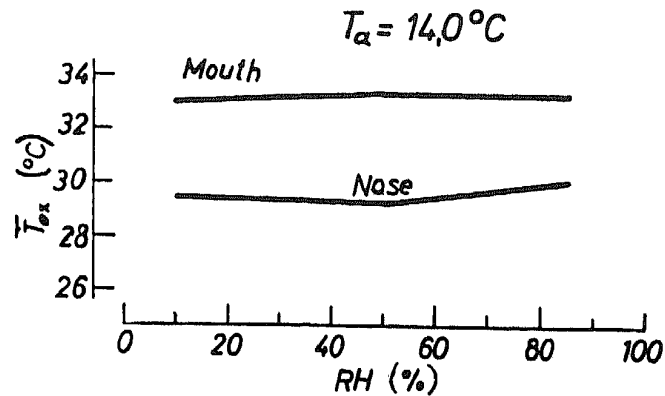


Figure 2.4: Exhalation temperature (T_{ex}) as a function of relative humidity (RH) [9]

Because of the minimal influence of the RH the influence is not considered. As long as the RH is within the interval given in figure 2.4 it can be neglected. Because of the insignificant influence of the RH only the ambient temperature is considered when determining the temperature of the exhalation jet.

It can be seen from figure 2.3 that with the possible indoor temperatures of 18 to 30°C the temperature of the exhalation jet from the mouth should be in the interval of 35 to 36°.

The respiration of a person is usually described using three important characteristics, these

are the amount of air inhaled per minute known as the pulmonary ventilation rate or minute volume (VM), the breathing frequency per minute (BF) and the last is the amount of air inhaled per breath known as the tidal volume (V_t). Hence, the frequency times the tidal volume equals pulmonary ventilation rate.

These three characteristics of the human respiration are highly dependent on the physical activity, the age and gender of the human. Figure 2.5 shows the difference in VM and BF for males and females at different activity levels, the graph is for humans in age 19 to 60.

Women				Men			
Activity	Met.	MV	Bf	Activity	Met.	MV	Bf
[-]	[met]	[l/m]	[br/m]	[-]	[met]	[l/m]	[br/m]
Lying(p.49)	0.7	7.12	14.4	Lying(p.52)	0.7	8.93	13.2
Sitting(p.49)	1	7.72	15.2	Sitting(p.52)	1	9.3	13.8
Standing(p.49)	1.2	8.36	15	Standing(p.52)	1.2	10.65	14.3
Walking 4 Km/h	2.5	19.23	21.7	Walking 4 Km/h	2.5	22.79	17.7
Walking 4.8 Km/h	2.9	23.81	24.2	Walking 5.3 Km/h	3.2	26.78	19.4
Runing 6.4 Km/h(p.66)	3.8	50.44	46.03	Walking 6.4 Km/h	3.8	35.56	21.9
Runing 7.2 Km/h(p.66)	4.25	48.89	47.86	Walking 7.2 Km/h	4.24	64.82	26.1
Driving	1,0-2,0	8.95	17.4	Walking 8 Km/h	4.67	58.74	33.3
Housework	2,0-3,4	17.47	21.9	Walking 9.7 Km/h	5.54	69.22	28.4
				Driving	1,0-2,1	10.79	16.8
				Woodworking	1,8	24.42	22
				Car maintenance	-	23.21	23
				Moving	-	36.55	24
				Yard work	-	26.07	21.1

Figure 2.5: The difference of activity levels between male and female.

Figure 2.6 shows the relation between the activity level and the MV and the activity level and BF.

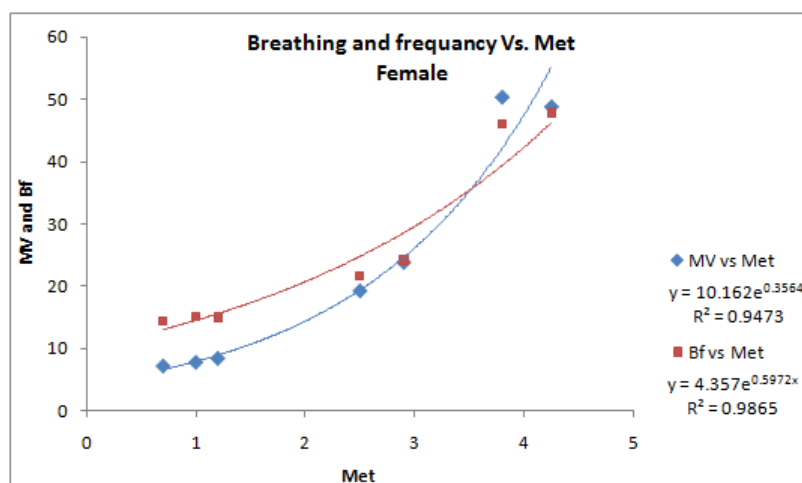


Figure 2.6: Relationship between breathing frequency and minute volume Vs. metabolic rate for females.

The equations shown in figure 2.6 will be used to calculate the MV and BF later in the project.

The respiration cycle for a human being is shown in figure 2.7 it is a periodic cycle that follows a sinus function.

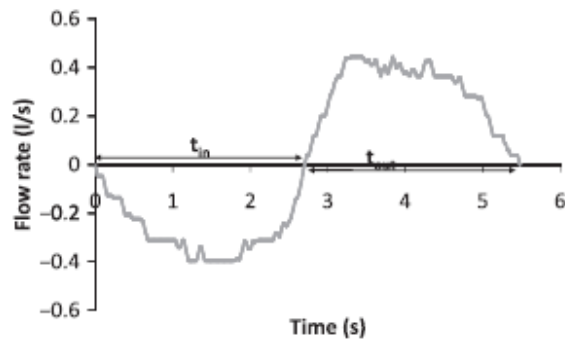


Figure 2.7: Breathing cycle for a human being [8].

The respiration pattern shown in figure 2.7 is almost the same as used in all cases conducted in Aalborg. A graph of the respiration pattern obtained using a artificial lung can be seen in figure 2.8.

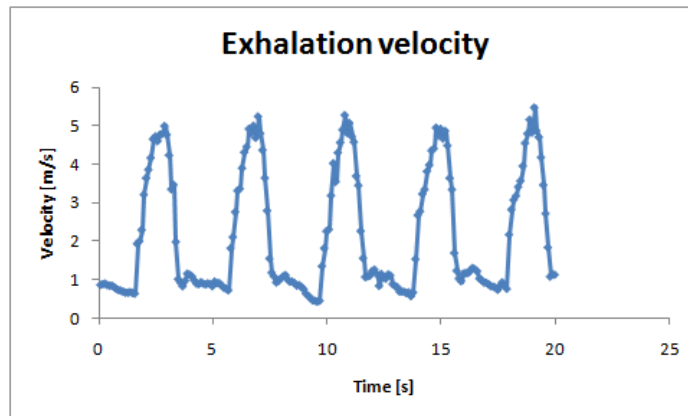


Figure 2.8: Breathing cycle using a artificial lung.

Figure 2.8 shows the velocities of the exhalation of the source manikin in case 2 see figure 4.4 on page 39 the velocities are measured 1cm from the mouth. Since only the exhalation is shown the two graph are not completely alike but if the inhalation had been present in figure 2.8 it too would follow a sinus function.

2.6 Manikin

The human respiration cycle is a rather complex process which entails mechanisms very complex to duplicate by use of surrogates, i.e manikins. However manikins has been used as substitutes in several extends and are given abilities very similar or at least sufficiently detailed in order to duplicate humans and their abilities.

A human being releases heat through the body surface in order to maintain thermal equilibrium [7]. This gives rise to a thermal plume to be created. Anticipated that a thermal

plume is presence for humans as well other heat sources this entails that room air flow patterns may be affected. The extent is however determined by the intensity of the thermal plume which depends on several other parameters such as the activity level, gender, body surface area etc. and for a passive heat source the effect in Watt. In addition, leave out of account CO_2 , humans can also act as contaminant sources, disseminating infectious agents through breathing, speaking, coughing or sneezing [2] [20] [15] [3]. Similar to the thermal plume intensity the dissemination of pathogen laden droplets depends on various parameters i.e, MV , V_t , BF , size of the expelled droplets, direction of the exhalation etc. Another parameter that affects the spread of infectious agents in an enclosed environment is whether the contaminant source remains stationary or moving [4]. A feature which may be difficult to adapt to a manikin.

Through an assay, are the abilities and disabilities of using a manikin instead of a human subjects in the specific case emphasized [23] and through the present study two manikins are utilized. One manikin is thought as a susceptible target and the other as a persistent source expelling contaminants through respiration. Although the manikins are limited with regard to imitate the exact and always varying real respiration processes and thermal abilities some applications of manikins are still acceptable. The total control of several crucial parameters are accessible and thus reducing discrepancies between manikins and real human subjects. Given that the manikins are thermal breathing manikins, the heat release as well as the breathing functions are controllable by the user. Only it has to be properly decided how parameters should be adjusted. The parameters referred to are described in the following.

2.6.1 Manikin construction

Before entering the more delicate abilities of the thermal breathing manikins used in this study and determining the parameters, firstly a description of the construction of the manikins is appropriate.

Besides the hollow aluminum cylinders which make up the body, heating devices and fans are installed inside the body. The manikin is then able to emit heat and subsequently the heat is distributed within the body by the help of two fans. In this manner heat is evenly distributed. This heating system is controllable by adjusting the potential. The range for the potential is $0V$ to $200V$ and the effect emitted from the manikins is within the range of $0W$ and $145W$. The fans within the manikin use $37W$ to operate, which must be included in the total heat load from the manikin. The appearance along with detailed construction of the manikin can be seen in figure 2.9

2.6.1. Manikin construction

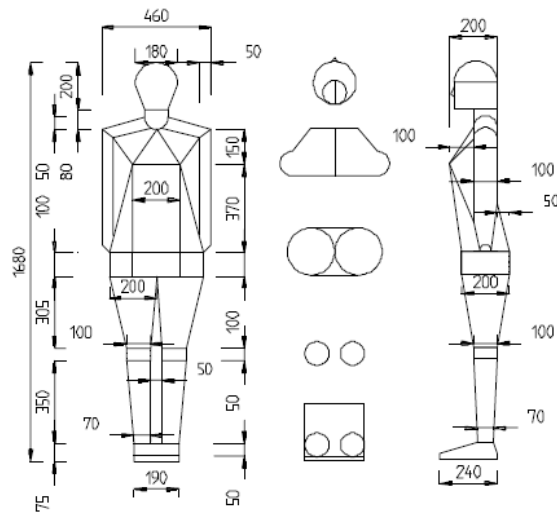


Figure 2.9: Detailed size description of the manikin [3].

There might be minor differences to the appearance of the manikins but in general they are made by the same template so they are internally the same. The Body surface area for the manikins are approximately $1.4m^2$. The height is $1.68m$. The height from the floor to the manikin mouth is $1.50m$ and floor to nose $1.53m$. The cross area of the mouth is $123mm^2$ and the nostrils $50mm^2$. The directions of the exhalation jet through the respiratory routes are given in table 2.1 and shown in figure 2.10[8].

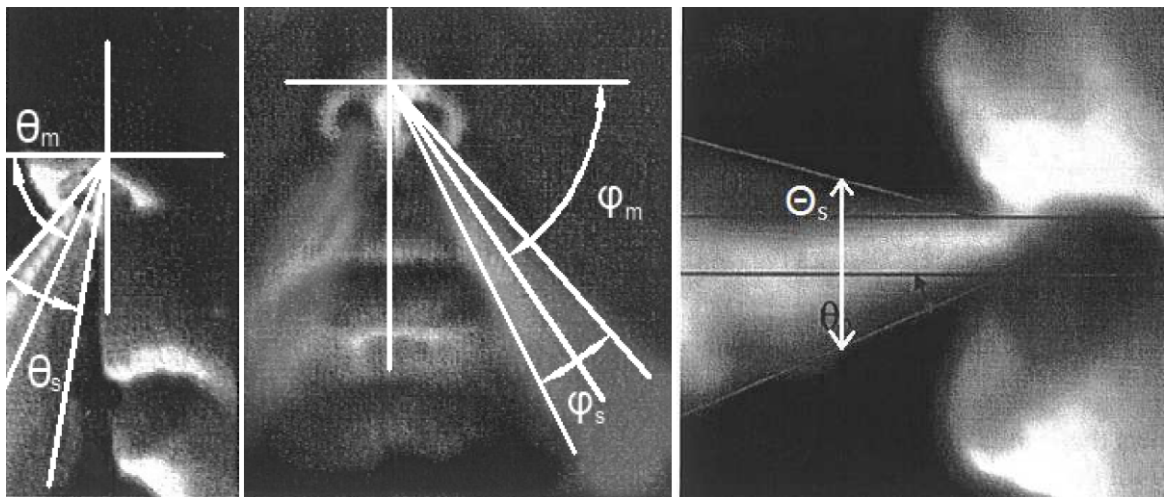


Figure 2.10: Exhalation from mouth and nose[?].

Naturally the exhalation jets from the nose and mouth are different. Respiration through the mouth is more or less horizontal while a downward exhalation jet is expected from the nose. Subsequently, due to buoyancy forces the exhalation jet tends to move upwards if the ambient room temperature is colder than that of the exhalation. Since the boundary layer

around humans is to be considered the exhalation jet from the nose may be affected. The direction of the exhalation jets are given in the table 2.1.

Angle	Description	Human	Manikins
θ_m	Mean side angle	60 ± 6	45
φ_m	Mean front angle	69 ± 8	60
θ_s	Front spreading angle	23 ± 14	22
φ_s	Side spreading angle	21 ± 10	21
θ_s	Front mouth spreading angle	30	20

Table 2.1: Angle of exhalation jets from mouth and nose.

The utilization of manikins through this study is an attempt to resemble real human subjects respiration cycle and heat release. Both abilities are covered by use of external units such as artificial lungs and heating units, the latter is to resemble real expiration temperatures. In the following both external devices will be described respectively.

2.6.2 Artificial lungs

The primary function of respiration is to obtain oxygen for use by body's cells and eliminate carbon dioxide that cells produce. In order to reconstruct the human respiration cycle artificial lungs are used. Below in figure 2.11 and 2.12 are two artificial lungs illustrated.

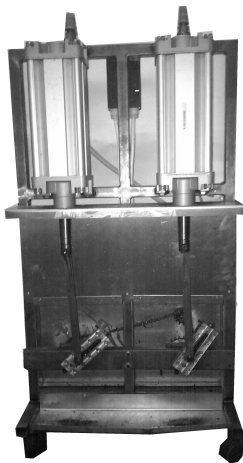


Figure 2.11: Piston driven lung.



Figure 2.12: Respiration helped along with a compressor inside the shell.

The artificial lung shown in figure 2.11 on the left, is driven by two cylindrical pistons, one handling exhalation and the other handling the inhalation. The construction of the artificial lungs allows adjustments by changing the stroke length of the piston and the frequency. Hence the volume of the artificial lungs can be set to deliver a desired exhale flow by adjusting the pistons penetration depth. Each chamber has the dimensions 125mm in diameter

2.6.3. Heating unit

and a maximum stroke length of 110.5mm providing a maximum pulmonary airflow of 1.35 liter pr. stroke. Furthermore the frequency can be set to a desired value as well. This is done by adjusting the potential on the motor that drives the pistons up and down. The other lung is controlled by a compressor which can be set to deliver desired frequency and pulmonary airflow. It also controls both exhalation and inhalation and can be seen in figure 2.12.

2.6.3 Heating unit

When the artificial lungs have delivered the desired amount of air, the air is then led through a heating unit which warms up the air in order to reach the same temperatures as real exhalation from a human. This is done with the heating unit shown in figure 2.13.



Figure 2.13: Heating unit used to heat up exhalation air.

The effect delivered to the exhalation air by the heating unit can be controlled by a Wattmeter. There are limits to as how much heat can be applied to the exhalation air. If the flow through the heating unit is very low the heat generated will not be removed by the air but is transported to fittings through convection. This leads to the fittings getting very warm and the tubes can melt.

Ventilation principles

for most buildings are the main objective for the ventilation system in a building is to deliver as fresh as possible to its occupants without creating any discomfort but in hospital settings it is also very important the ventilation removes as many of the airborne contaminants as possible and not create shortcuts aerosols. For a ventilation system to provide a satisfactory performance is it important to know the geometry of the ventilated space, the location of heat sources, electrical appliances and the number of occupants pl in the ventilated space as they play a vital role in the system working as intended.

3.1 Displacement ventilation

Displacement ventilation has proven to provide good results with respect to indoor air quality in the occupied zone in several applications, e.g. offices, industrial and domestic. By inducing slightly sub-cooled fresh air with low impulse close to the floor the fresh air progresses as a stratified flow. A illustration of how displacement ventilation works is shown in figure 3.1.

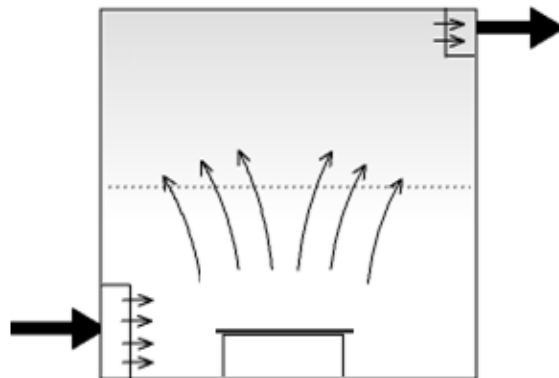


Figure 3.1: Illustration of the displacement principle.

This stratified flow will spread and progress across the floor until entrained into the ascending convective boundary layer flows that are formed close to heat sources. The entrained air is heated and lead towards the ceiling and in this manner a vertical temperature gradient arises. Thus two zones are created above and under the stratification height. The concept of stratification height is that volumetric flow rate of the convective flows equal the volumetric

flow rate from the inlet. The back draws of this principle is its sensitivity to movements induced by the occupants and the risk of draught [4]. Another unpleasant feature that has been observed in a hospital setting is that the stratification height is dangerously close to the breathing zone of bed bounded patients [21]. This gives rise to increased risks of cross infection between the patients.

3.2 Mixing ventilation

With regard to mixing ventilation a diluting process is expected in the entire ventilated space. This principle has upsides and downsides. On the upsides can be mentioned the fact that a uniform distribution of contaminants can be expected in the entire room this means that there are nowhere in the room where the concentration gets too high as can be the case with displacement ventilation. But this can also be seen as a downside as the personal exposure index will never be better than 1 if perfectly mixed air is supposed. When mixed ventilation is used the contaminants exhaled will be spread to the entire room and can spread contaminants to a large area. The mixing principle is illustrated in figure 3.2.

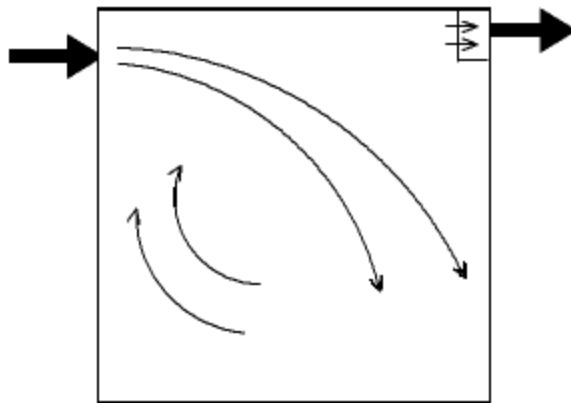


Figure 3.2: Illustration of the mixing principle.

At first this principle might seem inadequate in hospital ward settings since the primary aim is to reduce the risk of cross infection between the patients, but since a convective boundary layer is present around humans this might provide protection against direct exposure. Experimental studies conducted by [21] reveals personal exposure indexes close to 1 or less whereas higher personal exposure indexes has been found with displacement principle.

3.3 Piston ventilation

A ventilation form that are used when very clean rooms are wanted are piston ventilation. This form of ventilation is very efficient and used for clean rooms in laboratories. An illustration is shown in figure 3.3.

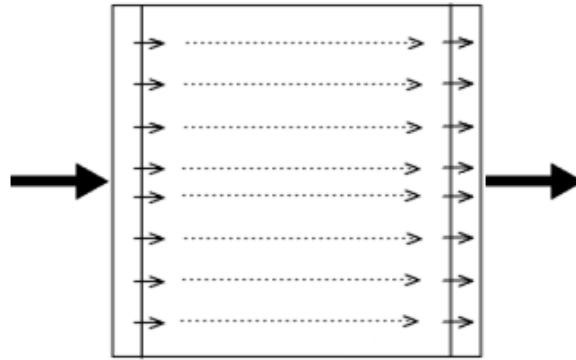


Figure 3.3: Illustration of the piston principle.

It is suggested by the CDC that air enters through the ceiling but the ACH they suggest are too low to overcome the thermal plumes of patients and equipment. It takes a high ACH to keep the room free of contaminants and that costs a lot of money and there is a great risk of draught when using high ACH.

3.4 Downward ventilation

A fourth option is to use downward ventilation which has shown good results earlier [18]. The downward ventilation works as a mixture of displacement ventilation and mixing ventilation, an illustration of the principle can be seen in figure 3.4.

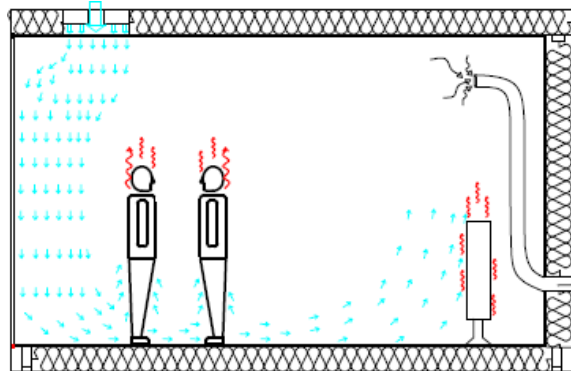


Figure 3.4: Illustration of the downward ventilation principle.

When the air exits the inlet diffuser and moves to the floor there is entrainment into the jet, like mixing ventilation. How much air is entrained depends on the speed and temperature of the inlet air. when the air reaches the floor it flows along the floor like the displacement principle. The fresh air then rises when it reaches a heat source, it follows the plume the heat source creates. If the heat source is a standing person or a person in bed the plume from that person transports the fresh air to the breathing zone. This fresh air makes sure that the risk of cross infection is minimized and works as a protective layer. It is chosen to

3.4. Downward ventilation

work with this kind of ventilation principle as it seems to give the best results when working with the kind of settings as are done in this project.

Set up in Aalborg

In this section is a description of the test room in which the measurements are executed and a description of the different cases examined. There are descriptions of where the equipment is positioned and why, the effect in the room and air changes used in the set ups.

4.1 The test room

The test room used for the measurements for this part of the project is located at Aalborg university. The test room has a steel skeleton and is covered with wood and glass. The test room is not very well insulated so in order to minimize heat transfer from the test room to the surroundings due to temperature differences is a heat source placed in the laboratory. The internal dimension of the test room are height 2.45m, width 3.6m and length 4.1m. A sketch of the room can be seen in figure 4.1.

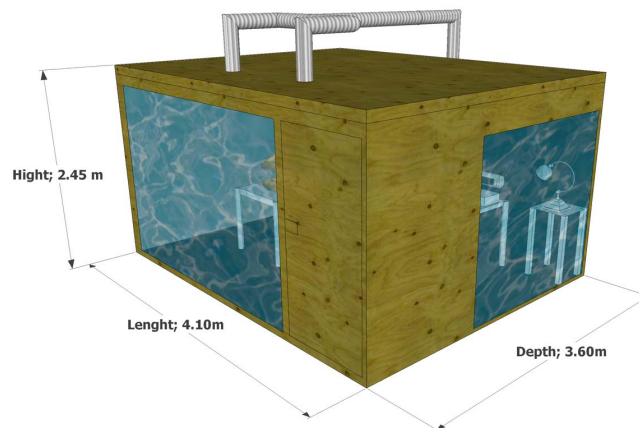


Figure 4.1: The dimensions shown on the figure are all internal.

Due to the ceiling construction is it possible to place the inlet different places in the room, which makes it possible to place the manikins directly under the inlet in the middle of the room but also have a vertical ventilated room where the Coanda effect can be utilized. It is also possible to place the exhaust opening different places in the room.

4.2 Setup for one standing manikin

In this set up is one thermal breathing manikin standing alone in the test room the manikin is located underneath the inlet diffuser shown if figure 4.2 or underneath the exhaust opening.

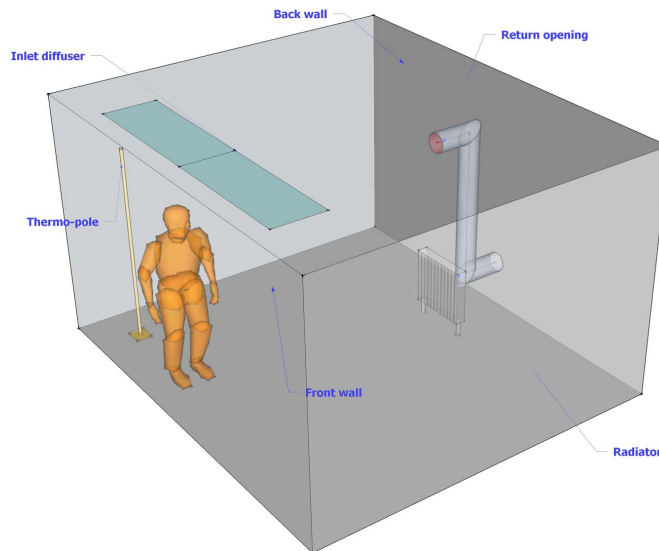


Figure 4.2: Manikin located underneath the inlet diffuser.

The air flow to the room is $128 \text{ m}^3/h$ which gives an air change rate per hour (ACH) of $3,5 \text{ h}^{-1}$ with a inlet temperature of $16 \text{ }^\circ\text{C}$. The velocity of the exhalation jet is measured at five different points from the manikin using hot sphere anemometers. The points chosen are where the jet has the highest velocity. The temperature in the room is measured two different places these are 15cm and 40 cm behind the manikin the temperature is measured at five different heights for each position. Besides these are the temperature of the exhalation jet measured.

The concentration of tracergas in the exhalation jet is measured in the same points as the velocity. The effect in the room is shown in table 4.1 it gives a total of 412W .

Heat source	Effect [W]
Manikin	100
Air heater	12
Radiator	300
total	412

Table 4.1: Effect from equipment and manikin inside the test room.

4.3 Setup for two standing manikins

Two thermal breathing manikins are placed facing each other with varying distances of 35, 50 and 110cm between each other. The manikins are placed under the inlet as in cases 3 to 8 or under the exhaust as in case 9, see figure 4.4 on page 39. The test room is in all cases supplied with the same airflow of $128 \text{ m}^3/h$ which gives an ACH of 3.5 h^{-1} . It is desired to have a inlet temperature close to 16°C as this will give a air temperature in the test room of 23°C which is assumed to be a comfortable temperature in a hospital environment.

In these setups is the temperature gradient measured three different places in the test room, 40 cm behind both the target- and the source manikin and in one of the corners. Besides these points the is temperature also measured in the inlet to secure it is close to the desired temperature of 16°C . The temperature of the exhalation of the source and target is measured to make sure it is within the interval given in section 2.5 on page 22.

The concentration of tracergas is measured several places in the test room. The concentration is measured in the exhalation of the source, the inhalation of the target, at chest height of both target and source, above the head of the target and in the exhaust air of the source. In addition to these points is the concentration gradient measured in one of the corners as well, the same corner as the temperature gradient is measured. These measuring points are chosen in order to learn where the exhalation jet moves and to calculate the personal exposure index and ventilation index.

The velocities are measured 25 and 35 cm above the manikins in some of the cases in order to check if there is an upward or downward flow around the manikin. It is done in order to check if the upward flow caused by the body plume is oppressed by the downward flow caused by the inlet as it is described in [5]. The effect in the room from equipment and manikins can be seen in table 4.2 it gives a total of $524W$.

Heat source	Effect [W]
Source manikin	100
Target manikin	100
Air heaters	24
Radiator	300
total	524

Table 4.2: Effect from equipment and manikins inside the test room.

4.4 Setup for the hospital ward

For the setup for the hospital ward are two thermal breathing manikins lying in beds. The manikins are positioned facing each other with 160cm from the mouth of the source to the mouth of the target. The set up can be seen in figure 4.3.

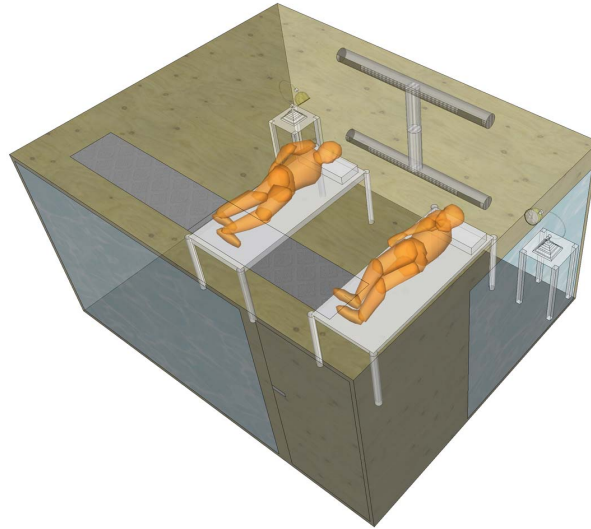


Figure 4.3: The setup for two manikins in bed.

The Exhaust opening is located in different heights in order to find the optimal position and to investigate if the guidelines given in [5] provides the best locations for exhausts. The exhaust is positioned at 10cm , 106cm , 180cm , 206cm and 235cm above floor level. Two different airflows is chosen, a low ACH and a high ACH, in order to see how the ACH influences the gas concentrations in the room. The low airflow to the room is set at $189\text{ m}^3/h$ which gives a ACH of 5.39 h^{-1} and the high airflow is set at $369\text{ m}^3/h$ which gives a ACH of 10.07 h^{-1} . These air change rates is within the interval given in [5] and should be able to keep the risk of cross infection at a minimum. The inlet temperature is calculated to be 19.1°C in order to keep a temperature inside the room of close to 23°C when the low ACH is used and 20.5°C in order to keep a temperature inside the room of 22.5°C for the high ACH. The reason why there is a difference in the desired room temperature is that it was found out after the first set of measurement that 22.5°C is better since it is closer to the temperature outside the room and the heat loss through the walls would be reduced.

The temperature is also in this setup measured several places in the test room in order to learn what happens inside the test room. Three poles with each ten thermocouples are placed in the room. One between the heads of the manikins, one at the foot end of the beds and one in the corner behind the source manikin. These poles are used to measure the temperature gradients in the room. The temperature of the inlet air is measured in order to keep the room air at the desired temperature. Three thermocouples are located in the exhaust in order to calculate dimensionless temperature profiles of the room. Besides these fixed measuring points there have also been made measurements of the exhalation of the manikins in order to make sure the temperature is within the interval given in section 2.5 on page 22.

The concentration of tracer gas is measured in twelve different locations. The two most obvious locations to measure is the inhalation of the target manikin and the exhaust, as these values are used to calculate the personal exposure index. The concentration is also measured between the manikins at head level, there are six measuring points in different heights. This is done in order to get a concentration gradient close to the exhaust and

see where the highest concentration is. There are also three measuring points behind the source, two of these are located at the height of the mouth of the source in order to see if the exhalation of the source stagnates at this height or near the ceiling where the third is located. The last is placed outside the test room to monitor if there are leakages. The heat load in the room from equipment and manikins can be seen in table 4.3 it gives a total of 249W.

Heat source	Effect [W]
Source manikin	75
Target manikin	75
Air heaters	19
Lamps	80
total	249

Table 4.3: Effect from equipment and manikins inside the test room.

4.5 Cases

Listed in the figure below are all the cases for the measurements performed in the test room in Aalborg. Each case have been given a number so it is easier to refer to them. The most important information about each case is written next to it so it easy to quickly gain knowledge of each case. A small sketch of the setup is to the right so it is easier to imagine the setup. Figure 4.4 show all the cases with standing manikins.

4.5. Cases

Case	ACH [h ⁻¹]	Mutual distances [cm]	Location of inlet	Location of manikins	Miscellaneous	Result [cr/ce]	
1	3.5	0	Near wall	Under inlet	One manikin		
2	3.5	0	Near wall	Under exhaust	One manikin		
3	3.5	35	Center of room	Middle	Two manikins	0.1	
	3.5	50	Center of room	Middle	Two manikins	0.3	
	3.5	100	Center of room	Middle	Two manikins	0.76	
4	3.5	35	Center of room	Right	Two manikins	0.1	
	3.5	50	Center of room	Right	Two manikins	0.4	
	3.5	100	Center of room	Right	Two manikins	0.8	
5	3.5	35	Center of room	Left	Two manikins	0.07	
	3.5	50	Center of room	Left	Two manikins	0.22	
	3.5	100	Center of room	Left	Two manikins	0.9	
6	3.5	35	Near wall	Left	Two manikins	0.24	
	3.5	50	Near wall	Left	Two manikins	0.18	
	3.5	100	Near wall	Left	Two manikins	0.82	
7	3.5	35	Near wall	Right	Two manikins	0.48	
	3.5	50	Near wall	Right	Two manikins	0.91	
	3.5	100	Near wall	Right	Two manikins	0.84	
8	3.5	35	Near wall	Middle	Two manikins	0.17	
	3.5	50	Near wall	Middle	Two manikins	0.55	
	3.5	100	Near wall	Middle	Two manikins	0.85	
9	3.5	35	Near wall	Under exhaust	Two manikins	1.12	
	3.5	50	Near wall	Under exhaust	Two manikins	1.1	
	3.5	100	Near wall	Under exhaust	Two manikins	1.19	

Figure 4.4: Cases 1 to 9.

Figure 4.5 Shows all the cases for the hospital ward.

Case	ACH [h ⁻¹]	Exhaust height [m]	Miscellaneous	Result [c _i /c _e]
10	10.1	1.06	Head under inlet	1.12
11	10.1	2.06	Head under inlet	0.8
12	10.1	1.06	Head under exhaust	1.97
13	10.1	2.06	Head under exhaust	2.71
14	10.1	2.06	Lying on the back	2.41
15	5.4	0.1 and 1.8	Two exhaust openings	1.15
16	10.1	0.1 and 1.8	Two exhaust openings	1.24
17	5.4	0.1	Head under exhaust	1.16
18	10.1	0.1	Head under exhaust	1.21
19	10.1	1.8	Head under exhaust	1.92
20	10.1	1.06 and 2.06	Two exhaust openings	2.95
21	5.4	1.06	Head under exhaust	3.27
22	5.4	2.06	Head under exhaust	3.41
23	5.4	2.35	Head under exhaust	2.32
24	10.1	2.35	Head under exhaust	2.35

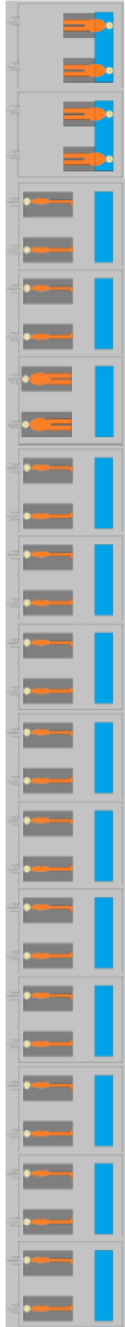


Figure 4.5: Cases 10 to 24.

One standing manikin

Introductory studies consisting of one manikin is carried out in order to study the exhalation flow under different conditions. The exhalation jet is studied by looking at the following:

- Visualization of the exhalation jet
- Measuring the N_2O concentration in the exhalation jet
- Drawing the velocity profile for the exhalation jet

Subsequently two cases are investigated, distinguished by the conditions during each experiments. In one case are the above mentioned parameters investigated while a manikin is placed underneath the inlet diffusers see figure 5.1. In case 2 is the manikin moved away from the inlet diffuser and placed under the return opening instead as seen in figure 5.8 on page 46.

5.1 One manikin under inlet diffuser; Case 1

During this experiment one thermal breathing manikin is located underneath the centerline of one of the two rectangular diffusers, see figure 5.1 and for information of case 1 see table 4.4 on page 39.

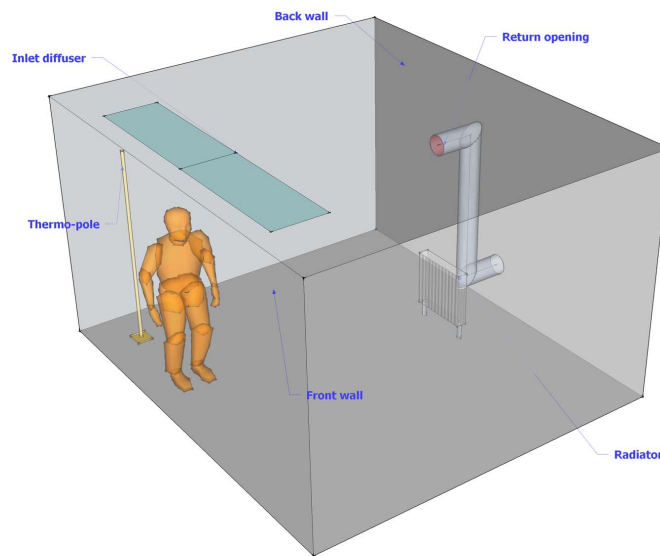


Figure 5.1: Manikin located underneath the inlet diffuser.

Meanwhile the manikin is situated underneath the inlet diffuser it is interesting to investigate whether the inlet air flow affects the velocity and N_2O concentration in the exhalation jet. Along with these parameters it is also convenient to investigate the temperature distribution in the test room in order to determine if stratifications is present.

5.1.1 Temperature distribution

The vertical temperature distribution provides information, about if stratification is developed or not. The presence of stratification means that the room is separated in two zones where the lowest zone contain fresh and clean supply air whereas the upper zone contain considerably higher amounts of contamination. Stratification and its height depend on the ventilation principle in use, air change rate as well as inlet temperature and type of heat source.

The vertical temperature gradient is measured with thermocouples placed at different heights on a pole. This pole is located 15cm behind the manikin. This distance, i.e 15cm , is assumed to be a sufficient distance between the manikin and the measurement points in order to avoid disturbance due to the heat release from the manikin, see figure 5.2 and 5.3.

5.1.2. Velocity of the exhalation jet

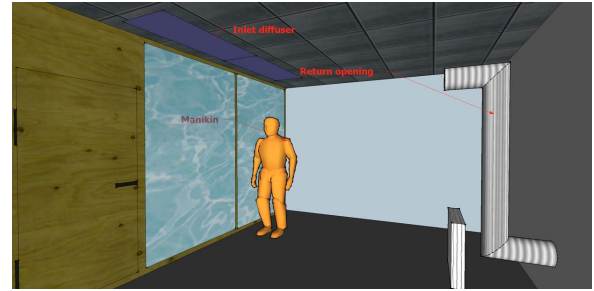
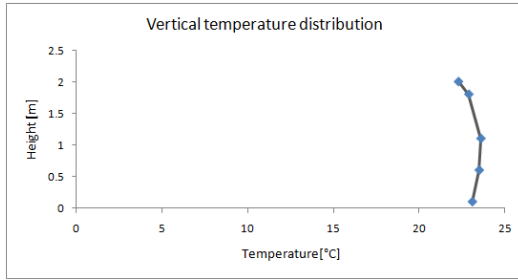


Figure 5.2: Vertical temperature distribution. Figure 5.3: Pole located 15cm behind the manikin.

As illustrated the vertical temperature distribution 15cm behind the manikin seems to be affected by the cold inlet air flow since the pole is located directly underneath the inlet diffuser. From 0.1m up to a height of 1.1m the temperature rises but subsequently at higher points i.e 1.8m and 2m the temperature seems to decline. Since the distance from floor to the manikins mouth is 1.5m, within the height range at which the temperature drops, it is interesting to observe how the exhalation jet develops in this area.

5.1.2 Velocity of the exhalation jet

The velocities of the exhalation jet from the manikin are measured. By using smoke the exhalation jet from the manikin mouth is visualized. This enables to position the hot-sphere anemometers within the core of the exhalation jet, see figure 5.4 and figure 5.5

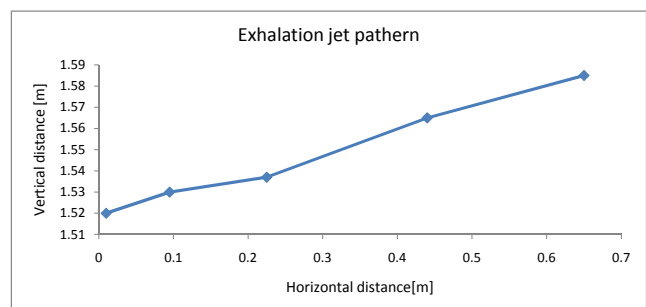
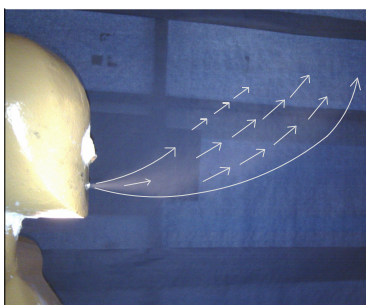


Figure 5.4: Exhalation jet with upward motion. Figure 5.5: Position of maximum velocity in the exhalation air.

Measurements of the exhalation velocities show that the initial maximum velocity, measured 1cm from the mouth, is approximately 4.5m/s whereas the velocity decreases to almost 0.5m/s at a distance of 65cm measured from the mouth. The decrease in maximum exhalation velocity can be seen in figure 5.6.

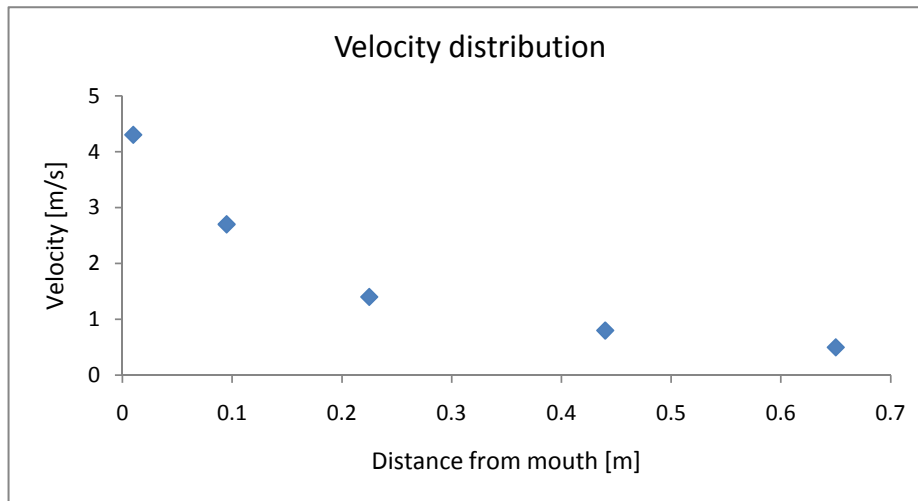


Figure 5.6: Velocities at different distances from the mouth.

This result indicates that although the manikin is situated underneath the air supply diffuser, the exhalation jet has a relatively large penetration depth in a horizontal direction. This may pose a risk of cross infection if the exhalation jet were to be pathogenic and another person is standing in front of the jet.

5.1.3 Concentration in the exhalation jet

N_2O tracer gas is injected into the exhalation of a thermal breathing manikin. By observing the exhalation jet from the mouth of the manikin, tracer gas sampling channels are located within the jet measuring the concentrations as air is expelled. Five sampling channels are used to measure the N_2O concentrations, see figure 5.7.

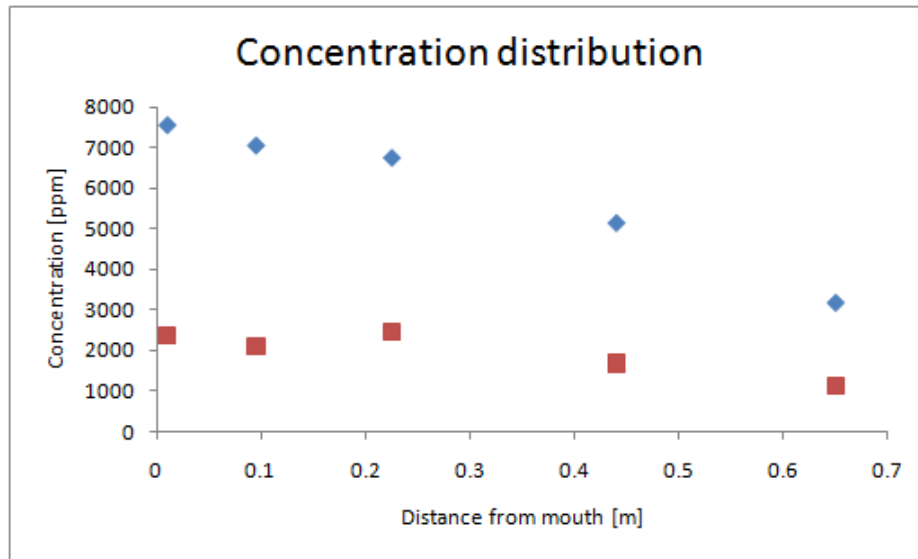


Figure 5.7: N_2O concentration distribution along the exhalation jet. Red; average concentration. Blue; maximum concentration.

The N_2O tracer gas concentration decreases as the measurement distances are increased from the mouth. Since the exhalation jet experiences a diluting process with the ambient air the concentration decreases to 1100ppm almost the half of its initial concentration of 2400ppm . For the average concentration and for the maximum concentration it decreases from 7500ppm to 3200ppm .

5.2 One manikin under the exhaust; Case 2

Regarding the second case see figure 4.4 on page 39, the manikin is moved to another position; underneath the return opening, see figure 5.8, while other parameters are kept unchanged, i.e. air change rate, inlet temperature, location of return opening etc.. It is now interesting to investigate whether there are any significant differences between the previous case 1 and the latter case 2. Hence vertical temperature distribution, concentration distribution and the exhalation jet velocities are measured likewise the previous case.

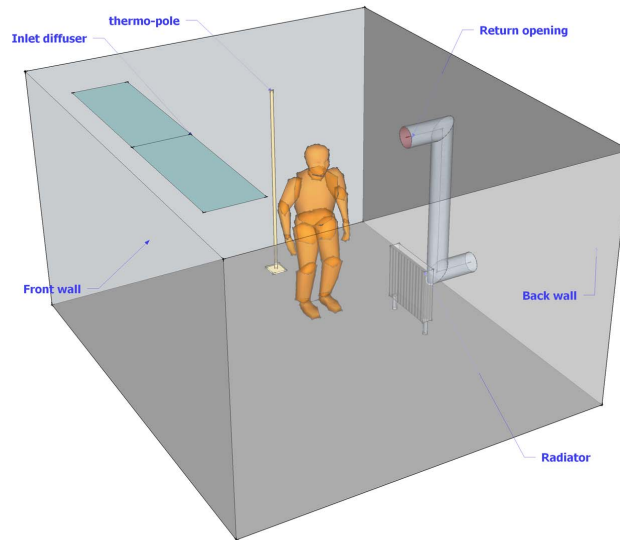


Figure 5.8: Manikin near the return opening

5.2.1 Temperature distribution

The vertical temperature distribution is measured with use of a pole, i.e. measuring temperatures in five heights, as can be seen in figure 5.9. The pole is located 40cm behind the manikin, see figure 5.10

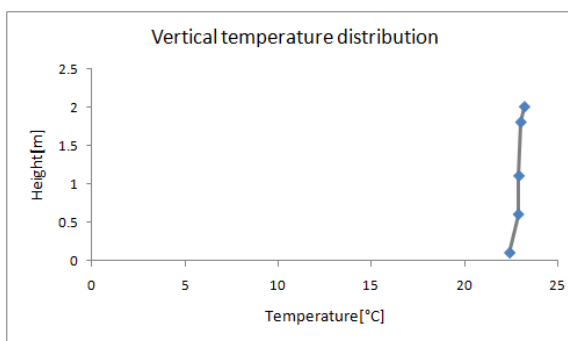


Figure 5.9: Vertical temperature distribution.

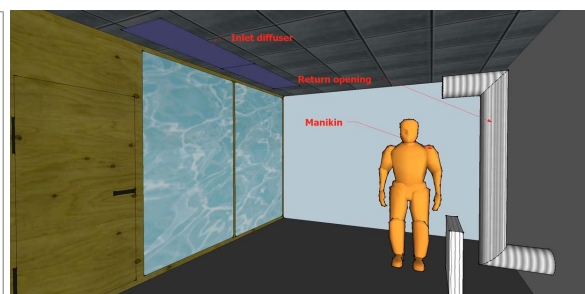


Figure 5.10: Pole located 40cm behind the manikin. Manikin located near exhaust.

In contrast to previous case, the vertical temperature distribution in this case is one of a more typical appearance, slightly indicating the presence of a temperature gradient. Although this gradient is not particularly large, the measurement result indicates that there might be stratification near the ceiling.

5.2.2 Velocity of the exhalation jet

The air flow velocities in the exhalation jet from the manikin mouth are measured. The place where the maximum velocity of the exhalation jet is measured is shown in figure 5.11 it is for both horizontal and vertical direction.

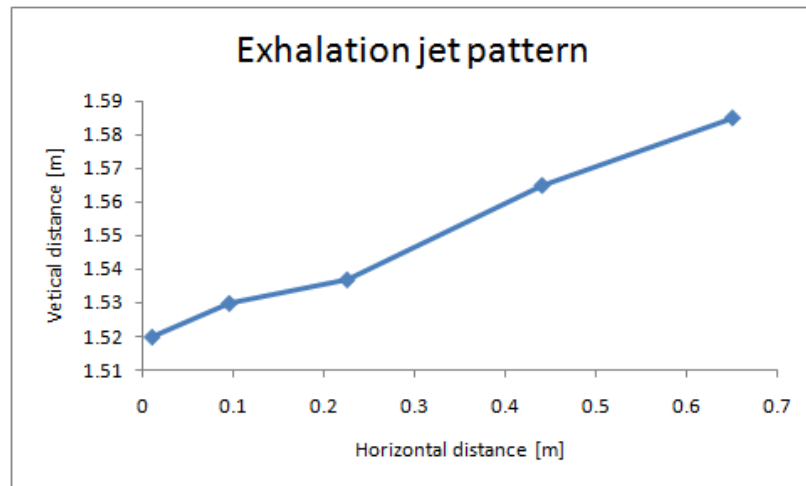


Figure 5.11: Position of maximum velocity in the exhalation air.

The maximum velocities measured in the points shown in figure 5.11 can be seen in figure 5.12.

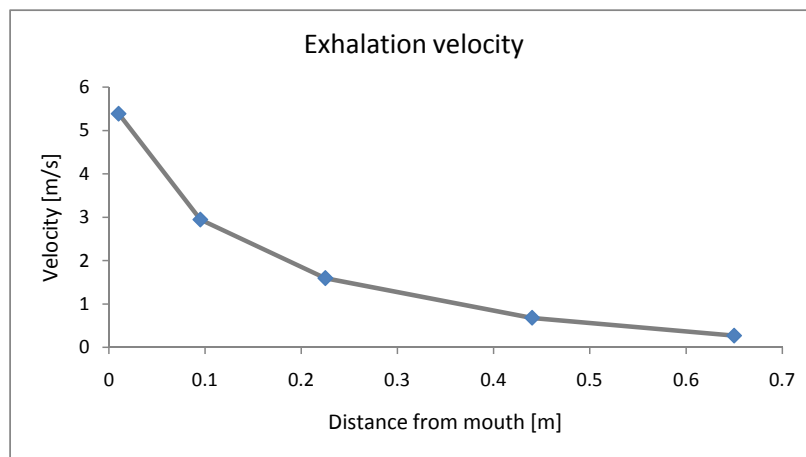


Figure 5.12: Exhalation flow velocities within the jet.

Like for case 1 the velocity decreases a lot when it is measured 65cm from the mouth.

5.2.3 N_2O concentration in the exhalation jet

The N_2O concentration is measured within the exhalation jet, see figure 5.13.

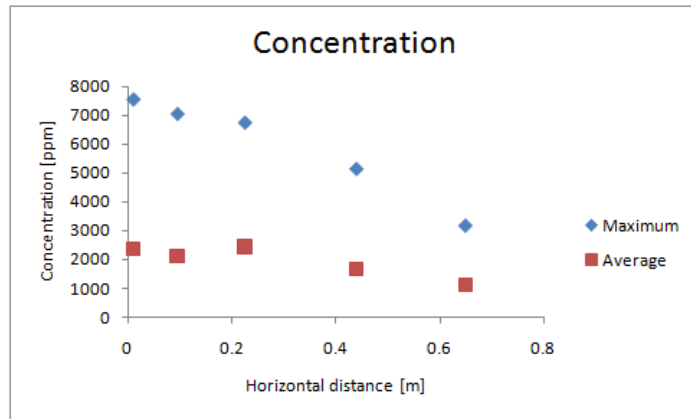


Figure 5.13: N_2O concentration, red; average concentration, blue; maximum concentration.

The average N_2O tracer gas concentration decreases to $555ppm$ $65cm$ from the mouth, from its initial concentration of approximately $3200ppm$ $1cm$ from the mouth and the maximum concentration goes from $9600ppm$ $1cm$ from the mouth to $2400ppm$ $65cm$ from the mouth.

5.3 Discussion

Comparing the exhalation velocities from case 1 and case 2 it is seen that even though the initial velocity is quite different the velocities get close to each other the further away from the mouth the velocity is measured, the velocities can be seen in figure 5.14.

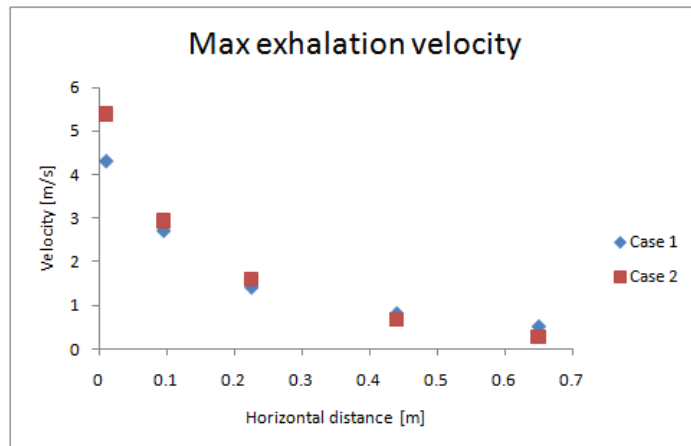


Figure 5.14: Comparison of the two exhalation jets.

Although the inlet diffuser is above the manikin in case 1 the exhalation jet is not affected at all. A possible explanation could be that that the high velocity of the exhalation jet is able to completely escape the thermal plume of the manikin and that the the flow from the inlet diffuser is on able to affect the jet. Based on CFD predictions for a laying manikin is

it calculated that the exhalation jet needs velocity of 2.7 m/s in order to completely escape the boundary layer of a laying person [10].

When comparing the velocities of the exhalation jet it is seen that they were almost identical but when looking at the concentration of tracer gas in the exhalation jet there are a big difference whether it is case 1 or case 2. The relative concentrations of the exhalation jet can be seen in figure 5.15. C_0 is chosen to be the concentration of gas of the measuring point closest to the mouth and c is the concentration in the point of interest.

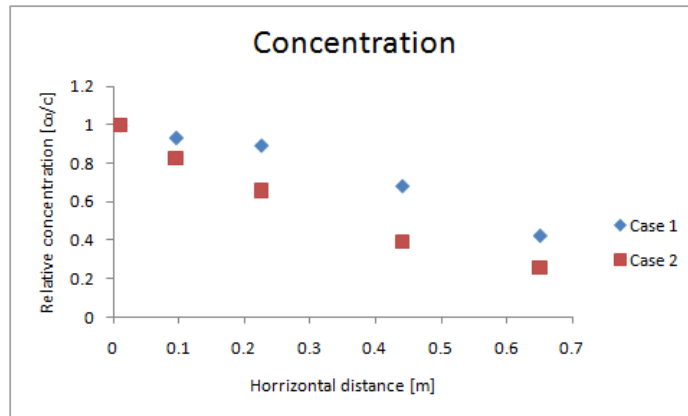


Figure 5.15: Relative concentration of tracer gas in the exhalation jet.

From figure 5.15 it can be seen that a high concentration of tracer gas is conserved for longer time in case 1 than case 2. A reason why this is could be because the points for maximum velocity were only found for case 1 and the same point were then used when measuring for case 2. It can not be expected that the exhalation flow behaves the same way in two different locations. When located under the inlet the exhalation jet it could be expected that the exhalation jet does not move as much upward due to the downward flow of the inlet as when it is very close to as powerful a heat source as the radiator. This means that using the same points for the two cases may result in maximum values for case 1 but not for case 2. For case two the error will increase with the distance if the jet travels as described.

5.4 Conclusion

Studies are conducted with use of one thermal breathing manikin positioned two different places within the test room, labeled as case 1 and case 2 see figure 4.4 on page 39. Measurements of the vertical temperature distributions imply presence of a small temperature gradient in case 1 at the lowest heights. At higher points the temperatures are possibly affected by the inlet air flow, see figure 5.16.

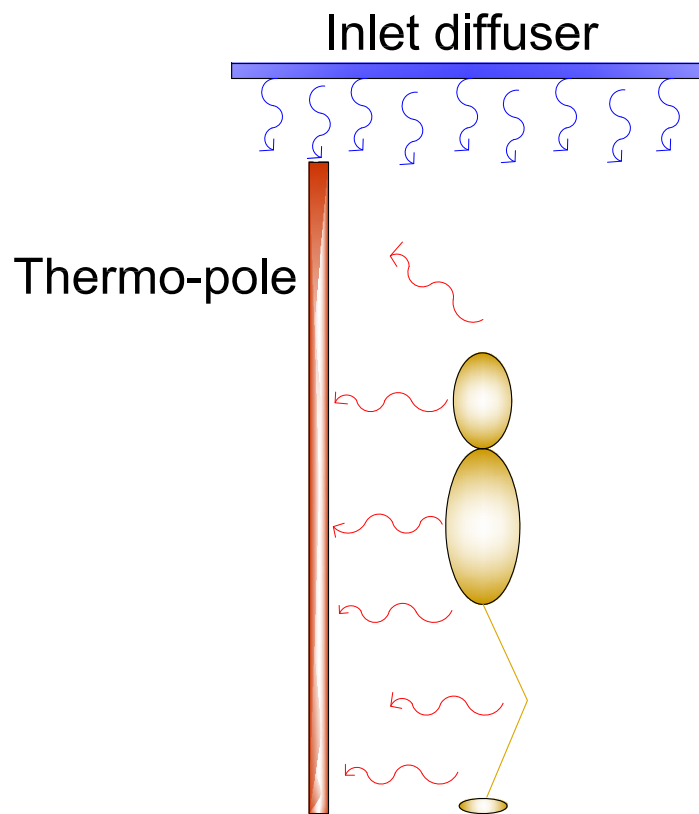


Figure 5.16: Possible scenario.

In case 2, since the manikin is moved away from the inlet diffuser, a small gradient is measured. Tracergas concentrations from the exhalation jet, measured underneath the supply air diffuser has the same trend to decrease likewise the tracergas concentration measured under the return openings. The same conclusion is valid for the velocity measurements on the exhalation jet. Besides the vertical temperature distributions, results of both studies are coincident events.

Micro environment between two standing persons

Experiments with two thermal breathing manikins are conducted and the risk of cross infection is showed by analyzing the micro environment. One manikin is labeled as the sick person, the source, dispersing tracergas into the environment through respiration. The other thermal breathing manikin, the target, is exposed to inhale what is exhaled from the source. The importance of distance between persons is showed simulating situations when two persons are at short conversation distances or any other situation involving two people close to each other. The experiments involve three locations in general and in two cases the manikins are always located underneath the inlet diffuser, see figures 6.1, 6.2 and 6.3 below. For information on all the cases see figure 4.4 on page 39

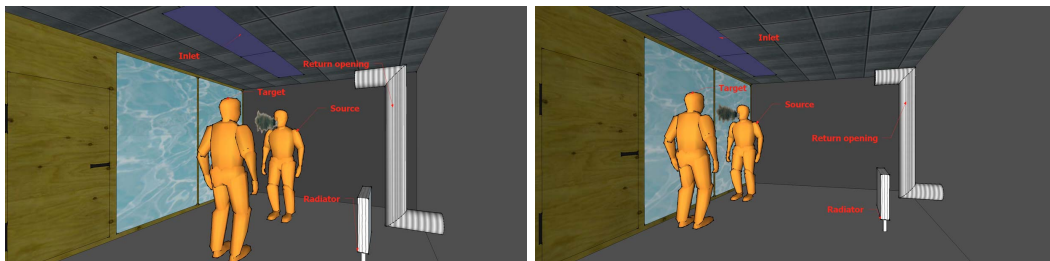


Figure 6.1: Inlet diffuser located in the middle of ceiling, cases 3, 4 and 5.

Figure 6.2: Inlet diffuser located near the front wall, cases 6, 7 and 8.

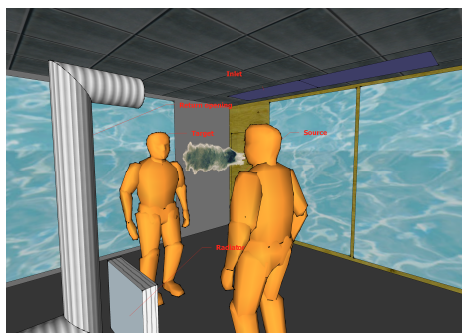


Figure 6.3: Inlet diffuser located near the front wall and manikins moved near the return opening at the back wall, case 9.

In three cases the inlet diffuser and manikins is located close to the front wall as seen in figure 6.2 and in another three cases the inlet diffuser and manikins is located in the middle of the ceiling as seen in figure 6.1. In the last case the inlet diffuser is located close to the front wall and the manikins are located under the exhaust at the back wall as shown in figure 6.3. The purpose of relocating the inlet diffuser during the experiments is to clarify whether it has any influence on the tracer gas distribution which is obtained in the micro environment developed by the manikins. The conditions investigated within the test room is given below:

- Temperature distributions
- N_2O concentration distributions
- Velocities above the manikin

A detailed description of the set up of the test room for these measurements can be seen in chapter 4 on page 34 these include where thermocouples and gas monitor channels are located, what the ACH are and what the effect released by manikins and equipment are.

6.1 Vertical temperature distribution

The vertical dimensionless temperature distribution can be seen in figure 6.4.

6.1. Vertical temperature distribution

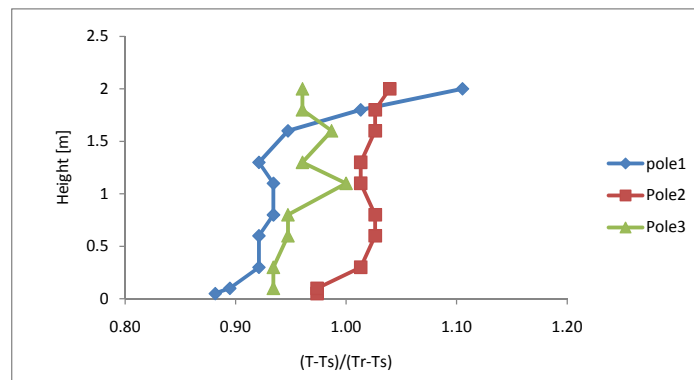


Figure 6.4: Pole 1; in corner, pole 2; behind source, pole 3; behind target.

This graph is valid for case 3 with a distance of 110cm between the manikins with the inlet diffuser in the middle of the room and the the manikins located in the center of the diffuser as seen in figure 6.5.

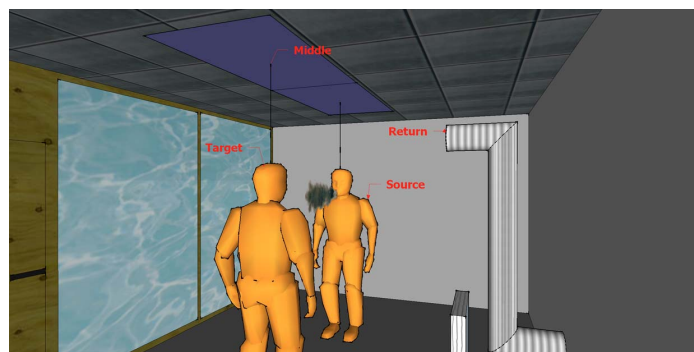


Figure 6.5: Illustration of case 3.

Pole 1, designated with blue line in figure 6.4 is placed at the corner of the test room during the experiments. Temperature measurements in this particular location show a clear temperature gradient, although not large. Furthermore this zone must be nearly unaffected by the cold inlet air flow although cooler inlet air is entrained. The situation is sketched in figure 6.6

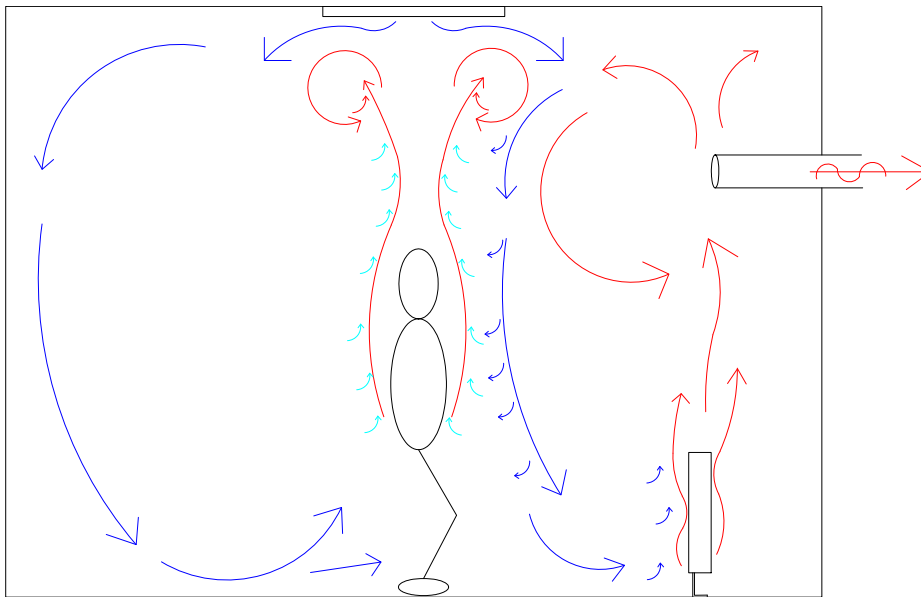


Figure 6.6: Possible air flow pattern. This pattern is dominated by the thermal plumes and convective forces from sources in the test room.

If looked upon the vertical temperature gradient for all cases for each pole it can be seen that there is a clear tendency that they follow the same pattern. In figure 6.7 is the dimensionless vertical temperature distribution for pole 1 shown for one distance for each case. It is located in the corner of the room as shown in chapter 4 on page 34.

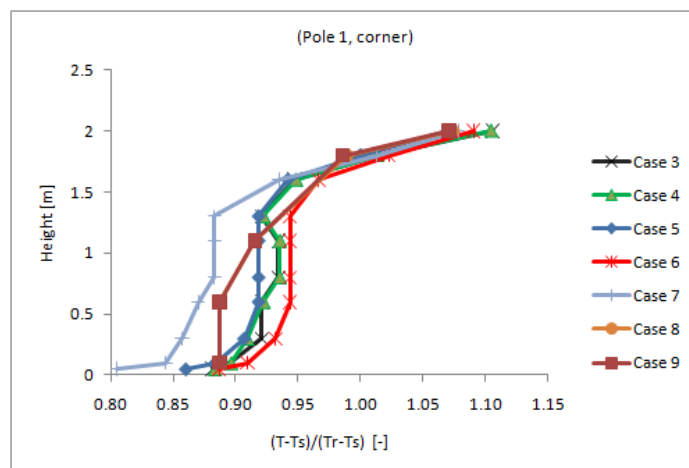


Figure 6.7: Pole located at the corner of the test room in cases 3 to 9.

It can be seen in figure 6.7 that there is a temperature gradient in the corner although it is not large. The pole located in the corner is the only one that is not influenced directly by the thermal streams or radiation from the inlet diffuser, manikins or radiator in the room. Figures 6.8 and 6.9 show the dimensionless vertical temperature of poles 2 and 3. The graphs show that the air is very well mixed in these parts of the room. That it is well mixed can

6.1. Vertical temperature distribution

be seen because the the dimensionless temperature do not vary that much and there are a lot of fluctuations in the graph.

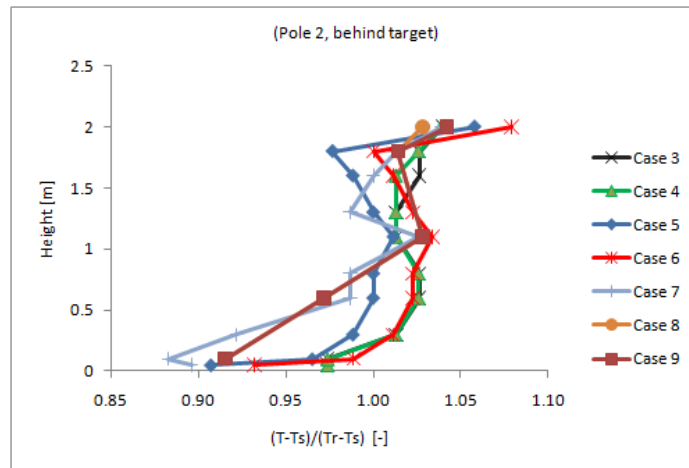


Figure 6.8: Pole 2 located behind the target manikin. Point temperatures slightly higher than those at return opening.

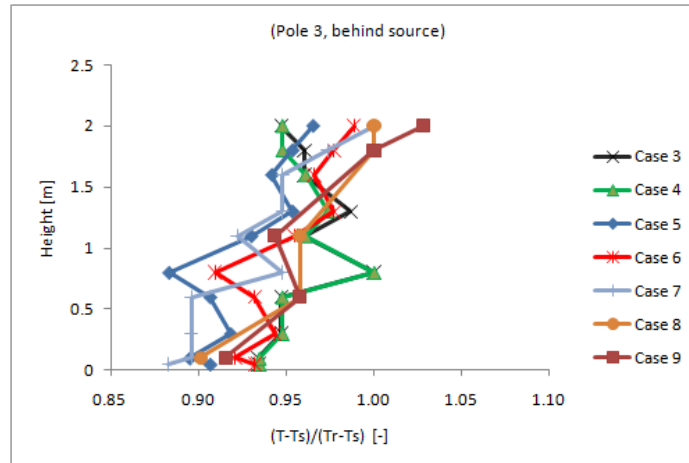


Figure 6.9: Pole 3 located behind the source manikin. Valid for all seven cases. Notice the temperature fluctuations.

The deviation in pole 2 for cases 3 and 5 at 1.8m are notable. Two possible situations could enroll since the deviation is so distinct. Either there is an error with regard to the equipment used to measure the temperatures or the thermal plume from the manikins could accumulate near the ceiling, between the front wall and the downward moving inlet air flow, at the same height the temperatures are measured, see figure 6.6.

6.2 Air velocity

The air velocities are measured at two height above the manikins 25cm and 35cm. It is measured to see whether the flow above the manikins are upward or downward. Since the hot sphere anemometers used to measure the air velocity are unable to tell the direction of a flow smoke visualization is used at the measuring points. The following four figures show velocity measurements for case 8 where the inlet diffuser is located close to the wall and the manikins are located in the middle. Results are only shown for one case as all the measurements show the same tendency.

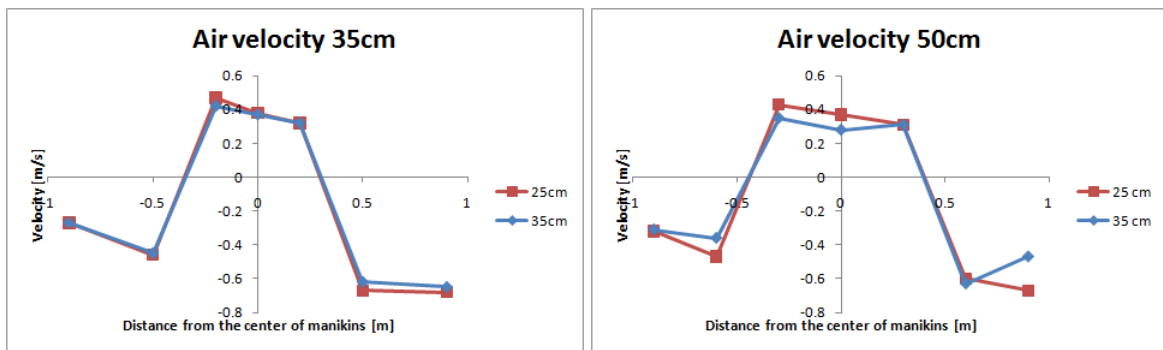


Figure 6.10: Air velocities 25 and 35cm above the manikins, for a distance between the the manikins, for a distance between the manikins of 35cm.

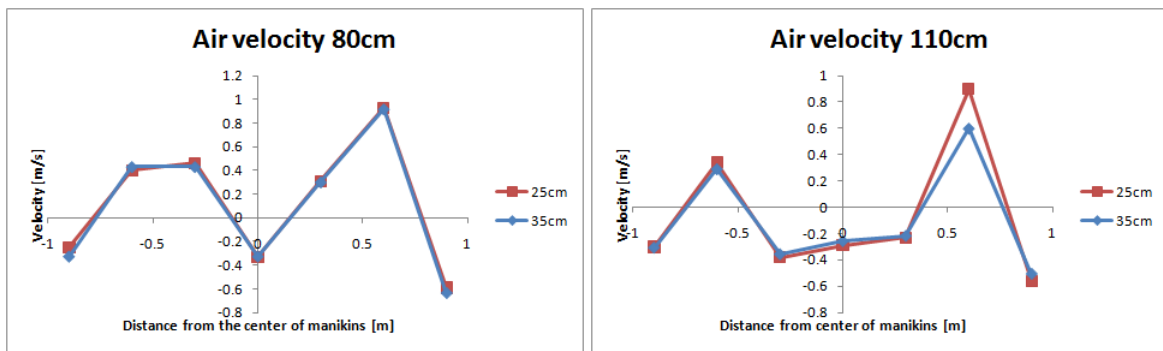


Figure 6.12: Air velocities 25 and 35cm above the manikins, for a distance between the the manikins, for a distance between the manikins of 80cm.

From the velocity measurements shown in figures 6.10, 6.11, 6.12 and 6.13 it can be seen that the velocities at the measuring points 25cm and 35cm are almost the same. More interesting is it that when the manikins stands close to each other their thermal plumes unite to make one strong plume. This phenomenon is clearly shown in figures 6.10 and 6.11 where the point in the middle of the manikins, the origo, has an upward flow. Figures 6.12 and 6.13 shows the velocities when there is a distance of 80cm and 110cm between the manikins now are the thermal plumes no longer united and air can move between the manikins. It can be

seen from the figures that when the plumes of the manikins are not united the velocities are much higher than when they unite. This is because when the plumes unite the flow is over a larger area and then the velocity drop.

6.3 Concentration

The vertical concentration distribution is presented in this section. These observations are regarding cases 3 to 9 as described in figure 4.4 on page 39. Three channels monitoring the N_2O concentrations are attached on a pole located in the test room. The concentration measurement at the return opening is used as the fourth measuring point, at a height of 1.8m above the floor. In figure 6.14 is the vertical concentration distribution illustrated.

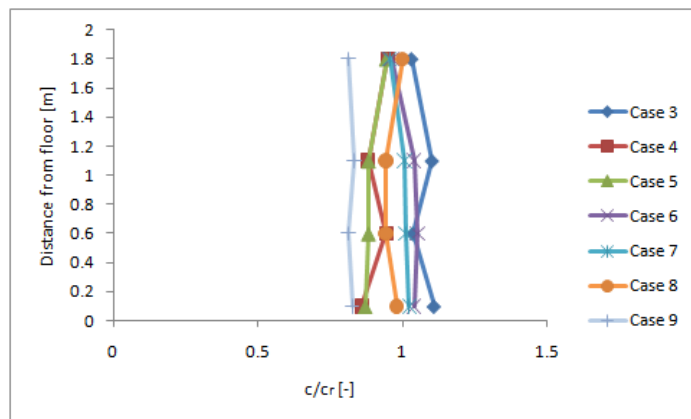


Figure 6.14: Vertical concentration distribution for cases 3-9 with a communal distance of 35cm.

Like the vertical temperature distribution, there are no clear vertical concentration gradients. Since the pole is located at a corner of the test room it only provides information regarding the concentration distribution in the macro-environment, not in the micro-environment. According to the vertical concentration distribution it is acknowledged that no stratification is present, hence the air must be fully mixed. In the following graph, see figure 6.15, the differences between the concentration measurements are illustrated. It can be seen that the concentrations measured at the source body are higher than those measured at the pole. This observation provides information about the conditions within the micro-environment and confirms that the micro-environment is developed. Part of N_2O expelled by the source manikin is captured within the micro-environment resulting a higher concentration.

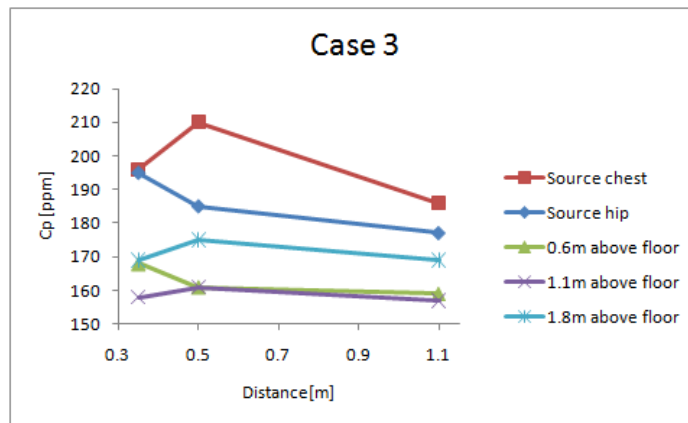


Figure 6.15: N_2O concentration measurements at the micro- and macroenvironment.

There are no accumulation of contaminants in the micro-environment since entrainment partly ensures removal of the contaminants. But the high concentrations in the micro-environment, compared with the macro-environment has an influence on the air quality experienced by the target manikin.

6.4 Personal exposure index

A high air quality is essential for the well being of occupants in any enclosed environment. Nevertheless in a hospital ward where the need for effective ventilation is of outermost importance not only to ensure thermal comfort but more important the removal of any airborne infections or diseases. A useful parameter used to quantify the air quality, experienced by the occupants, and thereby clarify the risk of cross infection is the personal exposure index which is defined in section 2.3.1 on page 19. In the following the personal exposure index is compared with the ventilation index see figure 6.16.

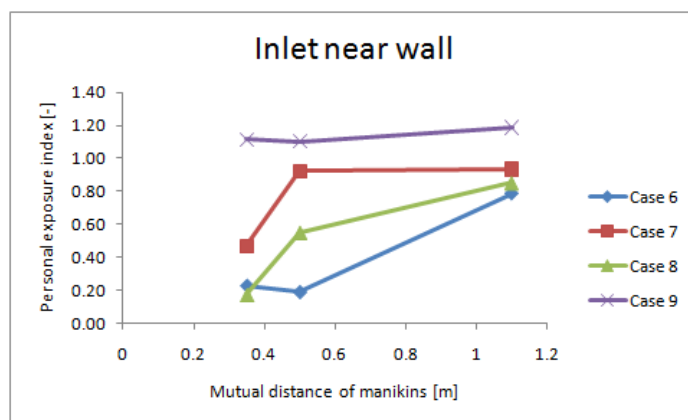


Figure 6.16: Inlet diffuser located Near the wall.

Offhandedly the personal exposure in case 7 seems to be higher than any other cases with a mutual distance of 50cm. Through several thought considerations it is concluded that there is a reasonable explanation for this particular type of deviation. The exhalation and inhalation of source and target manikin respectively must have occurred simultaneously. This involve tracer gas sampling at the instant the source exhales thus leading to high concentration measurements. As the distance between the manikins increase the personal exposure index decreases analogously. By recalling the observations made during the studies in case 1 and 2, the profile and penetration length of the exhalation jet is viewed once again. Only this time with two manikins. Additionally, the thermal plume from both manikins also play a vital role on the personal exposure. Obviously these two parameters are rationally linked together see figure 6.17

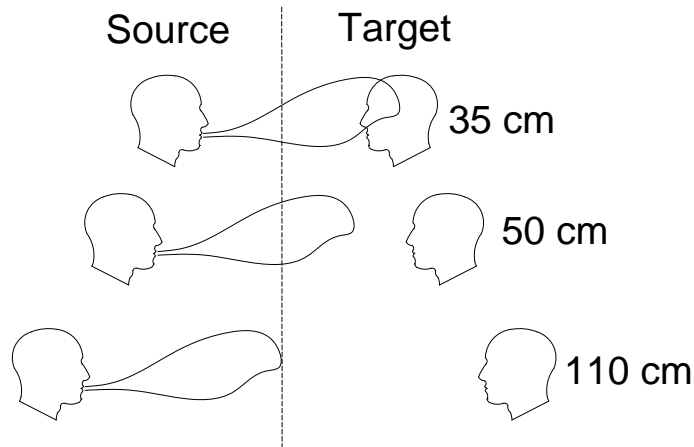


Figure 6.17: The communal distance influence on exposure.

Although both manikins are located underneath the inlet diffuser, the combined thermal plumes from both manikins seems to repel the downward inlet flow. Hence within the micro environment developed by two persons, the conditions are distinct from that in the macro environment. But as the distance between the manikins are increased the strength of the combined thermal plumes decreases analogously and at some point they stop to work as one plume but two plumes from two manikins. This give rise to a gap between the manikins in which the supply air is able to replenish. During this scenario the target manikin is no longer directly exposed to the contaminants expelled by the source, confer figure 6.16. Figure 6.18 illustrates the personal exposure indexes for the other location of the inlet diffuser.

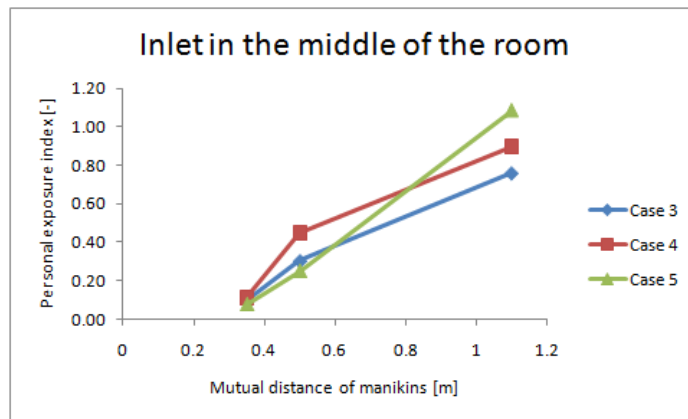


Figure 6.18: Inlet diffuser located in the middle of test room.

An overall view on the personal exposure index for the different cases indicate that there exists a declining trend. The further the manikins are moved from each other the better the personal exposure index and the smaller the chance of cross infection.

Results for the hospital ward

In this part of the report are the results from the hospital set up discussed. It will be looked upon the influence of the ACH, the location of the exhaust, the location of the manikins in the room and the performance of a high and low exhaust at the same time compared to only a high or low exhaust. Listed in figure 4.5 on page 40 is all the measurements made with two manikins in beds in the figure is most important information about each case. It is not looked upon the influence of the distance between the beds as it does not have an influence on the personal exposure index as long as the distance between the beds is large enough for a HCW to stand between the beds and do his/her job [21].

7.1 Where should the beds be located

It has to be investigated where the best location for the beds are. Is it with the heads of the manikins located under the inlet or is it with their heads located under the exhaust. It is natural to assume that the best location for the patients would be with their heads under the inlet as they would then be supplied with fresh air directly to the breathing zone but measurements in section 6.3 on page 57 with two standing manikins under the inlet shows that there is a very high risk of cross infection. This high risk of cross infection could be because of the upward thermal plume from the body destroys the downward jet from the inlet. The lying manikins do not have as strong a upward thermal plume as the standing manikins as the thermal plume is spread over a larger area and this gives it a lower velocity. The lower velocity of the plume may make it possible for the inlet air to penetrate into the breathing zone of the manikins. Figure 7.1 shows the personal exposure index of the manikins with their heads placed under the inlet and with the manikins heads placed under the exhaust. The ACH is approximately $10 h^{-1}$ with the exhaust located at $1.06m$ and $2.06m$ above the floor for both set ups. Figure 7.1 shows the personal exposure index dependent on the position of the manikins, the blue line is for when the manikins heads are under the inlet and the red line for when the heads are under the exhaust.

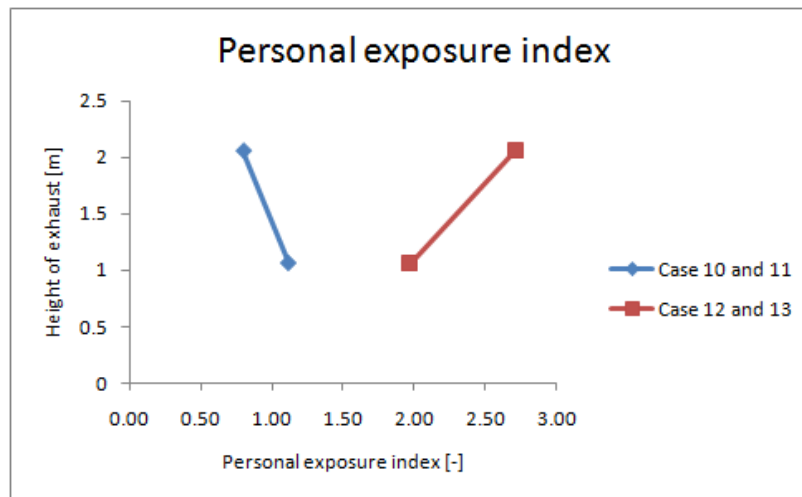


Figure 7.1: Personal exposure index when the manikins heads are located under the inlet and under the exhaust.

From figure 7.1 it is clearly seen that the best location of the manikins is under the exhaust as this gives the highest personal exposure indexes. This means that for the rest of the measurements are the manikins located with their heads under the exhaust. It is often mentioned that the beds should be located away from the inlet so the HCW's are in the cleanest part of the ward when they enter. This is probably still the cleanest zone as the contaminant source is moved and most of the contaminants are removed close to the source so it does not move to that zone.

7.2 Influence of position in the beds

In this section is it looked upon the influence of the position in the beds i.e. should the manikins face the ceiling or should they face each other. Previous studies with manikins in bed show that the results that gives the highest personal exposure indexes are when the manikins are facing the ceiling and the lowest are when the faces of the manikins are facing each other [18]. Because studies have already been made in this field there have not been made many measurements on this subject. Figure 7.2 show that the personal exposure indexes for the two cases are almost the same.

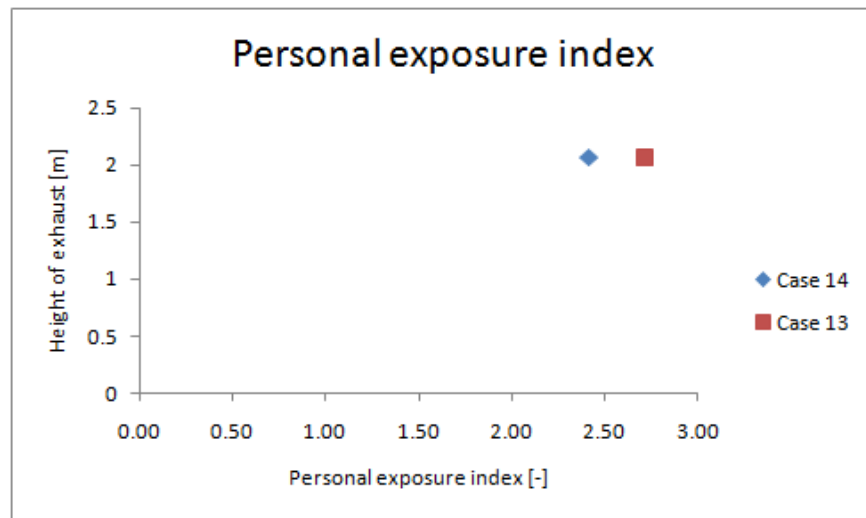


Figure 7.2: Personal exposure index when the manikins heads are facing each other and the ceiling with 10 ACH.

Because the two personal exposure indexes are almost the same and earlier studies showed that the lowest personal exposure indexes are reached when the manikins face each other this is chosen through the rest of the set ups.

7.3 Two exhaust heights compared to one

As described earlier in chapter 1 on page 15 the CDC recommends that the rooms exhaust openings should be located in a way where one is located near the ceiling and one near the floor. This is recommended because the low opening should remove the big droplets and the high opening should remove the airborne droplet nuclei which is caught in the updraft of the patients and equipment plumes or because of the exhalation is warmer than the surroundings. Figure 7.3 shows the personal exposure index when using two exhaust openings at the same time compared to one exhaust opening at a time and with two different ACH. The openings are located 0.1m and 1.8m above the floor. The height of the exhaust with two openings is entered in the graph with a height of 0.95m as it is the average of the heights of the openings.

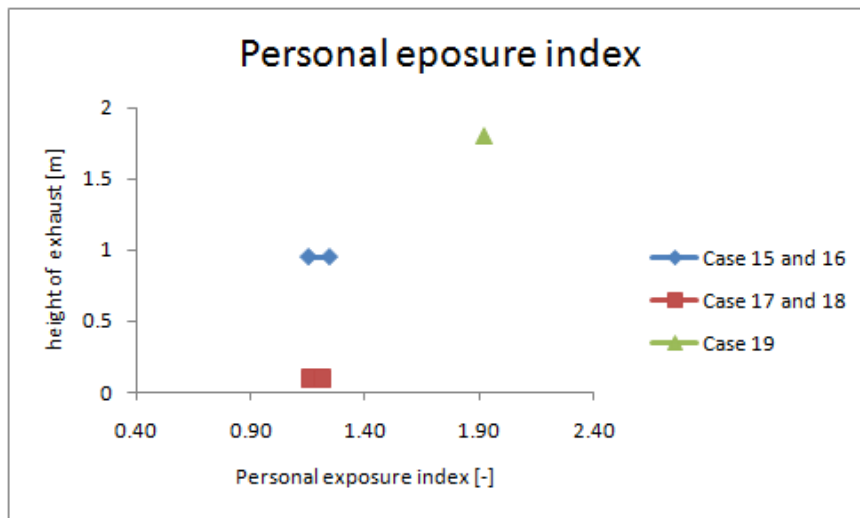


Figure 7.3: The points furthest to the left are for 5 ACH and the points furthest to the right are for 10 ACH.

Figure 7.3 shows that a high and low exhaust opening is not that efficient compared to just one located high in the room and that it gives as bad results as one located just above the floor.

Figure 7.4 shows the personal exposure index when using two exhaust openings at the same time compared to one exhaust opening at a time and with two different ACH. The openings are located $1.06m$ and $2.06m$ above the floor. The height of the exhaust with two openings is entered in the graph with a height of $1.56m$ as it is the average of the heights of the openings.



Figure 7.4: The points furthest to the left are for 5 ACH and the points furthest to the right are for 10 ACH.

Like figure 7.3, figure 7.4 shows that only one exhaust opening is better than two and in this case both the opening at $1.06m$ and the one at $2.06m$ gives better personal exposure indexes

than the solution that have openings at both 1.06m and 2,06m.

These results show that when it comes to removing droplet nuclei it is not the best solution to have two openings, one high and one low, as suggested in [5] but those guidelines are also intended to remove large droplets as well as airborne droplet nuclei.

Earlier work show that exhaust openings located high in the room is better than a high and low located opening. The work suggests that the large particles does not travel very far from the source and that a low exhaust opening won't be able to remove them but it would be better to clean the surfaces than to try and remove large particles by ventilation [11].

7.4 Influence of air changes on personal exposure index

It is interesting to look at how the ACH influences the personal exposure index, because a higher ACH costs more money and if a low ACH gives the same results or better then it might be worth considering. From equation 7.1 it is clear that a higher ACH gives a lower concentration in the inhalation of the target manikin and that gives a reduced chance of cross infection [16].

$$c_{exp} = \frac{S}{q_0 \cdot \varepsilon_p} \quad (7.1)$$

Where:

c_{exp}	Inhaled concentration of target [ppm/m^3]
S	Exhaled concentration of the source [ppm/m^3]
q_0	Air flow rate supplied to the room [m^3/s]
ε_p	Ventilation index [-]

Equation 7.1 shows that a high ACH gives a low concentration of pollutants for the target but also that the ventilation index plays a very important role in the concentration inhaled by the target. In table 7.1 is the ventilation indexes for when the exhaust is located at 1.06m and 2.06m for 5 ACH and 10 ACH listed. In this case the ventilation index is the same as the personal exposure index.

Case	Ventilation index
21	3.27
22	3.41
12	1.97
13	2.71

Table 7.1: Listed in the table is the ventilation indexes for two different air changes and exhaust heights.

Table 7.1 shows much higher ventilation indexes with the low air changes compared to the ones with higher air changes. But it also shows that they are not high enough to compensate

for the reduced air flow, then they should have been twice that of 10 ACH.

Figure 7.5 shows the personal exposure indexes for two different exhaust heights and two different ACH.

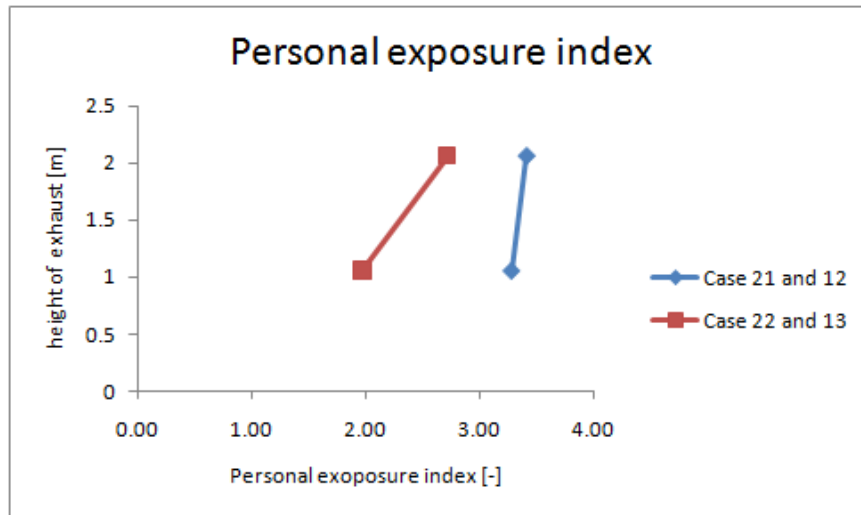


Figure 7.5: Personal exposures index at different heights dependent on air changes.

It is clear to see that for these two different heights of exhaust openings the highest personal exposure index is reached with the lowest ACH of $5 h^{-1}$. The reason why the personal exposure index decreases with an increasing ACH is that the ventilation principle becomes more like mixing ventilation. The reason why it becomes more like a mixing ventilation system is that the high velocities from the inlet diffuser creates more turbulence and due to that, entrains more of the air of the room into the jet. In order for this type of ventilation to work the currents in the room has to be driven by the heat sources such as the manikins and equipment and the faster air velocities from the inlet the less influence from the heat plumes.

Even though the personal exposure may be larger for the low ACH this does necessarily mean that the concentrations inhaled by the target are the lowest when using the low ACH of $5 h^{-1}$ compared to 10 ACH as the personal exposure index is dependent on the inhaled concentration and the concentration of the exhaust air as seen in 2.3.1 on page 19. It only means that the ratio between the concentration in the exhaust and the inhaled air is larger.

7.5 Influence of the exhaust height

Earlier studies suggest that the height of the exhaust might influence the personal exposure index [18]. The inlet diffuser in [18] is not the same as used in this project but there are similarities. Both diffusers are low impulse diffusers and they both provide a downward ventilation, but there are also discrepancies such as shape, surface area and location in the room, which can result in different flows in the room.

7.5. Influence of the exhaust height

Figure 7.6 shows the personal exposure indexes dependent on the exhaust height for two different air changes.



Figure 7.6: Personal exposure index dependent on the height of the exhaust and the ACH.

The figure shows that the location of the exhaust opening plays an important role in obtaining a high personal exposure index. The figure shows that an exhaust opening in this particular set up should be located relatively high and that an opening near the floor is the worst solution. These results are in good accordance with the assumptions on the flow described in section 3.4 on page 32.

The good result obtained in the measurement can seem a bit strange since it seems as if the air inside the room is well mixed. Figure 7.7 shows pole 2 which is located behind the source manikin. It is placed far enough behind the manikin so the heat release from it does not affect the temperature measurements.

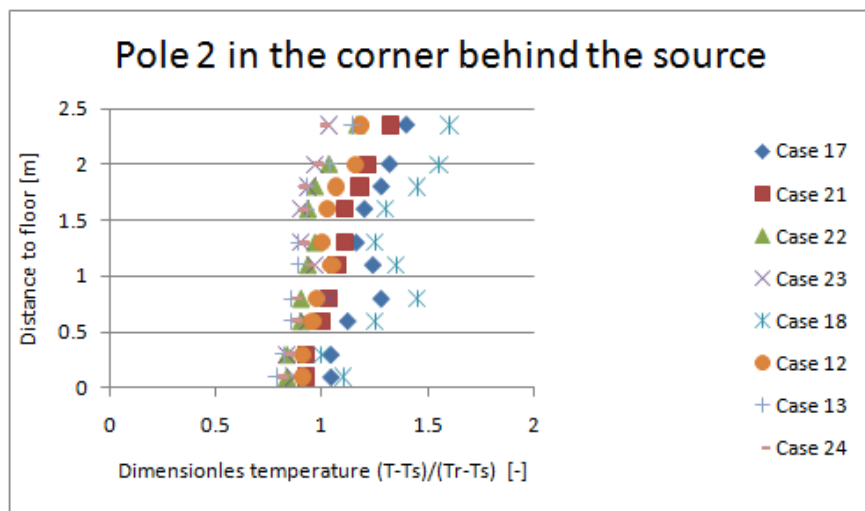


Figure 7.7: Dimensionless temperature in the macro environment.

If looking at the dimensionless temperatures in the room there is not a large temperature gradient which indicate that the air is very well mixed in the macro environment. If looking at figure 7.8 it shows the dimensionless temperature between the manikins.

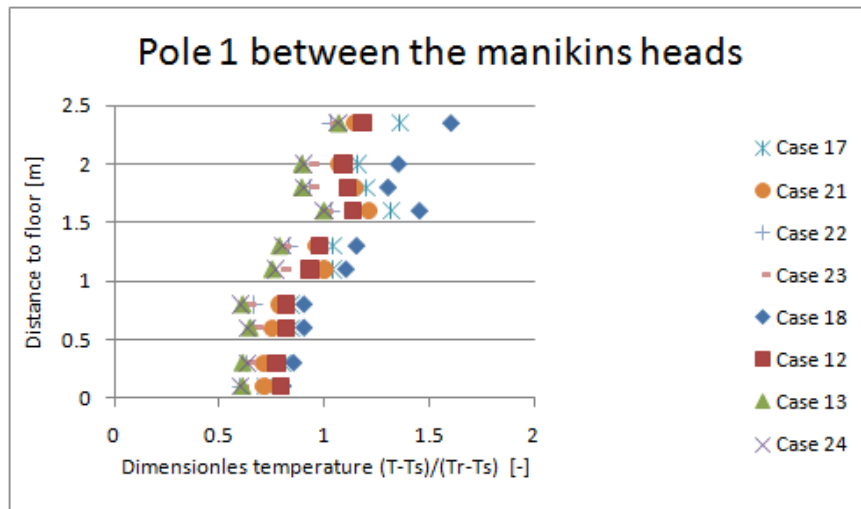


Figure 7.8: Dimensionless temperature in the micro environment between the manikins.

It shows that the gradient is generally larger than in the macro environment. This is because the air is heated by the manikin and moves upward in this part of the room. The warm exhalation jet is probably also a important factor in the temperature gradient since it is much warmer than the ambient air.

The dimensionless temperatures indicate that it is important were the exhaust openings are located, not only the height, but where in the room as well. If the exhaust openings are located too far away from the manikins, in the macro environment, it probably won't remove as much contaminant and the general concentration in the room will rise.

7.6 Conclusion

The measurements done for the hospital ward part of the report show that the location of heat source, inlet, exhaust and ACH all play a vital part in the personal exposure index. It was shown that when the manikins were located under the inlet that the personal exposure index were low compared to when they are under the exhaust. This is probably because the manikins are no longer supplied with the same amount of fresh air by their thermal plume. The flow inside the room is also completely changed as the manikins are the heat sources that partly creates the currents inside the room.

It was also investigated what influence the ACH of the room had. The measurements show that the ACH has a fairly big influence on the personal exposure index. This is because if the flow to the room is increased those currents are the dominant in the room and they create something similar to a mixing principle. If the thermal plumes of the manikins and are the dominant ones the entrainment of contaminated air to the inlet air is smaller and the air supplied to the manikins is going to be cleaner thereby increasing th personal exposure index.

Finally is the exhaust heights examined. It has been look upon the influence of having two openings in the same height and four openings in two different heights. If first considering four openings in two different height it showed that this was not a good solution for removing airborne contaminants. So for this to be considered it would have to be able to very efficiently remove large droplets. The two exhausts at the same height showed some interesting results. It showed that the location of the exhaust plays a big role when it comes to the personal exposure index. It show not surprisingly that at floor level were the worst solution. This is as expected as the air flowing there is very clean, what is surprising is that it still gives a personal exposure index above 1. meaning the air in the exhaust is still more polluted than the air the manikin breaths. Another surprising result is that the best personal exposure index is not achieved with the exhaust located just below the ceiling, as could have been expected that the warm plume from the manikin would accumulate contaminants just below the ceiling. Instead are the highest personal exposure index measured located at a height close of 2.06 *m* above the floor level. The results show that for this set up is vertical ventilation a very good solution since it gives very good result, but these measurements are done under steady state conditions, if there is movement inside the room the personal exposure will probably drop since the turbulence is increased.

Part II

Computational fluid dynamics

Computational Fluid Dynamic

CFD simulations of the current hospital setting are made for different locations of return openings. In the following chapter, is the simulations done for these setups presented. The simulations presented here contain a description of the temperature distribution, concentration distribution as well as the personal exposure index.

8.1 Introduction

The problem is defined as a hospital ward setting in which the flow patterns are dominated by the supply air flows from a ceiling mounted rectangular textile diffuser and the plumes above the persons in the room. Return openings are located at two different heights close to the bed bounded computer simulated persons (CSP). The geometry modeling and grid generation of the hospital setting are both defined using Gambit with a mix of structured hexahedral and unstructured tetrahedral cells. CSPs are defined both as heat and contamination sources. The entire simulated domain can be viewed in figure 8.1.

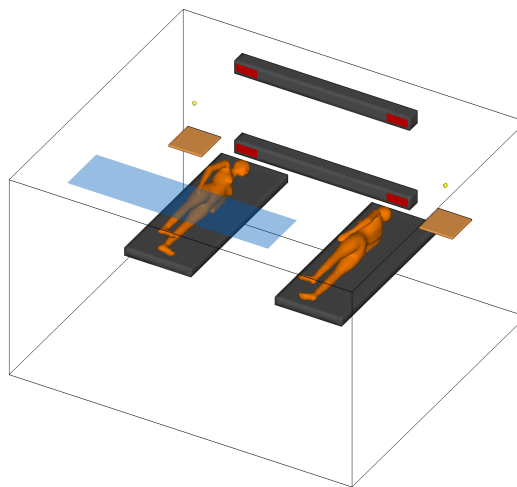


Figure 8.1: .

A commercial CFD code Fluent is used along RNG K- ϵ model with standard wall treatment. Furthermore a mixture template is selected as well in order to include contaminant transport. Convergence is accounted by monitoring the residuals. At the beginning the simulations are initialized by choosing default under-relaxation factors with standard pressure treatment and first order discretization scheme. Subsequently after 1000 iterations the default values are rearranged and switched to user defined values i.e. lower under-relaxation factors, PRESTO! pressure algorithm and second order upwind discretization scheme. When good convergence is reached the iterations are stopped and the results are analyzed using a post-processing software called Tecplot10. Tecplot10 is data visualization and technical plotting software with 2- and 3-D capabilities enabling to visualize data from analyses, simulations and experiments. The following simulations of the hospital wards setting are visualized using this software.

Five cases from the experiment list are simulated, see figure 8.2 along a single case, case 5, which does not exist in the experimental list.

Case	ACH [h ⁻¹]	Exhaust heigt [m]	Miscellaneous	Result [c _r /c _e]	CFD [c _r /c _e]	CFD Case no.	
21	5	1.06	Head under exhaust	3.27	1.4	1	
12	10	1.06	Head under exhaust	1.97	6.8	2	
22	5	2.06	Head under exhaust	3.41	1.8	3	
13	10	2.06	Head under exhaust	2.71	1.4	4	
-	5	1.06 & 2.06	Head under exhaust	-	3.8	5	
20	10	1.06 & 2.06	Head under exhaust	2.95	1.4	6	

Figure 8.2: CFD case numbers 1-6 to the right refers to experiment cases shown to the left.

8.1.1 Hospital ward setting

The model of the hospital ward setting with return openings at different heights is shown in figure 8.1. The source and the target patients both have a minute volume of 6 *l/min* corresponding to low activity level as the manikins are bed bound. The heat emitted from the patients corresponds to the chosen activity level i.e. 52W/m². The ACH and temperatures vary for each simulation. The main objective of these simulations is to compare the results from the CFD simulation with experimental results. The following CFD simulations refer to those experiments shown in 8.2.

8.2 Case 1

The experiment case for this simulation is case 21, confer figure 8.2. The source CSP disseminates pollutants by mean of respiration which is simulated as a constant flow in the CFD simulation. Both CSPs and the lamps emit heat which can be described as positive buoyant flows moving towards the ceiling. A vertical temperature profile reveals the flow pattern in this case.

8.2.1 Temperature distribution

Positioning of return openings at a height of 1.06m above floor level, heat emission from the CSPs, lamps and the supply air flow give rise to creation of a temperature profile as illustrated in figure 8.2.1 and figure 8.3.

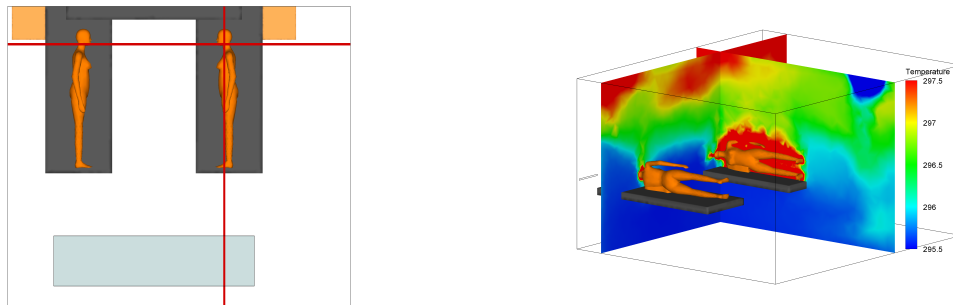


Figure 8.3: Right, source. Left, target. Temperatures given as Kelvin [K].

The regions with temperature differences are highlighted in the temperature contour. The supply air flow proceeds along the floor towards the opposite wall and beneath the beds on which CSPs are situated. Once the supply air flow has reached the opposite wall, recirculation takes place and part of the flow returns back towards the supply air flow while the rest of the recirculated air flow is entrained into the thermal plumes from the CSPs. Recirculation is especially prone beneath the beds as illustrated in figure 8.4.

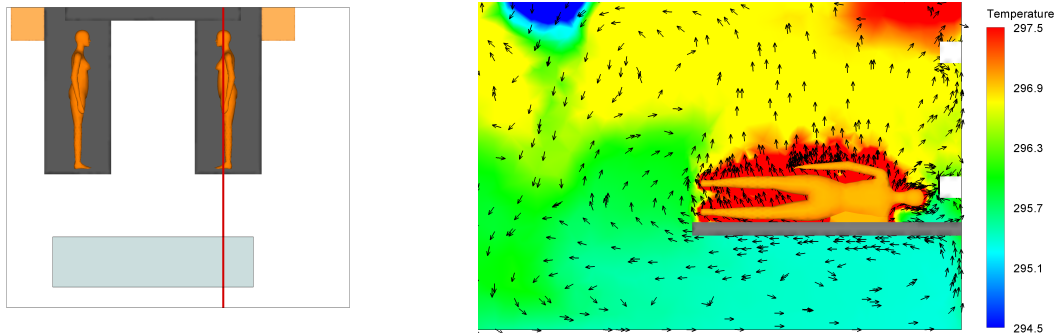


Figure 8.4: Temperature contour above the source CSP.

Due to the body heat emission from both CSPs, two buoyant plumes are expected to have upward motion towards the ceiling. When both plumes from the CSPs reach the ceiling, see figure 8.5, they tend to rise to the ceiling and accumulate there until eventually entrained into the supply air flow.

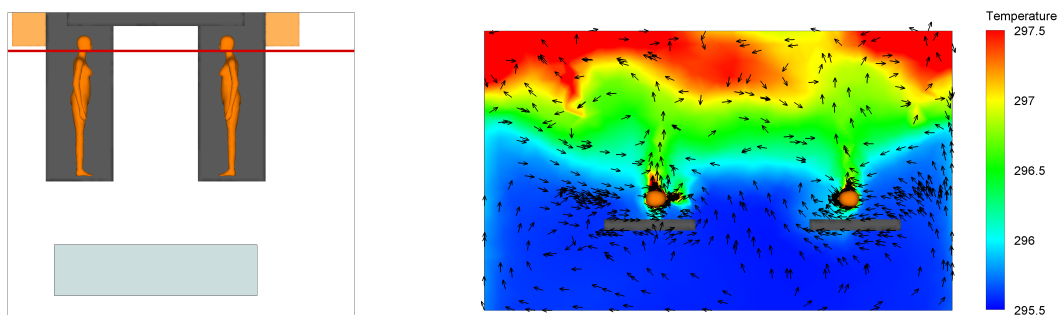


Figure 8.5: Due to body heat emission two positive buoyant plumes are created.

Heat seek upwards due to positive buoyancy. This is indeed in agreement with the CFD predictions, but since the inlet diffusers are attached at the ceiling, the supply air flow tends to entrain air from the vicinity and therefore a dilution process takes place. Due to this outcome the flow pattern can be described as well mixed. In order to check that no significant temperature gradients prevail in the hospital ward setting the temperature distribution obtained from the CFD predictions are held against the experiment, see figure 8.6.

8.2.2. Concentration distribution

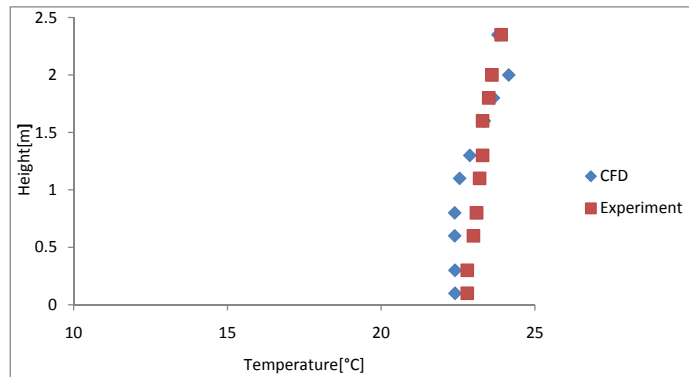


Figure 8.6: Vertical temperature distributions from CFD prediction and experiment.

From the comparison presented in figure 8.6, it can be seen that the CFD predictions are in good agreement with experiment results. Since mixing is widespread in the hospital ward setting the concentration distribution must have the same trend likewise the temperature distribution.

8.2.2 Concentration distribution

A vertical concentration contour of the hospital ward setting is presented. Offhandedly, it might seem like much of the contaminants that are expelled from the source CSP is accumulated below the ceiling and above the source CSP, confer figure 8.7.

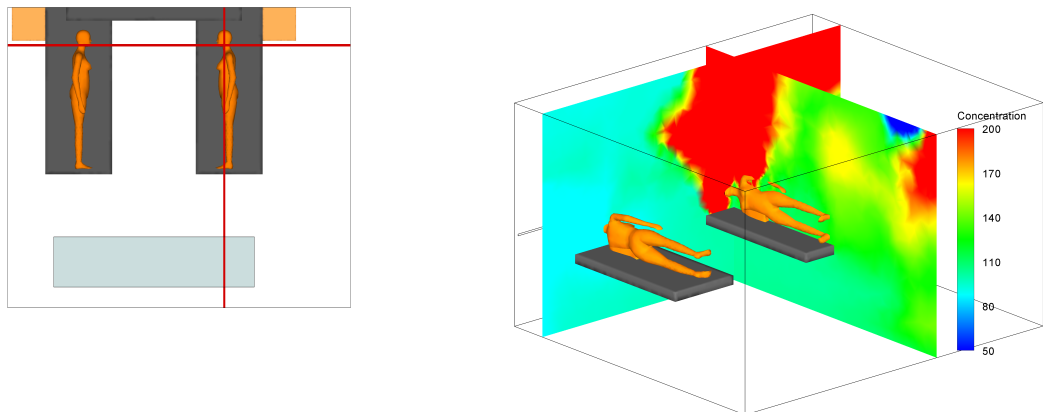


Figure 8.7: Right, source. Left, target. Concentration is defined as $\mu\text{g}/\text{m}^3$.

But by recalling the results of the CFD predictions with respect to the temperature distribution which moreover is in agreement with experiment results, a diluting process takes place in the hospital wards setting. This entails that the contaminants must be well mixed as well. The CFD predictions indicate that the target CSP is never exposed to a direct exhalation jet

from the source CSP. The exhalation jet from the source merely reaches the edge of the bed before it gradually rises towards the ceiling. According to a measured concentration distribution from the corresponding experiment case 21, an almost uniform vertical concentration distribution is present by sampling in different heights. This result is in agreement with the CFD prediction to a certain degree. In figure 8.8 the dimensionless vertical concentration distribution is shown.

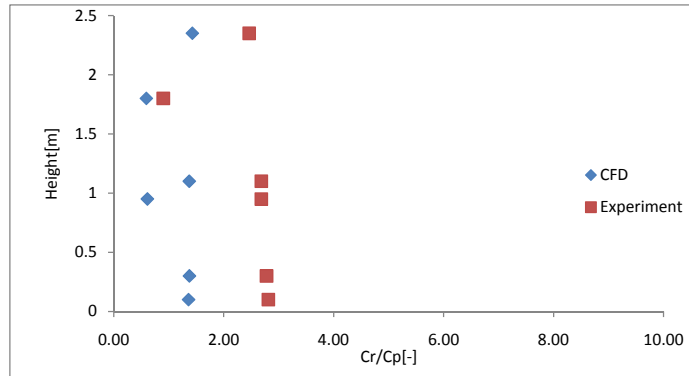


Figure 8.8: Comparison of contaminant distribution for CFD case 1 and experiment case 21.

A sudden variation in the local ventilation effectiveness is experienced at 1.8m. This observation is consistent in both CFD and experiment measurements. It is suggested that this sudden change may be caused by the exhalation jet from the source CSP that is locked at the height from which the concentrations are measured, see figure 8.9.

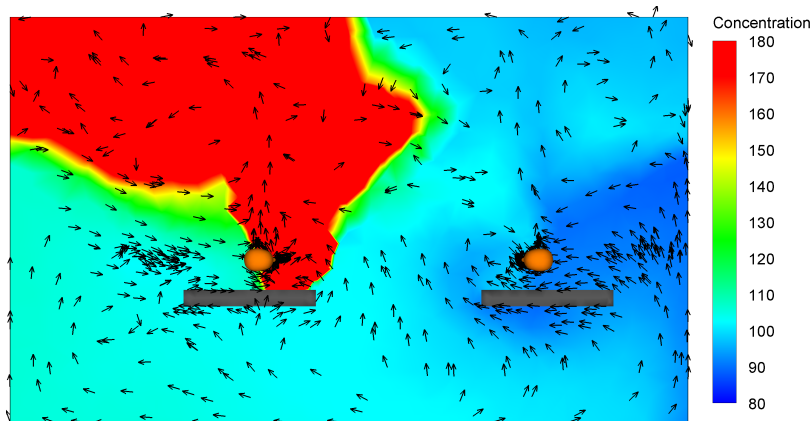


Figure 8.9: High concentration in 1.8 m above the floor.

From the temperature contour it is clearly illustrated that above the beds on which the CSPs are laying, there exists a layer of air with slightly higher temperature than below the beds. This is due to heat emission from both CSPs bodies and the exhalation jet from the source CSP which has a higher temperature than the surroundings. In the illustration shown below, figure 8.10 it can be seen that the contaminant distribution follows the temperature distribution. This might be a further explanation to a higher recorded concentration. The

8.2.3. Personal exposure index

measurement points for both temperature and concentration samplings are taking place in the middle of the beds.

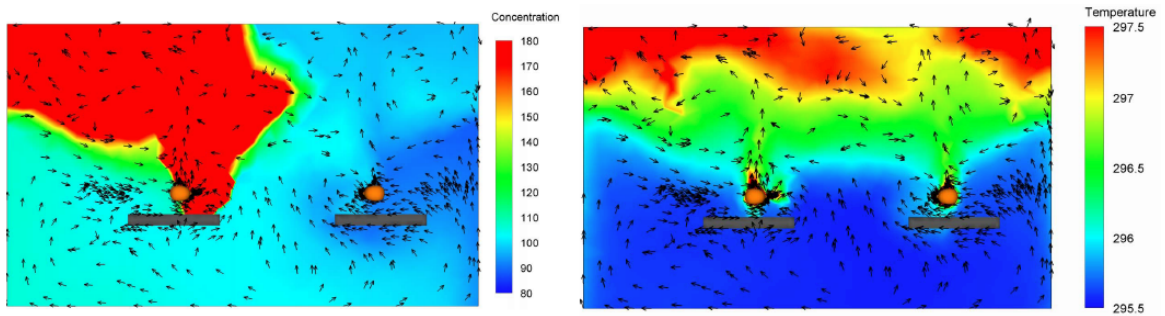


Figure 8.10: Left; concentration distribution. Right; temperature distribution.

8.2.3 Personal exposure index

A personal exposure index based on the CFD predictions and experiments are compared, conger figure 8.11. The concentrations at both return openings are averaged and held together with the concentrations at the target CPS's mouth.

Personal exposure index ϵ (5ACR & 1.06m)			
Experiment [ppm]		CFD[$\mu\text{g}/\text{kg}$]	
Exhaust	23.9	Exhaust	0.00011685
Target	7.3	Target	7.95215E-05
ϵ	3.27	ϵ	1.47

Figure 8.11: Personal exposure index for CFD prediction against experiment

A considerable discrepancy takes place between the two personal exposure indicies. The difference is larger than 200 %.

8.3 Case 2

The experiment case for this simulation is case 12, confer figure 8.2 on page 72. Since the amount of supplied air is increased compared to the previous case, less heat accumulation is expected below the ceiling. Heat accumulation is an indicator of how well the return openings are able to remove heated and contaminated air from the hospital ward. A vertical temperature profile reveals the flow pattern in this case.

8.3.1 Temperature distribution

Mixing is inevitable with the present ventilation system, since the supply air flows will entrain air from the surrounding. By increasing the air change rate from $5h^{-1}$ to $10h^{-1}$ mixing will take place more rapidly. In the same time a steep vertical temperature gradient

can be found in locations furthest away from the supply air flow. This temperature gradient is unavoidable unless very high air changes are used. According to CFD simulations as well as experiment measurements a steep temperature gradient is present in the hospital ward. But the gradient is very small and thus negligible. The temperature distribution can be seen in figure 8.12.

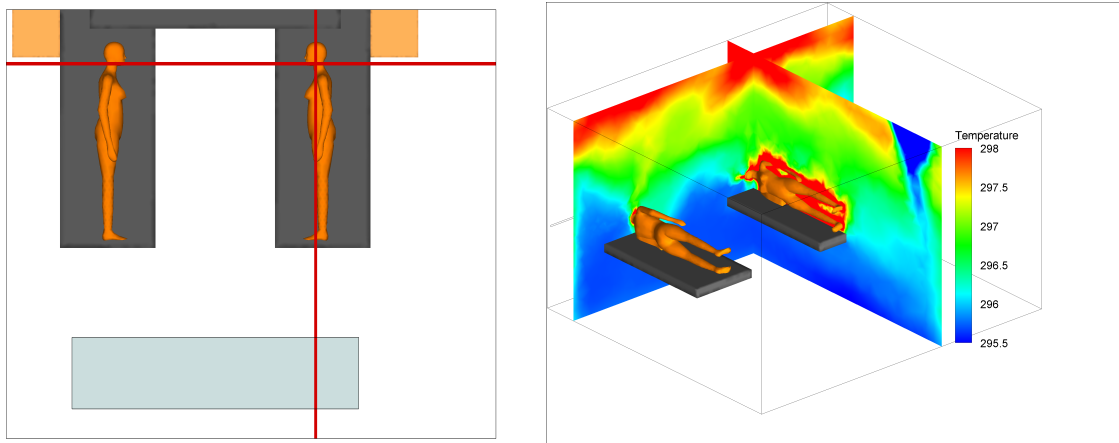


Figure 8.12: Right, source. Left, target. Temperatures given as Kelvin [K].

Similar to the previous case 1, it seems that heat emission from the CSPs are accumulated below the ceiling as if the hospital ward setting were ventilated with displacement ventilation principle, see figure 8.13. Near the inlet diffuser can it be seen that the heated air that is accumulated below the ceiling gets entrained into the supply air. Further away this tendency is less prominent. In order to prevent similar outcomes, the return opening need to be located at a higher location, e.g. below the ceiling. Another possibility is to increase the amount of supply air in order to create more mixing. But the latter will theoretically provide a ventilation efficiency no larger than 1.

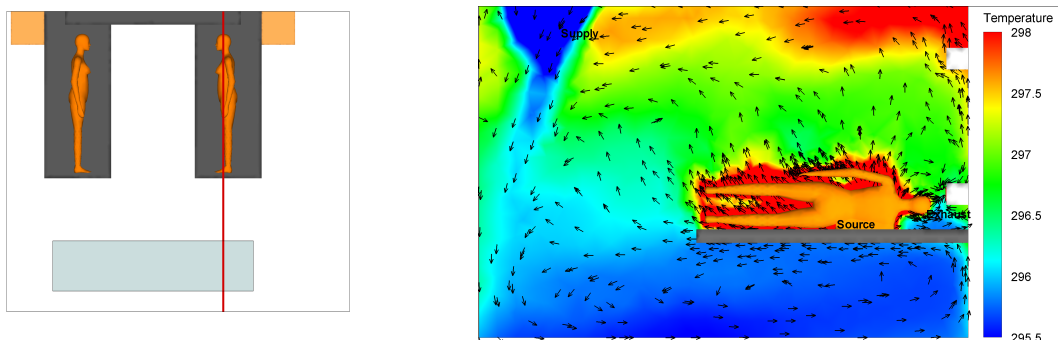


Figure 8.13: Temperature contour above the source CSP.

8.3.2. Concentration distribution

The plume from the source CSP is rising towards the ceiling while the supply air is proceeding along the floor, see figure 8.13. Above the manikin heads the temperature profile is almost similar to case 1, confer figure 8.14.

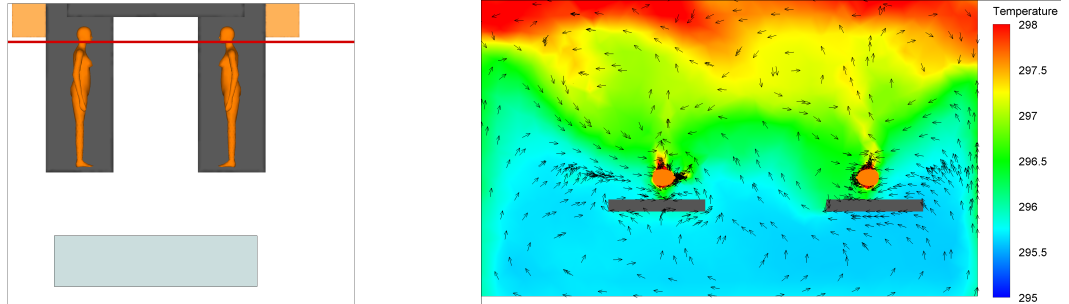


Figure 8.14: Due to body heat emission two positive buoyant plumes are created.

Comparison of CFD and experiment results can be seen in figure 8.15.

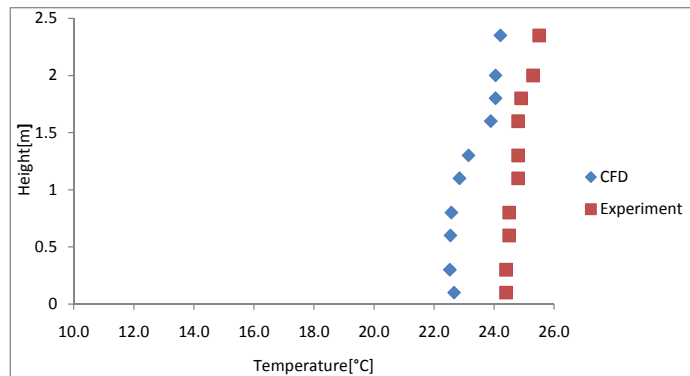


Figure 8.15: Vertical temperature distribution of CFD prediction vs. experiments.

8.3.2 Concentration distribution

The concentration contour highlights the highest concentrations above the source manikin. Contaminants from the exhalation jet tends to move behind the source after being expelled, see figure 8.16. This might be due to the general flow patterns that prevail in the hospital ward.

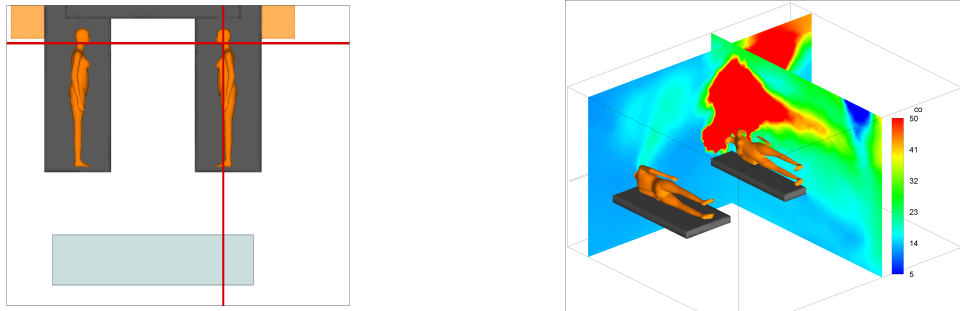


Figure 8.16: Contamination distribution in the hospital ward setting.

The contour in figure 8.16 indicates that the contaminants are clustered above the source CSP. It can also be seen that the contaminant distribution above the source CSP is not following the temperature distribution all the way to the ceiling but it rather cluster at some distance below the ceiling. Since the contaminants are expelled by the source with a certain temperature, the exhalation jet only reaches at locations where the temperatures are equal.

When comparing the local ventilation indexes for CFD and the corresponding experiment case a very distinguishable divergence is prominent, see figure 8.17.

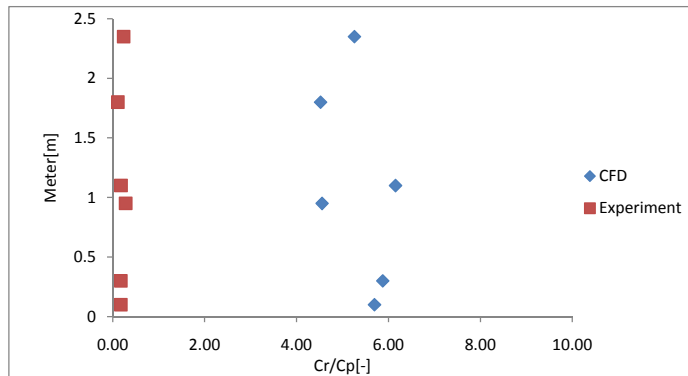


Figure 8.17: Local ventilation indexes from CFD prediction and experiment measurements.

The large difference might be caused by the fact that this CFD predicted local ventilation index is given by comparing the exhaust concentration with local concentrations between the beds. In figure 8.18 it can be seen that the CFD prediction suggests very high concentrations at the return opening besides to the source CSP while at the concentrations at the points between the beds are much lower.

8.3.3. Personal exposure index

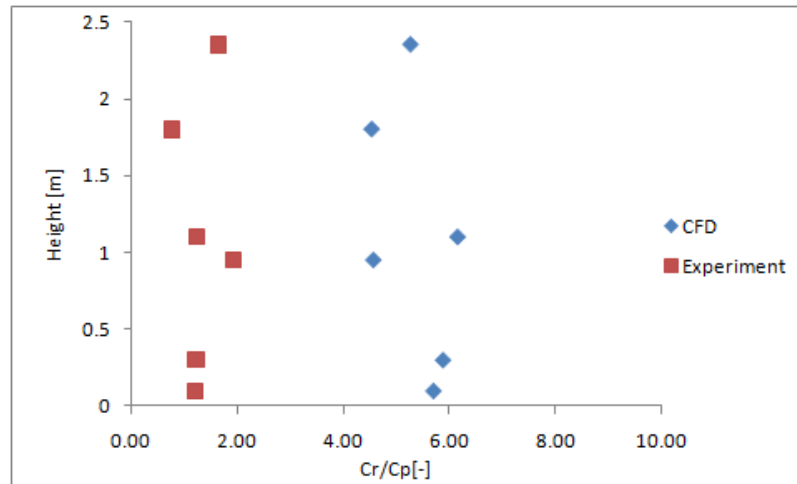


Figure 8.18: CFD, local ventilation index as the ratio between the exhaust concentration and the points between the beds

According to figure 8.18 the measurements and CFD predictions follow the same trend although the values are not the same.

8.3.3 Personal exposure index

A personal exposure index is calculated for this case and compared to the corresponding experiment case (case 12), see figure 8.19.

Personal exposure index ϵ (10ACR & 1.06m)			
Experiment [ppm]		CFD [$\mu\text{g}/\text{kg}$]	
Exhaust	164.9	Exhaust	6.32081E-05
Target	83.7	Target	1.35831E-05
ϵ	1.97	ϵ	4.65

Figure 8.19: Personal exposure indexes from experiment and CFD prediction.

The personal exposure index obtained from the CFD prediction is much higher than the personal exposure index from the experiment. The deviation is more than 200 %.

8.4 Case 3

In the following two cases, i.e. case 3 and 4, the return openings are located at 2.06m. It is of interest to investigate whether an improvement can be made through the changes in these cases and compare these results with measurements. It is expected that higher positioning of return openings will affect the contamination distribution as well as the temperature distribution.

8.4.1 Temperature distribution

The vertical temperature distribution can be seen in figure 8.20. This temperature contour clearly exhibits the plume on its way towards the ceiling and furthermore the entrainment into the supply air flow.

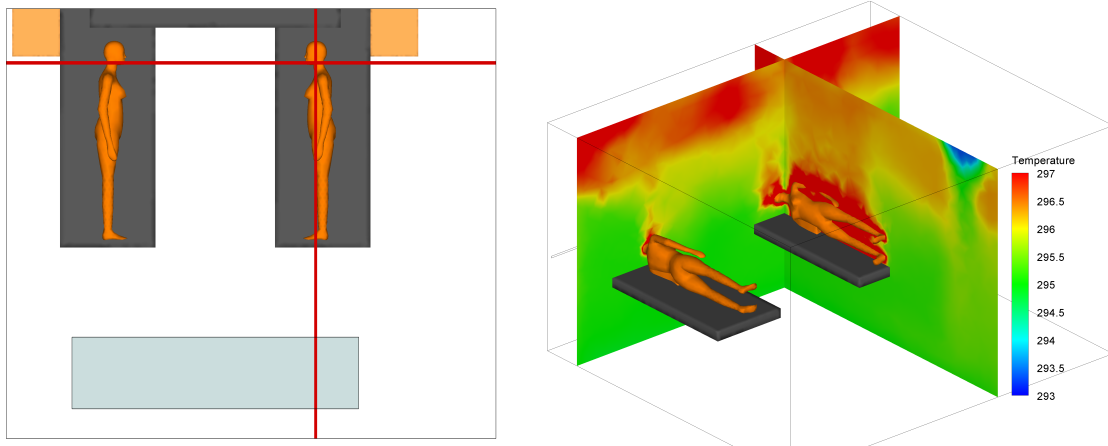


Figure 8.20: The contour reveals the vertical temperature distribution with return openings located at 2.06m above floor.

The temperature distribution below and above the source CSP is illustrated in figure 8.21. By recalling case 1 and comparing the temperature contours in both cases it can be seen that less heat is accumulated below the ceiling. This is especially the case near the highest return opening at 2.06m. This indicates that the higher positioning of the return openings is able to remove more heated air from the vicinity.

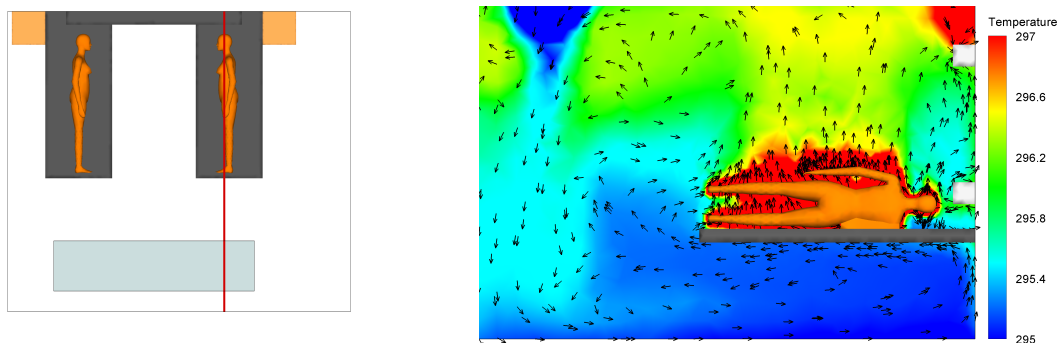


Figure 8.21: Temperature contour above the source CSP.

8.4.2. Concentration distribution

The latter incidence is also consistent when looking upon the temperature contour above the heads of CPSs, confer figure 8.22. Below the ceiling are two temperature pockets created in the vicinity of the return openings. Both return openings extract air locally.

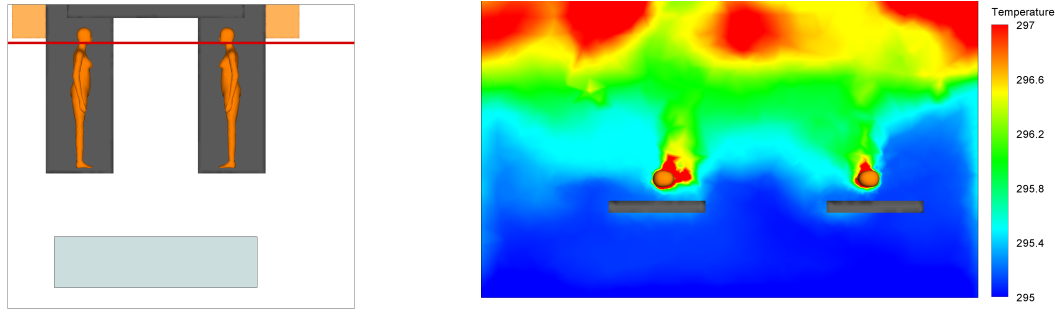


Figure 8.22: Vertical temperature contour above both manikins.

Vertical temperature distributions at the corresponding experiments case 22 and the present CFD prediction are compared, confer figure 8.23.

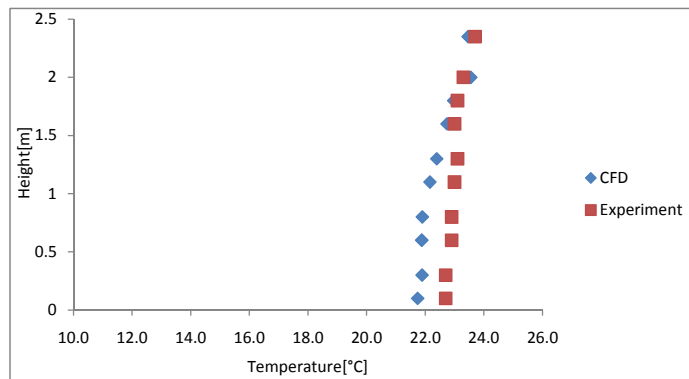


Figure 8.23: The CFD predictions of the vertical temperature distribution is slightly different from measurements.

According to both vertical temperature distributions, there are no significant temperature gradient in the hospital ward. In both cases the temperature differences between the lowest(0.1m) and highest(2.35m) measurement points is approximately 1 °C. In the following the outcome of this finding is presented with respect to concentration distribution.

8.4.2 Concentration distribution

The spread of contaminants in the hospital ward is illustrated in figure 8.24. The pollutants rise vertically until they reach the height at which the temperature is the same as the exhalation temperature, in this case all way up to 2.45m beneath the ceiling.

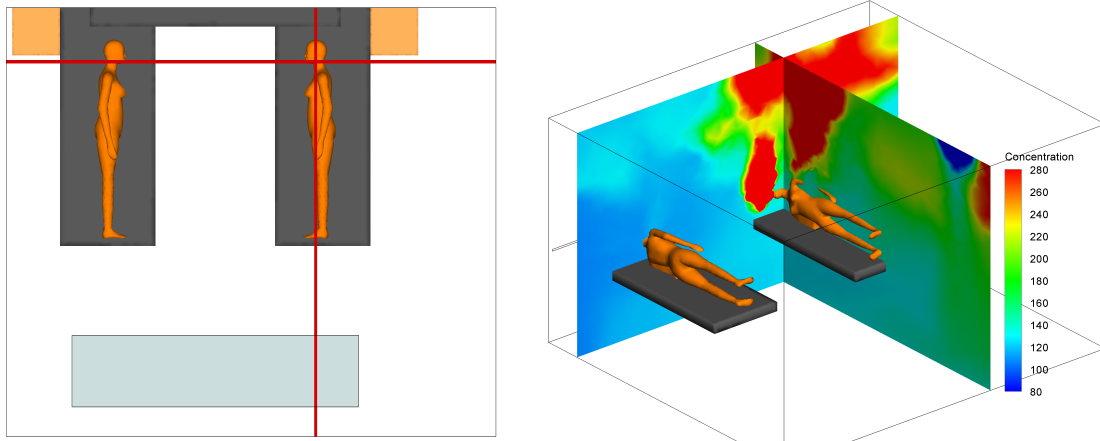


Figure 8.24: Contamination distribution in two planes.

It can be seen that the target CSP is not directly exposed to the exhalation jet from the source CSP. The contaminants are expelled from the source and accumulated at the ceiling where it is entrained into the main supply air flow. Hence a diluting process takes place and the target patient is exposed to a mixture of fresh and contaminated air. A comparison of the concentration distribution between the present case 3 and case 1 is illustrated in figure 8.25 and figure 8.26. This comparison reveals the difference and effect of variation of return opening heights at the same time.

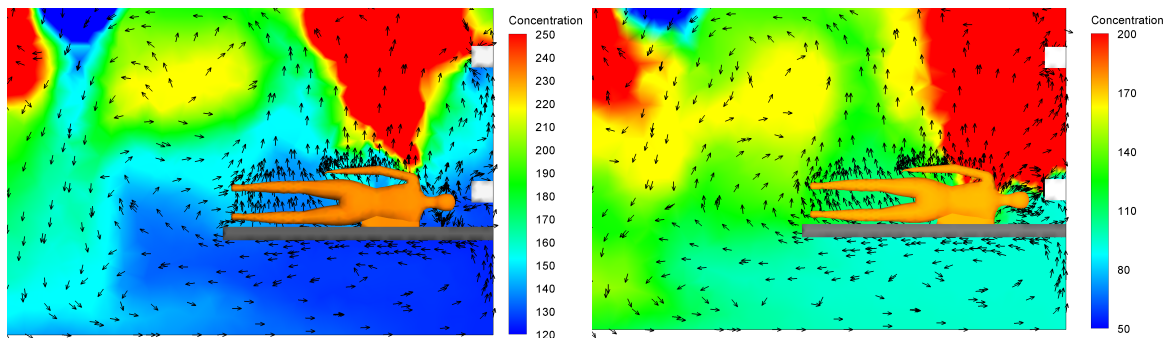


Figure 8.25: concentration contour for case 3. Figure 8.26: Concentration contour for case 1.

The illustration of the contaminant distribution for both cases exhibits the effect of the new location of return opening at 2.06m. This outcome is in agreement with expectations due to such modifications. The CFD predictions of temperature distribution for the present case is furthermore compared with measurements, case 22, see figure 8.27.

8.4.3. Personal exposure index

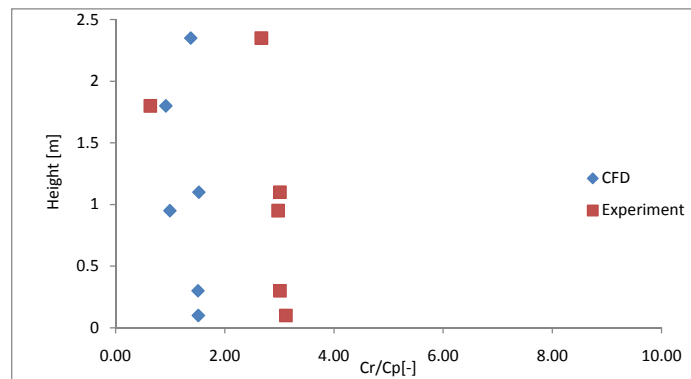


Figure 8.27: Comparison of local ventilation index for CFD case 3 and experiment case 22.

Similar to experiment case 21, confer table 8.2 on page 72, the present experiment case 22 undergoes a precipitous degradation with respect to local ventilation index at 1.8m. This scenario is consistent with the present CFD case as well, see figure 8.28 and figure 8.29

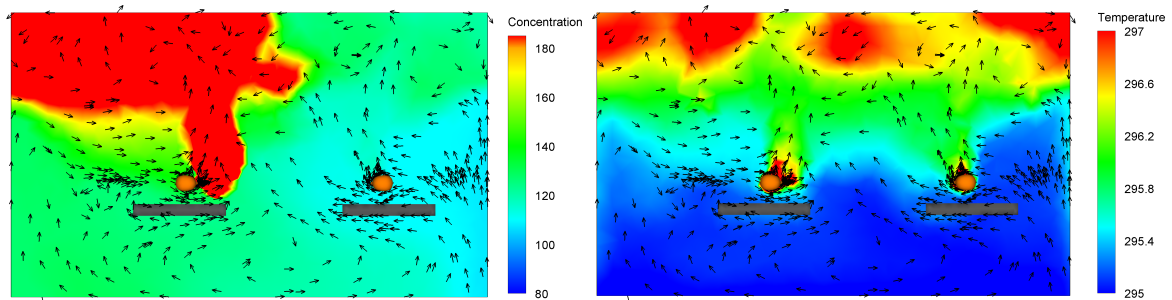


Figure 8.28: concentration contours for case 3. Figure 8.29: Concentration contours for case 1.

8.4.3 Personal exposure index

According to the CFD prediction, a slightly higher personal exposure index is obtained by locating the return openings at 2.06m instead of 1.06m. This observation is in agreement with personal exposure indexes obtained in the experiments, confer figure 8.11 on page 77 and figure 8.30

Personal exposure index ϵ (5ACR & 2.06m)			
Experiment [ppm]		CFD [$\mu\text{g}/\text{kg}$]	
Exhaust	25.9	Exhaust	0.000152357
Target	7.6	Target	9.50317E-05
ϵ	3.41	ϵ	1.60

Figure 8.30: Personal exposure index according to CFD prediction.

8.5 Case 4

This CFD simulation refers to experiment case 13, confer figure 8.2 on page 72. The heat generations from the lamps are accounted but not shown in neither of the following contours. It is now interesting to see if there is a difference between case 3 and the present case 4 with respect to temperature- and concentration distribution.

8.5.1 Temperature distribution

The temperature contour shown in figure 8.31 illustrates the vertical temperature distribution in two planes. This temperature distribution is anticipated. Heat is more likely to accumulate above the CPS heads near the ceiling than above the bodies, i.e. along the body, between the supply and return openings, due to entrainment into the supply air flow.

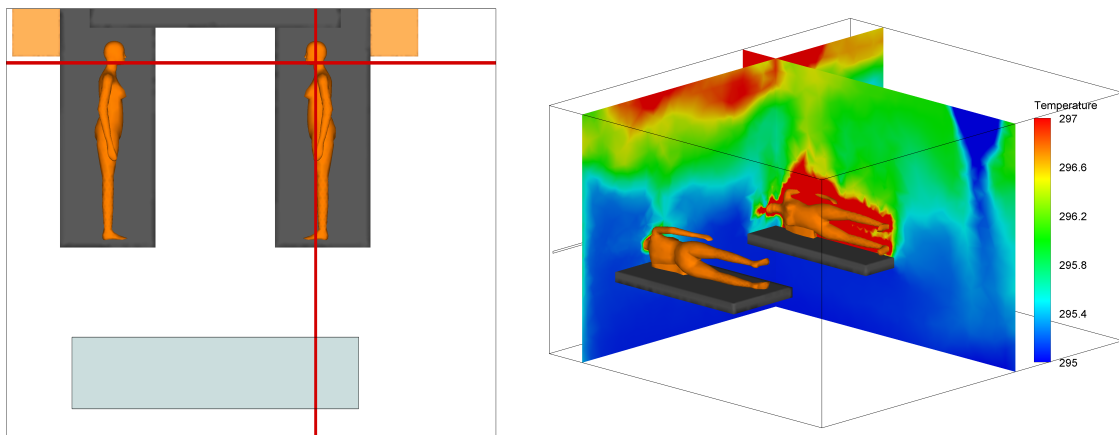


Figure 8.31: Temperature distribution in two planes.

The temperature difference between the lowest and highest measurement points is $1\text{ }^{\circ}\text{C}$. The vertical temperature distribution of this CFD prediction shares the same trend as the temperature distribution encountered in the experiment case 13, see figure 8.32.

8.5.2. Concentration distribution

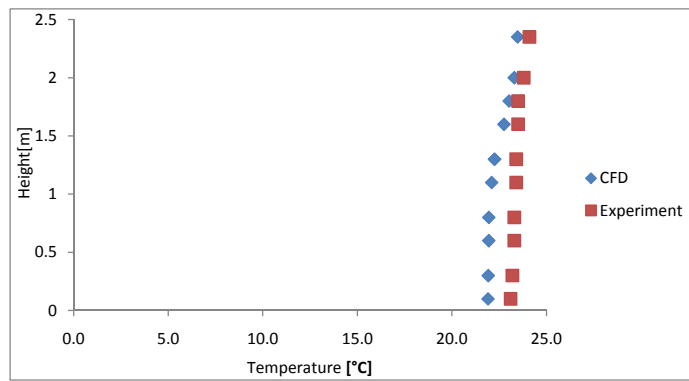


Figure 8.32: Vertical temperature distribution from CFD prediction and experiment are comparable.

8.5.2 Concentration distribution

The concentration distribution is in agreement with the temperature distribution. Contaminants are partly extracted by the return openings or entrained and diluted into the supply air flow, see figure 8.33

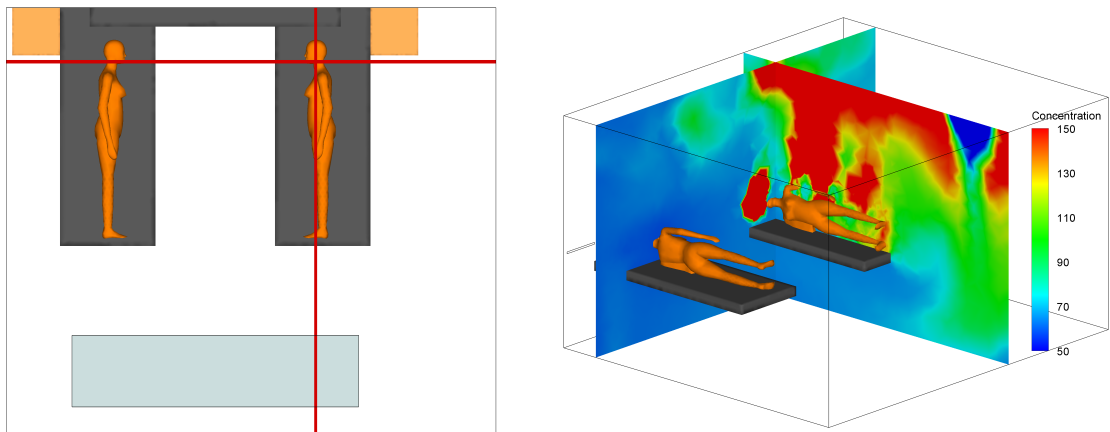


Figure 8.33: Contamination distribution in two planes.

Since the target CSP is not exposed to a direct exhalation jet from the source CSP, the contaminants inhaled by the target CSP must necessarily be the contaminants that are entrained, diluted and then brought to the breathing zone.

8.5.3 Personal exposure index

The CFD simulation of the present case predicts a lower personal exposure index than case 2 and 3. Compared with the experiment results the latter outcome is also consistent, see figure 8.34

Personal exposure index ϵ (10ACR & 2.06m)			
Experiment [ppm]		CFD[$\mu\text{g}/\text{kg}$]	
Exhaust	136.51	Exhaust	6.65028E-05
Target	50.35	Target	4.78088E-05
ϵ	2.71	ϵ	1.39

Figure 8.34: Personal exposure level of CFD prediction held against the experiment result.

The deviation between the personal exposure indexes from the experiment and CFD prediction is approximately 200 %.

8.6 Case 5

This particular case is simulated numerically without any corresponding experimental counterpart. Since no experimental data are to be inserted as boundary condition for this case, these are deliberately chosen from CFD case 1.

8.6.1 Temperature distribution

The temperature distribution for this case is shown in figure 8.35. The temperature distribution in the vertical direction shares the same trend as for the previous cases. If looking close near the walls behind the target CSP. It can be seen that the walls effectively emit heat since they are given temperatures from the experiments.

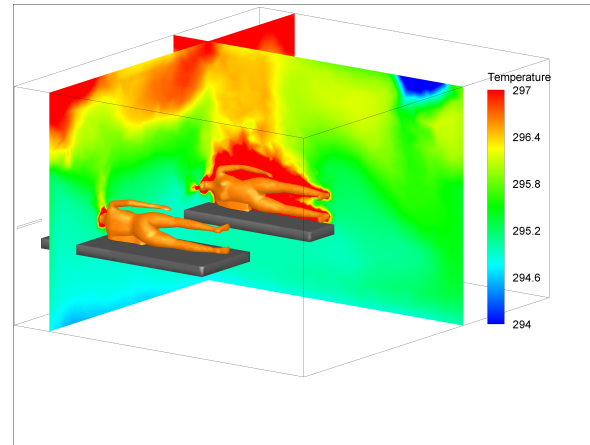
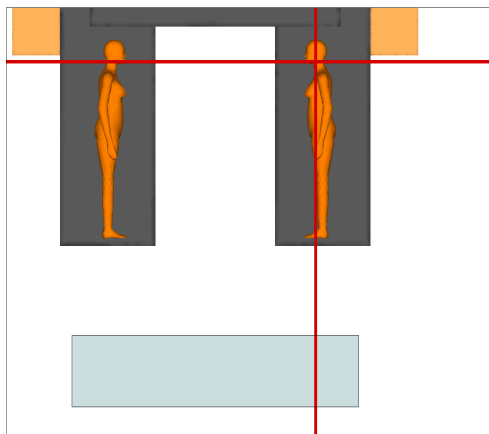


Figure 8.35: Temperature distribution as a result of exhaust openings at two different heights.

8.6.2 Concentration distribution

The concentration distribution can be seen in figure 8.36. From this concentration contour it can be seen that the target CSP is surrounded by very by air with small concentrations of contaminants. This behavior is consistent with other cases and might me due to the asymmetry of the hospital ward setting. At the breathing zone of the target CSP it can be seen from the concentration contour that the CSP inhales air with relatively lower concentrations than the surrounding. This might be caused by the supply air flow which is recirculating that height.

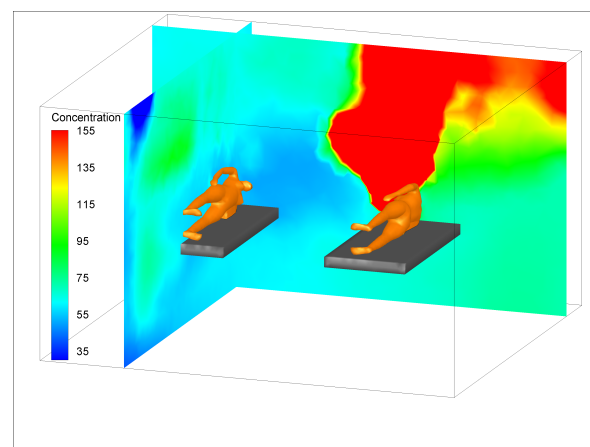
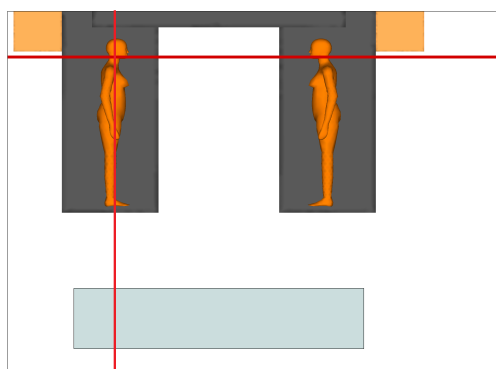


Figure 8.36: Contaminant distribution as a result of exhaust openings at two different heights.

8.6.3 Velocity distribution

The velocity distribution can be seen in figure 8.37. From the velocity predictions for this case it can be seen that the largest velocities prevail along the boundaries of the simulated domain. Expectedly, the highest velocities are encountered at the return openings. But also at the floor below the inlet diffuser a region with high velocity is exhibited. this incident might be due an accelerated negative buoyant supply air flow as it collides with the floor once it reaches it.

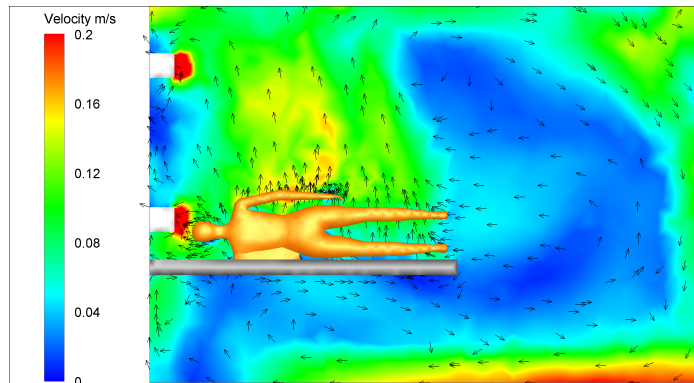


Figure 8.37: Velocity contour in a section through the target patient.

8.6.4 Personal exposure index

The personal exposure index for this CFD prediction, confer figure 8.38 is not compared with an experimental data counterpart. For this reason a conclusion can not be given conveniently.

Personal exposure index ϵ (5ACR & 1.06m + 2.06m)			
Experiment [ppm]		CFD[$\mu\text{g}/\text{kg}$]	
Exhaust	-	Exhaust	0.000161724
Target	-	Target	4.20817E-05
ϵ	-	ϵ	3.84

Figure 8.38: Personal exposure index for the target CSP bed bound upon the left bed.

8.7 Case 6

This CFD simulation is the last case to be compared with an experiment.

8.7.1 Temperature distribution

The temperature distribution of this case is shown in figure 8.39.

8.7.1. Temperature distribution

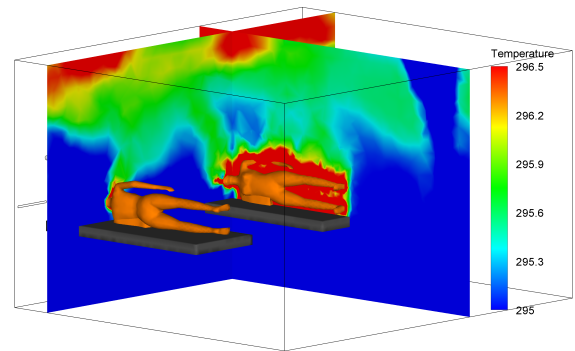
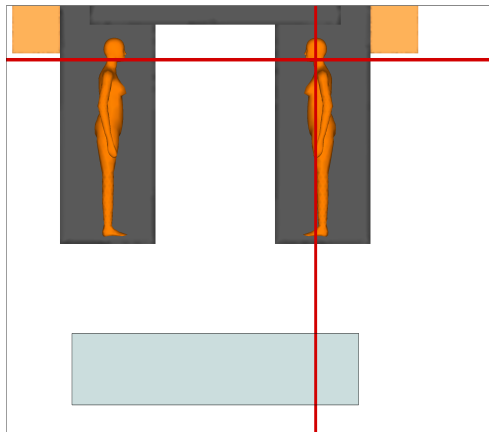


Figure 8.39: Temperature distribution as a result of exhaust openings at two different heights.

The vertical temperature distribution above the source CSP and both CSPs heads are shown in figure 8.40 and figure 8.41 respectively.

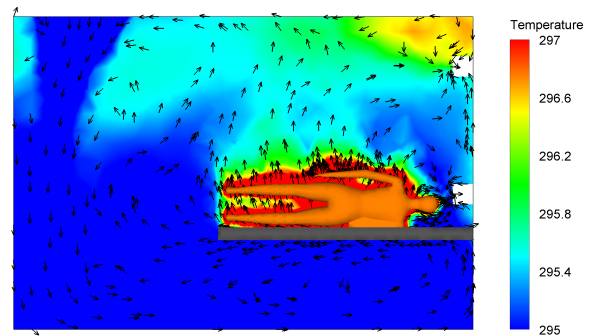
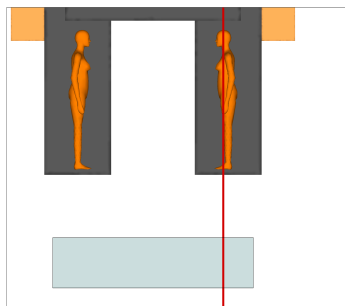


Figure 8.40: Temperature contour above the source CSP.

By extracting air via all four return openings it can be seen, according to the temperature contour, that heat is effectively removed locally.

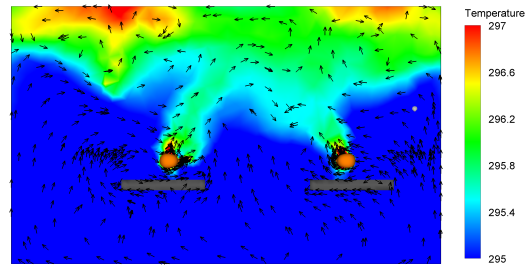
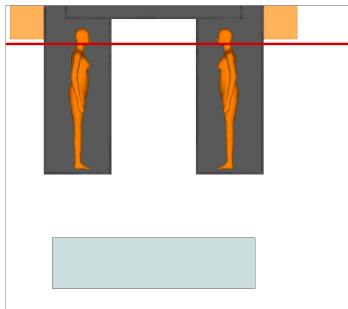


Figure 8.41: Vertical temperature contour above both manikins.

By comparing this CFD prediction with measurements a very good convergence is reached, confer figure 8.42.

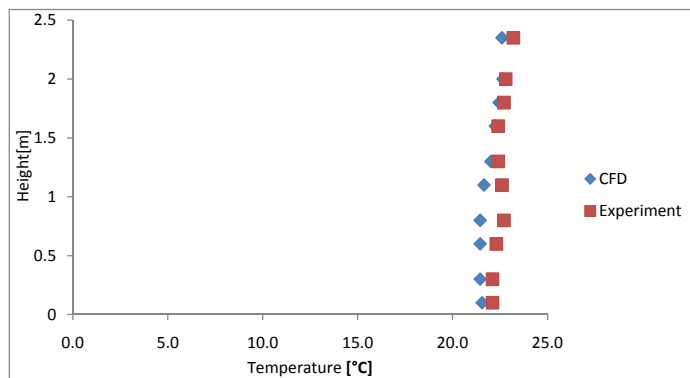


Figure 8.42: CFD prediction of temperature distribution vs experiment measurements.

8.7.2 Concentration distribution

The concentration distribution of this case is shown in figure 8.43

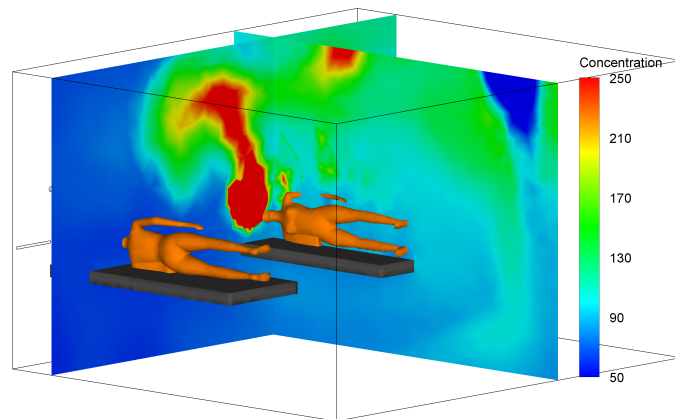


Figure 8.43: entrainment is very prominent along the supply air flow.

Above the source CSP it can be seen that contaminants are both extracted by the return opening and entrained into the supply air flow to the left, see figure 8.44.

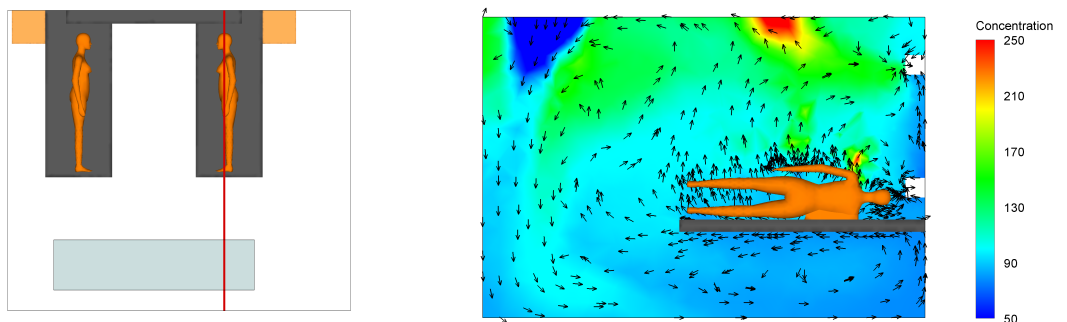


Figure 8.44: Concentration contour above the source CSP.

Similarly the concentration above both CSPs heads indicate effective removal of contaminants locally, see figure 8.45.

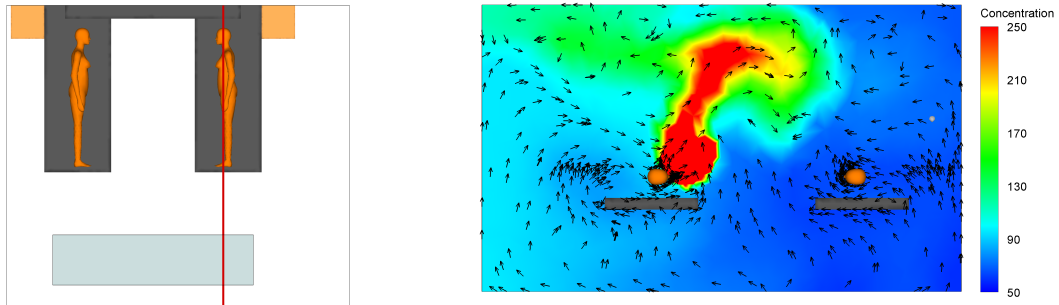


Figure 8.45: Concentration contour above the source CSP.

Unlike other CFD predictions the concentration distribution is not sharing the same trend as the measurements, see figure 8.46

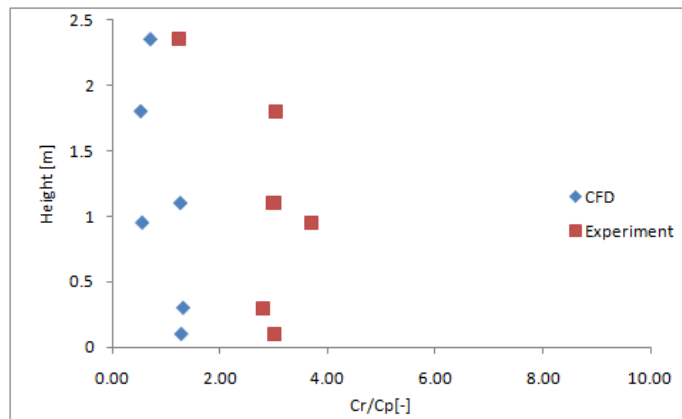


Figure 8.46: Similarities in the relative values.

8.7.3 Personal exposure index

The personal exposure index from the numerical predictions for the present case and the corresponding experiment case 20 occurs with a difference of more than 200 %, see figure 8.47.

Personal exposure index ϵ (10ACR & 1.06m + 2.06m)			
Experiment [ppm]		CFD[$\mu\text{g}/\text{kg}$]	
Exhaust	14.19	Exhaust	7.41662E-05
Target	4.81	Target	5.39536E-05
ϵ	2.95	ϵ	1.37

Figure 8.47: Personal exposure index, CFD vs experiment.

8.8 Conclusion

In total six experiments have been used as measurement criterion for the CFD predictions. All six cases share the same characteristics when speaking of boundary conditions. Two parameters are chosen as variables for all 6 CFD simulations. These are the air change rates and location of return openings. Air flow patterns obtained through the CFD predictions confirms that the general air flow patterns in the hospital ward are created by two main flows. These are the supply air flow and thermal plumes from both manikins and lamps. The nature of these flows, i.e. the supply air flow with lower temperature and thermal plumes above the manikins which tends to move towards the ceiling while the supply air flow proceeds along the floor and beneath the beds. This flow pattern creates a diluting process since the heated and contaminated air above the computer simulated persons (CSPs) are entrained into the supply air flow, which further explains the higher temperature and concentration readings in the supply air flows. Furthermore the target CSP is never exposed to a direct hit from the exhalation jet from the source CSP. This finding indicates again that no temperature stratification is present in the hospital ward. The latter fortifies the fact that mixing is prevailing. Thus the contaminants inhaled by the target CSP must necessary be originated from the diluted air with contaminations expelled by the source CSP. This finding is consistent in all CFD predictions and also in the corresponding experiment measurements. Experiment results indicate that the positioning of return openings indeed affects the ventilation effectiveness perceived by the target patient. The personal exposure index is highest when the air change rate is $5h^{-1}$ with return opening at 2.06m. According to the CFD simulations the best result with respect to personal exposure index are achieved with low positioning of return openings at 1.06m and $10h^{-1}$. Several conditions may influence the latter outcome and the consistent diverging with respect to concentration distribution. One of the main decisive parameters that distinguishes the CFD prediction with real situations is state of the simulations. The CFD predictions are confined due the choice of constant exhalation from the source CSP. This action may underestimate the exhalation jet from the source CSP, since with constant exhalation the maximum velocities, due to the pulsating nature of exhalation, are omitted. This might be the explanation to the higher personal exposure indices achieved with CFD predictions.

Part III

Particle distribution

Set up in Hong Kong

In this section is a description of the test room in which the measurements are executed and a description of the different cases examined. In addition to this there are accounts of where the equipment is positioned and why and the effect in the room.

9.1 The test room

The test room used in Hong Kong university was built right after the severe outbreak of SARS in Hong Kong. The purpose of the room is to investigate how to minimize the risk of cross infection of diseases like SARS with various ventilation principles. It can be fitted with beds and thermal manikins which are used to simulate people. The reason for the manikins is to generate the same flows inside the room as in a normal hospital ward. The room is insulated to minimize heat transfer through the surfaces. It has windows which makes it possible to observe what happens inside. The ventilation inside the room makes it possible to have displacement, mixing and vertical ventilation. The ventilation system is cable of delivering ACH of up to $16h^{-1}$. The system runs on 100% outdoor air. The control of the system including the inlet temperatue and the flow has proven to not be very good which means it is hard to keep a constant temperature inside the room. The internal dimensions of the room with out the lowered ceiling are for height, width and length: $3m$, $6.7m$ and $6.7m$.

9.2 Equipment

A lot of the equipment used in the Hong Kong measurement are similar to that used i Aalborg this is the manikins, the artificial lung and the air heater. The artificial lung shown chapter 2.12 on page 28 are used for the source instead of the one shown in chapter 2.11 on page 28 which were used in Aalborg. This is because it is lighter and therefore easier to transport. Unfortunately it is not possible to determine the exact air flow through the lung since the settings on it is not correct and it was not possible to completely calibrate it as the equipment for that were not sufficiently large to cope with the largest flows from the lung. Because of this only smaller flows were calibrated to see if there were a clear tendency between increasing the MV and the BF. A tendency between MV and BF are seen and this is used when deciding a MV and BF for a given activity level. The maximum velocity is then measured using a *Tsi INCORPORATED Veloci calc plus*. This measurement will at a

later time when the equipment arrives at Aalborg be transformed into a MV.

Also new equipment is used in Hong Kong, this is mainly a microscope and a particle generator. The microscope is used for counting particles and the particle generator is made to ensure an even distribution of particle to the exhalation air. The particle generator can be seen in figure 9.1.

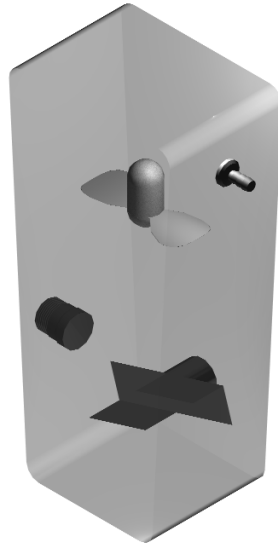


Figure 9.1: A sketch of the particle generator.

It is in principle a box with a paddle wheel and a fan. The wheel throws dust up in the air and the fan makes it stay in the air. The only way to control the amount of particles released to the exhalation air is by decreasing the effect for the paddle wheel and fan or adding less powder to the generator. It is not possible to control the exact number of particles or range of particles released so it is not possible to represent the exhalation of a real human being.

9.3 The setup for one manikin

The dimensions for the platform located in the center of the room are for height, width and length: $0.01m$, $2m$ and $3m$. The reason why a glass platform is located on the floor is to make sure the floor is totally even. This is not the case with the existing floor which is a bit uneven. The platform is covered with black cardboard in order to better see the pattern of the exhaled particles, as it is much easier than with the glass. A thermal breathing manikin as described in section 2.6 on page 25 is located at one end of the platform.

Several thermocouples are located inside the room. They are used to measure the surface temperatures of the ceiling, the floor and all the walls, as well as to measure the temperature distribution inside the room. The surface temperatures are measured as they are to be used as boundary conditions if CFD predictions are made for the experiments. Originally it were desired not to have a temperature gradient inside the room. But since it was not possible due to the poor control of the ventilation system and further it was not possible to get a cooling surface the gradient in the room is recorded in order to document the conditions inside the room. The concentration of particles are sampled with small glass plates located

9.4. The setup for two manikins

on the platform after the measurement is done. Using a microscope and a software developed at Hong Kong University the particles are counted. The particles used for these experiments are ISO 12103-1, A4 COARSE TEST DUST [12]. The particle concentrations are measured in 7 to 14 different places in order to get a good view of how they deposit on the floor, the distance from the manikin where the particles are measured can be seen in figure 9.2.



Figure 9.2: The distance between the white lines are 20 *cm* for the first 2 *m* after that is it 50 *cm*.

9.4 The setup for two manikins

The two manikins are located on the platform with a mutual distance of 1*m* in case 6 and 1.5*m* in case 7. The platform is located the same place as for the setup for one manikin how ever the manikins are moved, so they have the same distance to the center of the room. The temperatures are measured the same places as with only one manikin in the room. The particles are measured several places between the manikins. The mutual distance of measuring points are 10 *cm*. Location of sampling plates for case 7 can be seen in figure 9.3.

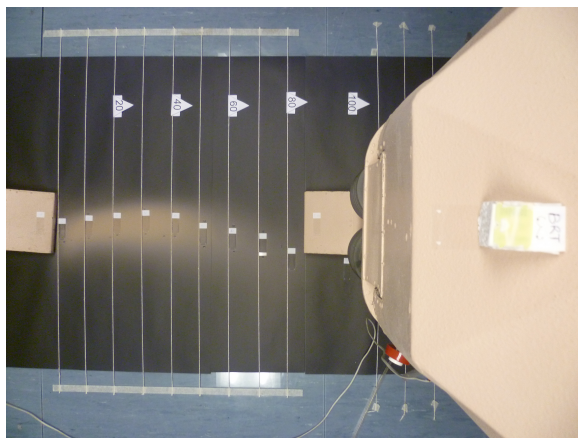


Figure 9.3: The position of sampling plates for case 7.

9.5 Cases

Listed in table 9.1 are the measurements executed in Hong Kong, also listed in the table is the important information about each case. From now on refers case 1 to 7 to this table and not figure 4.4 on page 39.

Case no.	Effect [W]	Activity level [MET]	Max velocity [m/s]	BF [min ⁻¹]	Number of manikins	Exhalation temperature °C
1	0	0	4.31	15	1	-
2	0	0	7.55	30	1	-
3	112.7	1.32	4.31	15	1	35.3
4	200.6	2.4	7.55	30	1	40.6
5	79.9	0.89	4	10	1	36.2
6	228	1.36	4.31	15	2	37.6
7	228	1.36	4.31	15	2	37.6

Table 9.1: The important variables of each case.

Particle deposition

In this part of the report the distance a particle can travel is examined. It is of interest to determine how far a particle can travel. Based on this it can be concluded how far a healthy person should be from a contaminated person without being in risk of being infected. In general practice $1m$ is used, but without any documentation as to why it is chosen [1].

In the following are different distances from the manikin examined. Not all measuring points are shown neither are all the data acquired as it is hard to illustrate in a clear way and a lot of the data does not really give any relevant information about the subject of interest. For example, most of the particles deposited after one meter are of the same size and distribution and therefore not illustrated in the graphs in this section. For a more detailed distribution of the particles see Appendix G. A detailed description on the procedure of the measurements can be seen in appendix H.

10.1 Isothermal flows

Cases 1 and 2 are made as reference cases, which means they are the basic cases, where everything is kept as simple as possible. Later on heat is added to the manikin as well as exhalation flow and other manikins will be added.

Figures 10.1 and 10.3 shows the patterns the exhalation jet creates at the floor and figures 10.2 and 10.4 shows the temperature distribution in the room for the two cases. Index a on the temperature distribution indicates that the temperature is measured during the deposition measurements for the pattern on the floor and b indicates it was measured during the deposition on the sample plates. This is done in order to see whether the same temperature distribution is present for the two measurements so that they are comparable.

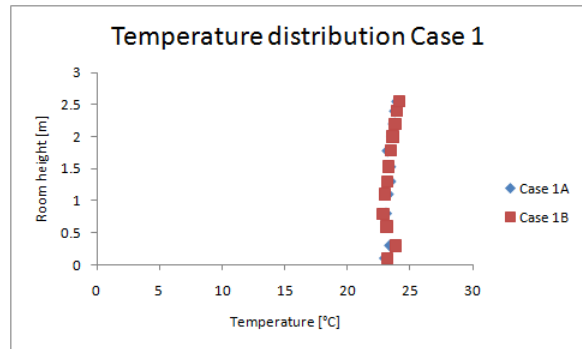
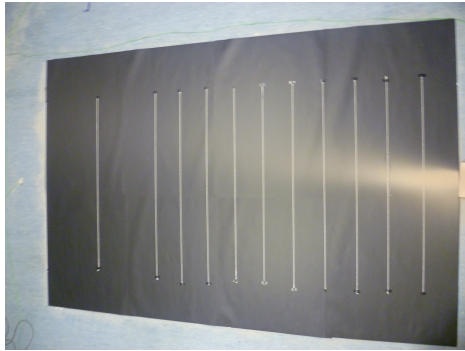


Figure 10.1: Illustration of deposited particles from the exhalation jet, case 1.

Figure 10.2: Temperature distribution for case 1.

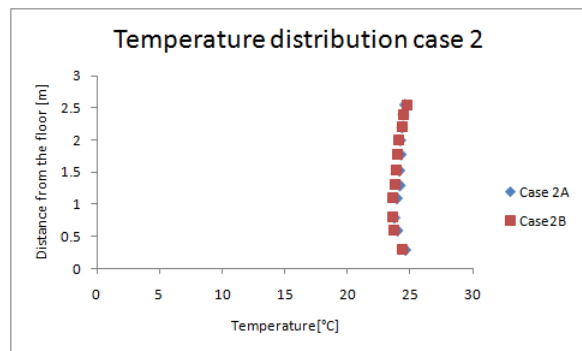
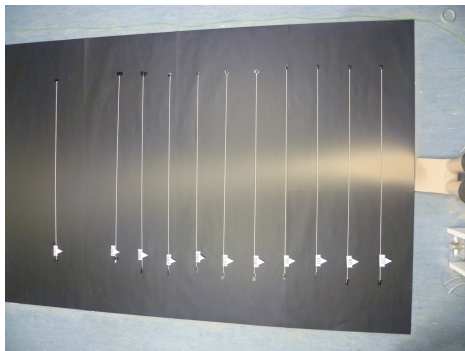


Figure 10.3: Illustration of deposited particles from the exhalation jet, case 2.

Figure 10.4: Temperature distribution for case 2.

It can be seen from figures 10.2 and 10.4 that the temperatures inside the room are almost without a gradient which was desired. Figures 10.1 and 10.3 show the pattern on the floor. It can be seen that case 2 deposits particle further in the room than case 1. This was as expected since case 2 has a larger MV and therefore also exhales more particles per minute. The average velocity is also greater for case 2 than for case 1 which means the particles are able to travel a larger distance.

The distribution of particles can be seen in figure 10.5. To make it easier to assess the results obtained the particles are divided into small intervals.

10.2. Comparison between isothermal and non isothermal flow

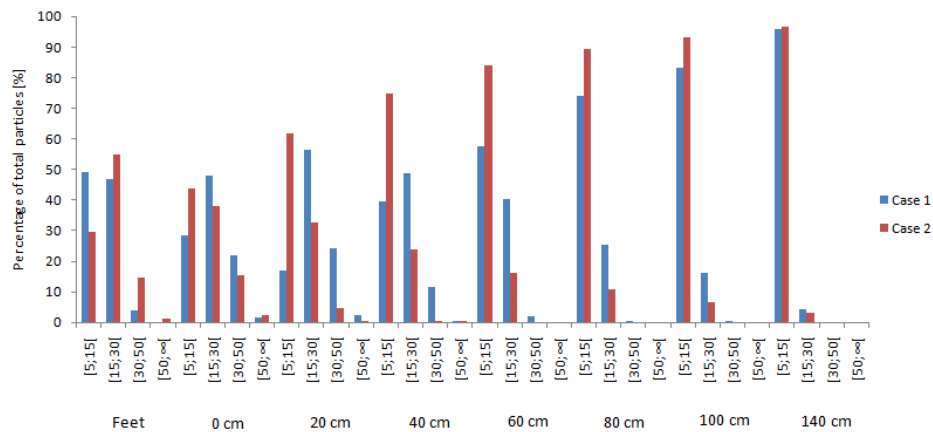


Figure 10.5: On the x-axis is the distance from the manikin and the particle sizes the interval is in μm .

From figure 10.5 it appears that in case 1 larger particles are able to travel further than case 2, this may be because of the way the particles were measured in the first two cases were they measured in a straight line from the manikin instead of following where there were the most particles. This does not have that great an influence closest to the manikin where the particles drop straight down and further away is it mainly smaller particles that deposit.

10.2 Comparison between isothermal and non isothermal flow

Here it has been looked upon the influence of a couple of key parameters when considering the exhalation flow of a person. These parameters are the thermal plume of the manikin, which changes the flow close to the manikin and the exhalation air which is heated and there by changes direction as it leaves the mouth.

Figures 10.6 and 10.7 show the deposited particles from the exhalation jet of cases 1 and 3.

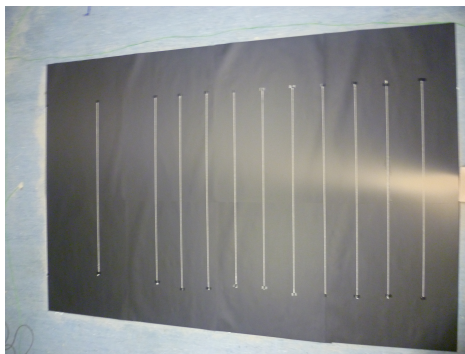


Figure 10.6: Illustration of deposited particles from the exhalation jet, case 1.

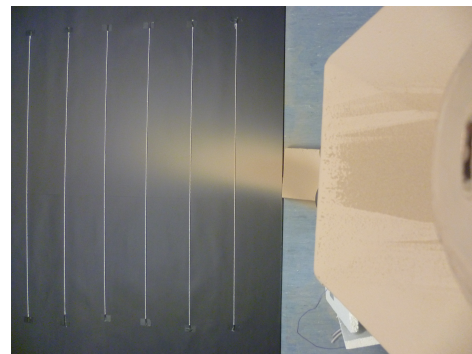


Figure 10.7: Illustration of deposited particles from the exhalation jet, case 3.

It is easy to see that the jet travels the furthest for case 1 but the amount of particles deposited very close to the manikin are larger for case 3. This can be seen by the amount of particles on the chest and feet in case 3, the chest and feet are not shown for case 1 as there were nothing noticeable.

Figure 10.8 shows the percentage of deposited particles at different distances from the manikin for case 1 and 3.

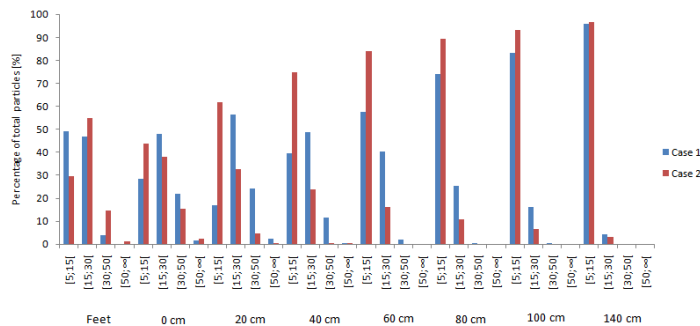


Figure 10.8: On the x-axis is it the distance from the manikin and the particle sizes the interval is in μm .

From figure 10.8 it is noticed that in case 3 particles larger than $30 \mu m$ does not reach $60 cm$ and there are hardly any at $40 cm$ either while in case 1 particles larger than $30 \mu m$ can be recorded as far away as $100 cm$ from the source. A reason for why the large particle deposit close to the manikin when it is heated could be that in the beginning and end of the exhalation the horizontal velocity is quite low, see section 2.5 on page 22 and is not able to penetrate the upward flow of the thermal plume from the manikin. This phenomenon can be seen in figure 10.9, the jet mainly has an upward direction and the horizontal is almost without influence. This means the particles have a high upward and a small forward velocity and this may result in the particles depositing close to the manikin.



Figure 10.9: Upward flow around the maninikin.

10.3. Influence of varying activity levels

Figures 10.10 and 10.11 show the deposited particles on the floor from the exhalation jet for cases 2 and 4.

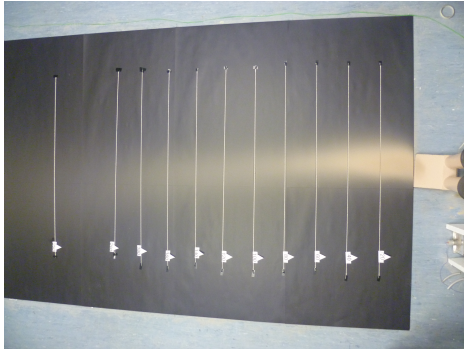


Figure 10.10: Illustration of deposited particles from the exhalation jet, case 2.

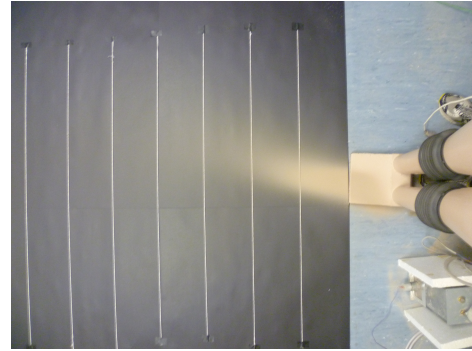


Figure 10.11: Illustration of deposited particles from the exhalation jet, case 4.

Again it can be observed that the deposition of particles can be seen further away from the manikin when it is not heated compared to when it is and that there is a larger concentration of particles close to the manikin in case 4 than case 2.

10.3 Influence of varying activity levels

In the following section influence of changing the activity level and appertaining MV and BF on the deposited particles of the exhalation jet is examined. The activity levels correspond to a standing woman, case 3, a woman walking $4km/h$, case 4, and a woman lying down, case 5. These activity levels have been chosen as they correspond to activity levels which can be expected in a hospital surrounding and due to the limitations of the equipment. This limitation is due to the equipments inability to have a larger MV than the one used for case 4.

Figure 10.12 shows the deposited particles on the floor for cases 3, 4 and 5.

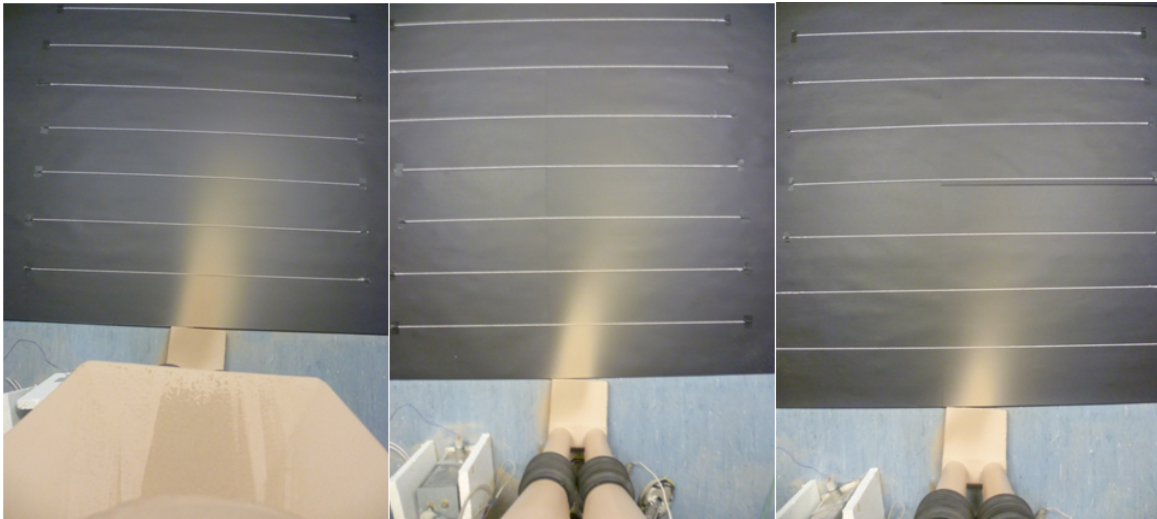


Figure 10.12: From left to right is it case 3, 4 and 5.

It can be seen from figure 10.12 that in cases 3 and 4 the main part of the particles have deposited within the first 40 cm from the manikin and hardly any deposition is seen beyond 60 cm. For case 5 the main part of the particle is deposited within the first 20 cm and hardly anything have deposited beyond 40 cm.

None of the three cases show signs of larger particles have deposited more than 1m from the manikin which is what is investigated in this part of the project.

Figure 10.13 shows the distribution of particles along the floor. It has to be noticed that the exhalation air temperature of case 4 is too high, it is above 40°C . The reason for this is the construction of the manikin, when the manikin is very warm a lot of heat is transferred to the air which results in too high air temperature. It is presumed that this does not have a big influence on the deposited particles since they do not follow the exhalation for long before they drop to the ground.

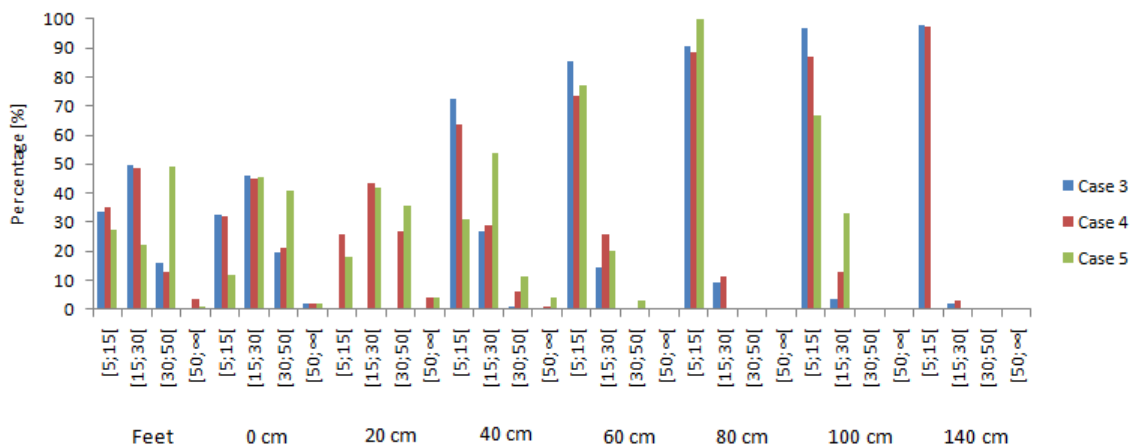


Figure 10.13: On the x-axis is it the distance from the manikin and the particle sizes the interval is in μm .

It can be seen from 10.13 that cases 3 and 4 have almost the same percentage of deposited particles for all distances while in case 5 there are a larger fraction of big particles close to the manikin. This does not mean that more large particles deposit far from the manikin in case 5 than the other two, since it is percentage wise of the total amount of particles found. For example, particles are only measured up to one meter in case 5 since there were hardly any particles deposited on the floor at that distance from the manikin.

10.4 Micro environment between two people

In chapter 6 on page 51 the micro environment between two people is examined. In these investigations it was observed, using smoke visualization and through measurements that with a mutual distance between the manikins of $1.1m$ the personal exposure index were the highest of the measured and the exhalation jet did not reach the target before it was diluted. These result were obtained with ventilation in the room, the measurements in Hong Kong are without ventilation and they show different results. Figure 10.14 shows how the exhalation jet of the source manikin reaches the breathing zone of the target, the picture is taken as the exhalation has stopped and before the next starts..



Figure 10.14: The source is located to the right and the target to the left.

The observation that the exhalation jet break through the thermal plume of the target is underpinned by the particle measurement at the chest of the target, these can be seen in figure 10.15

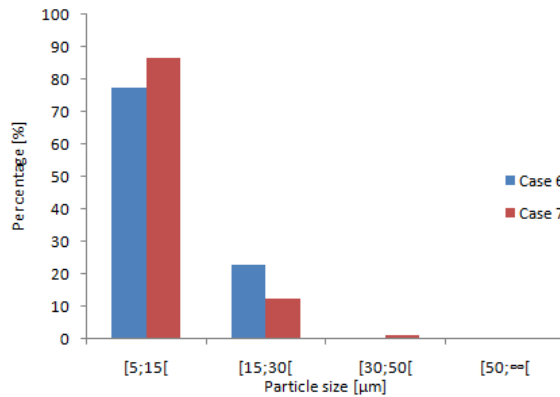


Figure 10.15: Particles measured on the chest of the manikin on a horizontal sample plate.

It is seen that particles above 15 μm settle on the plate on the chest. These can be considered as larger particles as they are not part of those that are usually considered to be airborne which is 5 μm to 10 μm .

Figure 10.16 shows the distribution of deposited particles on the floor. There are more points in case 8 than case 7 since the distance between the manikins is larger. The point 100cm in case 7 is located next to the manikin to see how many particle deposited there.

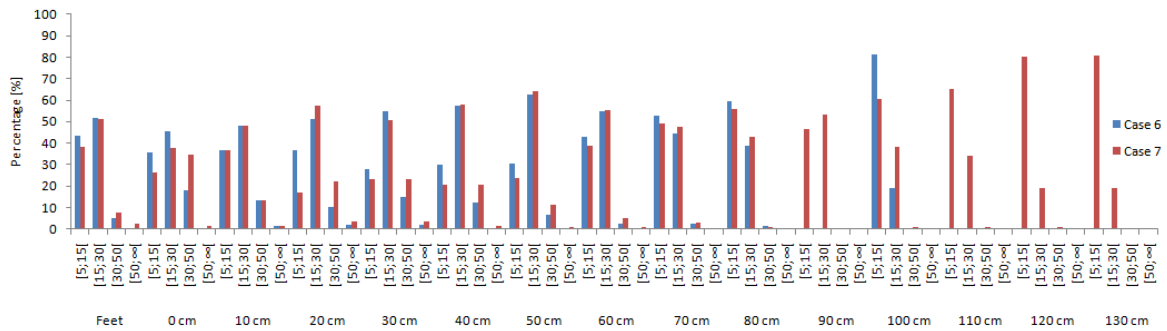


Figure 10.16: On the x-axis is it the distance from the manikin and the particle sizes the interval is in μm .

Figure 10.16 shows that large particle travel much further with two manikins standing opposite each other than when one manikin stands alone, see case 3 section 10.2 on page 103. It is presumed the reason for this could be that the plumes of the two manikins interact and thereby give extra updraft to the particles and thereby enable them to travel further.

10.5 Uncertainties

There are some uncertainties concerning the measurements conducted in Hong Kong, these both concern how the measurements are performed but also the equipment used for the

10.5.1. Equipment

measurements. This section is used to clarify those uncertainties and what influence they have on the results presented above.

10.5.1 Equipment

The equipment in the laboratory in Hong Kong was insufficient to deal with the task at hand.

The settings on the artificial lungs are not correct and needed to be controlled in order deliver the right flow for the measurements. In Aalborg it was calibrated using equipment which was reproduced in Hong kong, unfortunately it was not big enough to calibrate the largest flows the lung are able to generate. The calibration equipment constructed in Hong Kong can be seen in figure 10.17



Figure 10.17: Equipment for calibrating the minute volume of the artificial lung.

As a result of not being able to determine the correct flow from the lung the settings for MV on the lung were decided based on measurements of lower flows which the equipment were able to handle and finding a tendency in the deviation from the setting on the manikin, a more detail description of this can be seen in appendix I. This means that the settings for MV may not fit the activity level correctly.

The particle generator is constructed in a way which should secure that particles are suspended inside it at all time, so when the flow from the lung enters it, it entrains particles of all sizes. But it is questionable whether it is able to keep the largest particles suspended in the air as the largest particles counted on the sample plates are below $80 \mu m$ and approximately 10 % of the particles should be above this size. Another reason why particles larger than $70 \mu m$ is only counted once could be that they deposit before the first sample plate or

they are stuck inside the manikin.

It has not been possible to control the amount of particles exhaled. The only form of control is varying the speed of the wheel and fan inside the generator and adjusting how much powder is put into the generator. However when it is not controlled how much powder exits the generator it is impossible to guarantee the same amount is in the generator for the next measurement.

Another problem with the generator is that it is not possible to see or hear whether it is working or not. The reason why it is not possible to see if it is working or not is that particles stick to the glass and it is therefore not transparent anymore.

10.5.2 The manikins

The construction of the manikins makes it very hard to control the temperature of the exhalation jet. The exhalation air runs through the manikin in a tube and when the heat release of the manikin is high like in case 4 it is impossible to keep the temperature at the desired temperature of 35 to 36 °C.

The construction of the mouth of the manikins is not made properly resulting in the jet do not enter and exit the mouth straight, this can be seen in figure 10.18



Figure 10.18: Crooked pattern on the floor.

This solution has been to the manikin has to be turned in order to get a pattern on the floor which is more or less straight. This is not a big problem when only one manikin is used but when two is used it is important to know the exhalation jet is pointed directly towards the other manikin.

10.5.3 Execution of experiments

There are also uncertainties concerning the execution of the experiments. The way the measurements in this report is performed is by removing the sample plates at different times dependent on the distance from the manikin. By doing this we have to enter the room during measurements and that creates disturbances in the flows inside the room. When removing the sample plates turbulence is created close to where they are located at this may result in large particle to change direction and deposit further from the manikin than they initially would do. As described above are the sample plates not removed from the test room at the same time. This is done in order to get an acceptable amount of particles on each sample plate. If the sample plates are in the room for too long too many particle deposit on them and if they are in the room for too short a time not enough particle have deposited to be able to get an acceptable count of the particles.

10.5.4 Counting particles

The way the particles are counted in this project is by sample plates on the floor and only particles deposited on the floor is counted. The sample slides are put in a microscope where pictures are taken of them. It is very important to try and find the right place to take the picture in order to make sure no particles lie on top of each other nor that not too many particles have sharp edges as this can lead to miscounting in the software used for counting. A picture of the particles can be seen in figure 10.19

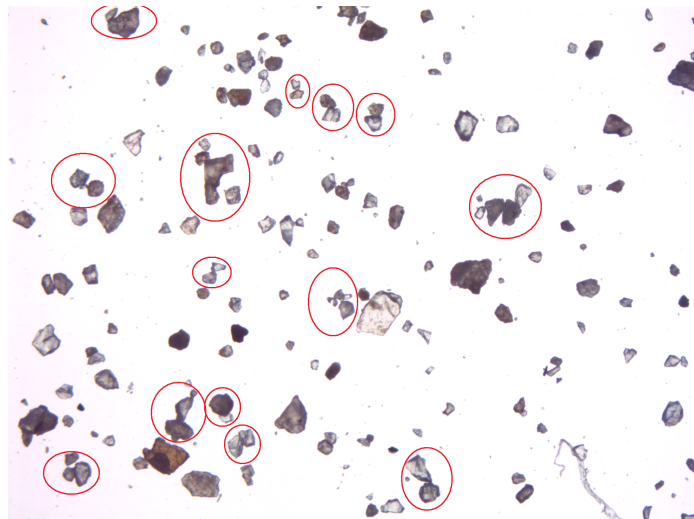


Figure 10.19: Examples of particles on top of each other.

If the particle lie on top of each other as shown in the figure above the software will count them as one particle and thereby increase the count of large particle. The joint particles may even be the largest particles in the frame creating extra errors as it is then assumed that a particle size travels further than it actually did.

10.5.5 The use of particles compared to droplets

In this project particles are used to represent droplets. This may be problematic as the density of the particles may differ from that of saliva and the shape is also different. These two properties play an important role in the trajectory of the particle/droplet. Another property that plays an important role on the trajectory of the particle/droplet is the evaporation. The particles have the same mass and volume from when it leaves the mouth till it lands on the floor. This is not the case with droplets they evaporate from their starting size to between 1/2 to 1/4 of its original size [15]. The evaporation is expected to increase the distance the droplet travels compared to the particle.

10.6 Conclusion

With the conditions under which the experiments are conducted, that is one manikin standing by itself with a thermal plume, a heated exhalation jet and almost no temperature gradient in the room it is unable to deposit particles larger than $30\ \mu\text{m}$ $1\ \text{m}$ from the manikin. This is independent of the activity level, MV and BF. When two manikins are located in front of each other is it interesting to see how much further the large particle travel. It indicates that large particles are able to travel more than $1\ \text{m}$ between two standing persons it is believed that the thermal plume gives updraft to the particles and thereby enable them to travel further.

Part IV

Conclusion

Conclusion

The subdivision of the of the project in three major parts justifies three conclusions. The first part deals with tracergas measurements at a simulated hospital ward in Aalborg. The second part of the conclusion is based on the CFD work done about the hospital ward as well. The third and final part is about particle deposition from standing manikins.

The part of measurement with tracergas is furthermore divided into three parts. With respect to this arrangement, the first part is about a single manikin breathing under different conditions. The second part is about two manikins standing opposite each other. In this scenario one of the thermal breathing manikins is labeled as the source and the other as the susceptible target. The investigation is based upon the personal exposure index for a person who is encountered with two different varying parameters which are the persons position in the room and mutual distance to a simulated infectious person. Subsequently the same investigation is repeated with varying location of inlet diffusers. The third part deals with two bed bounded patients in a hospital ward. Once again attention is turned towards the personal exposure index, but now for a bed bounded person who is encountered to variations with respect to its position in the room, varying air change rates and exhaust heights.

The measurements show that the exhalation jet from the manikin in both cases 1 and 2 are more or less unaffected by the position in the room when it comes to the core velocity. This is an interesting finding since the conditions of the flow trajectories are very different. The following observation has been made in case 1. The exhalation jet is affected by two flows, one which is originated from the inlet diffuser and the other, the thermal plume from the manikin itself. In case 2 the exhalation jet is affected by the thermal plume of both the manikin and the radiator which is located close to it. A reason why they seem to have the same trajectory could be that the exhalation jet in both cases penetrates the upward moving boundary layer flows that surrounds the manikins, without being effected much by it. Furthermore the supply air flows from the inlet do not possess the necessary speeds to pose any retarding affect on the exhalation jets trajectory.

For the micro environment created between two manikins the most interesting findings indicates that when the two manikins stand close to each other. Due to entrainment of both manikins plumes, they get enclosed in a "bubble" where the concentration of tracergas larger than in the macro environment. The reason why the micro environment is obtain is probably because the plumes of the two manikins coincide and thereby oppresses the downward flow of the inlet air. When the distance between the manikins are increased the joint plumes are spread over a larger area and the velocity is thereby reduced. At a certain point the

velocities of the plumes are too low to overcome the flow of the inlet and the plumes are split into two single plumes. The measurements show that because of the micro environment which is develop between the manikins the lowest personal exposure indicies are measured when the manikins are located underneath the inlet diffuser. The highest personal exposure indicies are measured when the manikins are located outside the direct downward flow of the inlet diffuser. The reason for the higher personal exposure indicies is that the exhalation jet is able to escape the micro environment qua to its higher temperature than the ambient air.

A lot of important information are obtained by the measurements done in the hospital ward. The most important result is that the location of the return openings plays an important role when a high personal exposure index is desired. This finding is in contrast to the presumed understanding that the highest personal exposure indicies are not reached with the exhaust located just below the ceiling. There can be several reasons for this outcome. It can be that the contaminants lies in a layer below the ceiling due to the temperature of the exhalation jet or it could be that they accumulate somewhere else in the room than where the exhaust is located in these measurements. Other interesting results are that a high and low exhaust at the same time does not deliver as good results as a high located exhaust. The aim of having a high and low exhaust is that the one located high should remove the airborne contaminants and the low should remove large droplets but it has been indicated that the large droplets can not be removed by ventilation. It is shown that an increased air change does not improve the personal exposure index. This is because an increased air change rate increases the turbulence in the room and there by entrain more contaminants to the fresh air.

CFD predictions has been carried out, with the aim to compare these numerical simulations with the 5 corresponding experiment results. Furthermore an additional case with no experimental counterpart has been made as well. The quantities that are compared between the experiments and the CFD simulations are, temperature and concentration distribution, local ventilation as well as personal exposure indicies. The CFD predictions of the temperatures are in good agreement with the experiment measurements. Both results reveal uniform vertical temperature distributions which furthermore imply that a well mixed flow pattern prevails in the hospital ward. According to the CFD predictions the demonstrated flow patterns are created by two dominant forces, i.e the supply air flows and the thermal plumes. Entrainment of the contaminated air into the supply air flow is consistent through all CFD simulations. The latter ensures a uniform concentration distribution in the hospital ward except in few cases(CFD case 1 & 2) where a sudden deterioration is found with respect to local ventilation index. The latter needs further explanation. Furthermore this finding is also consistent with the experiment cases 12 & 21. For the experiment cases, there has been surmises that this behavior was caused by the exhalation jet that tend to transport the contaminants to the tracergas samplers at 1.8m. At this height, 1.8 m above the floor and between the source and target manikins, it was thought that a layer of contaminants was hovering, and that this layer did not reach all the way up to the ceiling. However this conjecture is partly true and only partly since the following finding is handed out by CFD predictions. According to the numerical results the high concentration at 1.8m is consistent since the contaminants from the exhalation jet is able to just reach 1.8m before it is reversed due to the flow patterns that prevail in the ward. However, although unity is generally consistent with respect to temperature distribution, this likeness between CFD predictions and experiments are overshadowed by huge discrepancies with respect to contaminant distribu-

tions. By a comparison between the personal exposure indices between the two approaches, i.e. CFD and experiments, not less than 200% divergence appear. Thus it can be recommended that more refined approaches need to be taken. These refinements should include grid dependency investigations, transient conditions instead of steady state conditions that omits maximum velocities from the exhalation jet. Suitable boundary condition for more aberrant inlet diffusers is also expected to yield better results. But in general CFD can be used as a tool to at least provide a good estimation of the actual conditions and even more accurate if made with care and good understanding of all precautions.

The objective with the particle deposition was to investigate how far from a person particle deposit. This has been done for with manikins standing by themselves and exhaling particle at different activity levels with appertaining minute volume and breathing frequencies. The results from the single manikins showed that the large particle deposited close to the mouth. A lot of particles were seen on the chest and feet of the manikins as well as the first 20 to 60 *cm* from the manikin but further than that were hardly a clear deposition of particles. So under the conditions inside the room and the uncertainties in mind can it be concluded that a large particles are not able to travel further than 1 *m* from a person but when two manikins are opposite each other are different results seen. When two manikins are located opposite each other can large particle be measured much further away from the source. Particles larger than 30 μm were measured at the chest of the target which indicates that a distance of 1 *m* is not enough to ensure that a person is without the reach of large particles exhaled by another person if they are standing in front of each other.

Bibliography

Bibliography

- [1] Infektionshygiejnisk afdeling. Hygiejne håndbog. Technical report, 2007.
- [2] J. P. Duguid and. The size and the duration of air-carriage of respiratory droplets and droplet-nuclei. -, pages 471–479, 1946.
- [3] Erik Bjørn. *Interacting Airflows and Contaminant Transport around Persons*. PhD thesis, Aalborg University, 1999.
- [4] H. Brohus, K.D. Balling, and D. Jeppesen. Influence of movements on contaminant transport in an operating room. *Indoor Air*, 16:356–372, 2006.
- [5] Carmine J. Bozzi Dale R. Burwen, Samuel W. Dooley, Patricia M. Simone, Consuelo Beck-Sague, Elizabeth A. Bolyard, William R. Jarvis, Philip J. Bierbaum, Christine A. Hudson, Robert T. Hughes, Linda S. Martin, Robert J. Mullan, and Brian M. Willis. Guidelines for preventing the transmission of mycobacterium tuberculosis in health-care facilities. <http://www.cdc.gov/mmwr/preview/mmwrhtml/00035909.htm>.
- [6] Eugene C. Cole and Carl E. Cook. Characterization of infectious aerosols in health care facilities: An aid to effective engineering controls and preventive strategies. *DynCorp Health Research Services*, pages 453–464, 1998.
- [7] P. O. fanger, K.D. Balling, and D. Jeppesen. Assesment of mant’s thermal comfort in practice. *British Journal of Industrial medicine*, 30:313–324, 1973.
- [8] Jitenda K. Gupta, Chao-Hsin Lin, and Qingyan Chen. Characterizing exhaled airflow from breathing and talking. *Indoor air*, 20:31–39, 2010.
- [9] P. Höppe. Temperatures of expired air under varying climatic conditions. *Int. J. Biometeor*, vol 25:127–132, 1981.
- [10] Q. Hua, P. V. Nielsen, Y. Li, and C. E. Hyldgaard. Airflow and contaminant distribution in hospital wards with a displacement ventilation system. *China Environmental Science Press*, pages 355–364, 2004.
- [11] Qian Hua and Yuguo Li. Removal of exhaled particles by ventilation and deposition in a multibed airborne infection isolation room. *Indoor air*, 20:284–297, 2010.
- [12] Powder Technology Inc. Iso 12103-1 test dust grades from powder technology inc. <http://www.powdertechnologyinc.com/products/test-dust/test-dust.php>.
- [13] Donald G. McNeil Jr. In new theory, swine flu started in asia, not mexico. http://www.nytimes.com/2009/06/24/health/24flu.html?_r=3, 2009.
- [14] Sehulster LM, Chinn RYW, Arduino MJ, Carpenter J, Donlan R, Ashford D, Besser R, Fields B, McNeil MM, Whitney C, Wong S, Juranek D, and Cleveland J. Guidelines for environmental infection control in health-care facilities. Technical report, 2003.
- [15] M. Nicas, W. W. Nazaroff, and A. Hubbard. Toward understanding the risk of secondary airborne infection-emission of respirable pathogens. *Journal of Occupational and Environmental Hygiene*, 2:143–154, 2005.
- [16] Peter V. Nielsen. Control of airborne infectious diseases in ventilated spaces. *J. R. Soc. Interface*, 6(747-755), 2009.

-
- [17] Peter V. Nielsen, F. V. Winther, M. Buus, and M. Thilageswaran. Thermal environmental conditions for human occupancy. *American Society of Heating, Refrigerating, and Air conditioning Engineers*.
- [18] Peter V. Nielsen, Frederik V. Winther, Morten Buus, and Yuguo Li. Risk of cross-infection in a hospital ward with downward ventilation. *Building an environment*, 45(2008-2014), 2010.
- [19] Peter W. Nielsen. Thermal building dynamics. lecture, 2009.
- [20] R. S. Papineni and F. S. Rosenthal. The size distribution of droplets in the exhaled breath of healthy human subjects. *Journal of aerosol medicine*, 10(2):105–116, 1997.
- [21] H. Qian, Y. Li, P. V. Nielsen, C.E. Hyldgaard, T. W. Wong, and A. T. Y. Chwang. Dispersion of exhaled droplet nuclei in a two-bed hospital ward with three different ventilation systems. *Indoor Air*, 16:111–128, 2006.
- [22] JJY Sung, I Yu, NS Zhong, and K Tsoi. Super-spreading events of sars in a hospitalsetting: who, when and why? *Hong Kong Med J*, 15, 2009, pages = 29-33,.
- [23] J. W. Tang, C. J. Noakes, P. V. Nilesen, I. Eames, A. Nicoll, Y. Li, and G. S. Settles. Observing and quantifying airflows in the infection control of aerosol- and airborne-transmitted diseases: an overview of approaches. *Journal of Hospital infection*, 2010, pages = ,.
- [24] Raymond Tellier. Aerosol transmission of influenza a virus: a review of new studies. *J. R. Soc. Interface*, 6:783–790, 2009.